2007

Singlet Oxygen Generation Using New Fluorene-based Photosensitizers Under One- And Two-photon Excitation

Stephen James Andrasik
University of Central Florida

SINGLET OXYGEN GENERATION USING NEW FLUORENE-BASED PHOTOSENSITIZERS UNDER ONE- AND TWO-PHOTON EXCITATION

by

STEPHEN J. ANDRASIK
B.S. University of Central Florida, 2001
M.S. University of Central Florida, 2004

A dissertation submitted in partial fulfillment of the requirements
for the degree of Doctor of Philosophy
in the Department of Chemistry
in the College of Sciences
at the University of Central Florida
Orlando, Florida

Fall Term
2007

Major Professor: Kevin D. Belfield

ABSTRACT

Molecular oxygen in its lowest electronically excited state plays an important roll in the field of chemistry. This excited state is often referred to as singlet oxygen and can be generated in a photosensitized process under one- or two-photon excitation of a photosensitizer. It is particularly useful in the field of photodynamic cancer therapy (PDT) where singlet oxygen formation can be used to destroy cancerous tumors. The use of two-photon activated photosensitizers possesses great potential in the field of PDT since near-IR light is used to activate the sensitizer, resulting in deeper penetration of light into biological tissue, less photo-bleaching of the sensitizer, and greatly improved resolution of excitation.

The synthesis and photophysical characterization of new fluorene-based photosensitizers for efficient singlet oxygen production were investigated. The spectral properties for singlet oxygen production were measured at room temperature and 77 K. Two-photon absorption (2PA) cross-sections of the fluorene derivatives were measured by the open aperture Z-scan method. The quantum yields of singlet oxygen generation under one- and two-photon excitation (Φ_Δ and ${}^{2PA}\Phi_\Delta$, respectively) were determined by the direct measurement of singlet oxygen luminescence at ≈ 1270 nm. The values of Φ_Δ were independent of excitation wavelength, ranging from 0.6 - 0.9. The singlet oxygen quantum yields under two-photon excitation were ${}^{2PA}\Phi_\Delta \approx ½\Phi_\Delta$, indicating that the two processes exhibited the same mechanism of singlet oxygen production, independent of the mechanism of photon absorption.

To my wife Hong

and my little girls

Heather Rose Ling

and

Abby Mingmei

ACKNOWLEDGMENTS

I would like to express my sincere gratitude towards Dr. Kevin D. Belfield. He has had a significant contribution in the development of my education as a result of his support and guidance over the past several years. I feel privileged to have had the opportunity to study under his direction and to share in his enthusiasm for chemistry. Additionally, I deeply appreciate the time and effort extended to me by Dr. Mykhailo Bondar. Both Dr. Belfield and Dr. Bondar have been outstanding mentors for which I am truly grateful for.

TABLE OF CONTENTS

LIST OF FIGURES

LIST OF TABLES

LIST OF EQUATIONS

LIST OF SCHEMES

LIST OF ACRONYMS/ABBREVIATIONS

ACN	Acetonitrile
A1A	5-Aminolevulinic acid
Ar	Argon
BPD-MA	Benzoporphyrin monoacid ring A
cm	Centimeter (10^{-3} m)
C	Concentration
°C	Degrees Celsius
CT	Charge transfer
pCT	Partial charge transfer
ΔE	Excess energy
FDA	Food and Drug Administration
GM	Göppert Mayer (10^{-50} cm^4 s $photon^{-1}$ $molecules^{-1}$)
g	Gram
HpD	Hematoporphyrin derivative
h	Hour
IV	Intravenous
IR	Infrared
K	Kelvin
k_d	Deactivation rate constant
L	Liter
MHz	Megahertz (10^6 Hz)

m-THPC	Meta-tetra hydroxyphenyl chlorin
μs	Microsecond (10^{-6} s)
mL	Milliliter (10^{-3} L)
mmole	Milimoles (10^{-3} mole)
min	Minute
ε	Molar absorptivity (M^{-1} cm^{-1})
nm	Nanometer (10^{-9} m)
NMR	Nuclear magnetic resonance
OD	Optical density
ppm	Parts per million
PBS	Phosphate buffered saline
PDT	Photodynamic therapy
1PA	One photon absorption
1PE	One photon excitation
psi	Pounds per square inch
PMT	Photomultiplier tube
PS	Photosensitizer
^{1}H NMR	Proton nuclear magnetic resonance
PpIX	Protoporphyrin IX
QY	Quantum yield
RT	Room temperature
Φ_{Δ}	Singlet oxygen quantum yield by one photon absorption
$^{2PA}\Phi_{\Delta}$	Singlet oxygen quantum yield by two photon absorption

SI	International System of Units
S_1	First excited singlet state
S_0	Ground singlet state
$^1O_2$	Singlet state oxygen
TMS	Tetramethylsilane
TLC	Thin layer chromatography
T_1	First excited triplet state
$^3O_2$	Triplet state oxygen
2PA	Two-photon absorption
2PE	Two-photon excitation
δ	Two photon absorption cross section (GM)
M	Molar (mol/L)
λ_{max}	Maximum wavelength
λ	Wavelength
UV	Ultraviolet
wks	Weeks
Xe	Xenon

CHAPTER 1: INTRODUCTION

Ground state molecular oxygen, O_2, is essential for life in all aerobic organisms on earth. It is highly abundant throughout the universe and is the most common component of the earth's crust. It can undergo excitation in a photosensitized process to become a powerful oxidant where it can undergo destructive reactions with organic compounds. Excited state O_2 is commonly referred to as singlet oxygen ($^1O_2$) and its photosensitized production has given rise to a fascinating field of medicine known as photodynamic therapy (PDT).

This chapter will introduce the intriguing properties of $^1O_2$ and its photosensitized production. Recently, there have been heightened interests in the fields of chemistry, biology, and medicine to produce new compounds capable of photosensitizing $^1O_2$ for use in PDT. The central objective of this dissertation is in the development of $^1O_2$ sensitizers that can efficiently produce $^1O_2$ under one- or two-photon excitation. Section 1.1 describes $^1O_2$, how it can be produced, and its use in PDT. A description of two-photon excitation (2PE) and the benefits of its use to enhance $^1O_2$ sensitization in PDT will be discussed. The dissertation statement will be presented in section 1.2 and an outline for this work will be provided in the final section.

1.1 Background and Significance

Ground state molecular oxygen, $^3O_2$, has two unpaired π electrons in separate degenerate orbitals giving rise to a triplet state and its paramagnetic behavior. There are two electronically excited singlet states of molecular oxygen that have the same electron configuration but with spin pairing of the two electrons. The excited singlet states lay 94 and 157 kJ mol^{-1} above the ground triplet state. However, the higher energy excited state is very short lived and quickly

decays to the lower excited singlet state. Phosphorescence emission at 1270 nm results upon relaxation from the lower excited state to the ground state. Additionally, it is this lower excited state that is associated with much of the chemistry of $^1O_2$.

The formation of $^1O_2$ can occur by a number of different pathways such as thermally, chemically, or by means of a photosensitizer. Cyclic organic peroxides can readily undergo thermal decomposition resulting in $^1O_2$ formation. Khan and Kasha, who performed some of the earliest direct spectroscopic studies on $^1O_2$, used the chemical reaction between sodium hypochlorite and hydrogen peroxide to form $^1O_2$.[1] Singlet oxygen can also be generated in an energy transfer process between a photosensitizer and $^3O_2$.[2] Some of the more common types of photosensitizers are highly conjugated organic compounds, transition metal complexes, and porphyrins. Many of theses compounds are associated with a number of photochemical and photobiological processes, and are involved in the photodegradation of organic compounds and polymers, bleaching processes and the purification of water, and the destruction of biological material in PDT.[3-6]

Biological tissue is very sensitive to $^1O_2$ and is quickly destroyed in its presence. In recent years there has been a heightened interest in utilizing compounds that can photosensitize the formation of $^1O_2$ for use in PDT of cancer. Singlet oxygen is very reactive towards biological tissue and will quickly react with unsaturated organic compounds and fatty acids. Cell membranes such as plasma, mitochondrial, and nuclear membranes are rapidly destroyed by $^1O_2$.[7] Enzymes and cellular proteins become cross-linked, and may become bound to and inactivate DNA and RNA.[8-11]

Photodynamic therapy of cancer has great potential to treat a variety of different types of neoplastic diseases such as skin, head and neck, esophageal, and lung cancer. In PDT of cancer,

a photosensitizer (PS) is administered topically or by intravenous injection to a patient. This is pictorially represented in Figure 1. Initially inert, the PS travels throughout the body and is taken up and retained by the tumor. In some circumstances the PS has a lower affinity for healthy cells and is removed from the body through the liver and kidneys. The sensitizer is then activated by exposing the treatment area to a wavelength of light were the PS undergoes excitation from the ground state, S_0, to the first excited state, S_1. The S_1 state is short-lived, and the PS quickly undergoes intersystem crossing from the S_1 to the triplet state T_1. Collisional interaction between the PS T_1 and ground state $^3O_2$ result in the formation of $^1O_2$. The use of PDT allows the possibility to reduce or completely remove a cancerous tumor, in some cases, without the need for surgery, chemotherapy, or radiation.

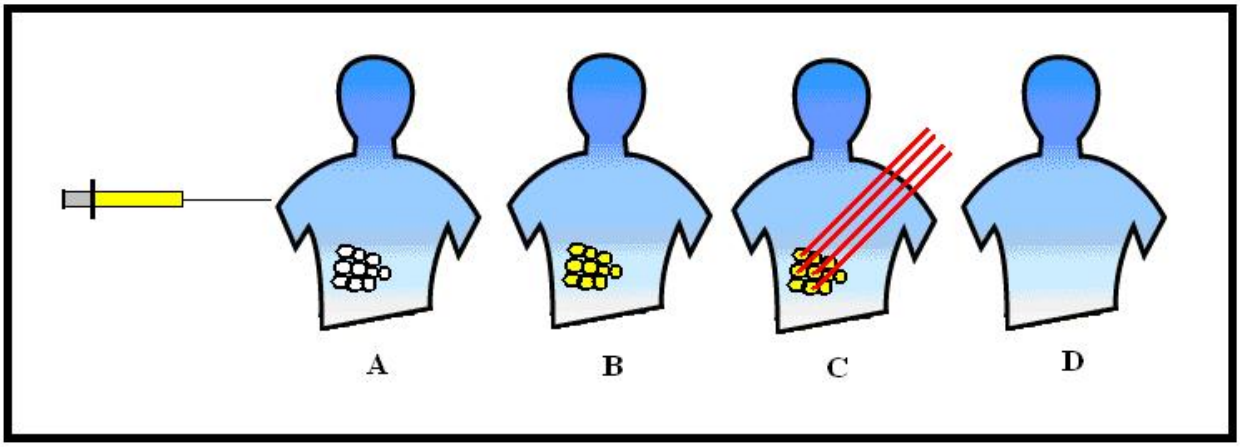

Figure 1. Graphical representation of PDT. A) Injection of PS into patient, B) localization of PS in tumor, C) activation of PS with light, D) tumor eradicated.

One of the most important requirements in PDT is to get enough light to the PS to adequately excite it. Most PS's have absorption maxima in the visible to near IR region. Scattering and absorption by biological tissue are significant in this region (Figure 2) and greatly

reduce the ability to excite the PS. Synthetic efforts on commercial PS's have been on shifting the absorption maxima to longer wavelengths, out towards the absorption minimum of biological tissue to 700-1000 nm. The ability to maintain a high $^1O_2$ quantum yield and photostability at longer wavelengths has been difficult, and many of the commercial PS's approved by the FDA have absorption maxima at or below 680 nm.[12] This has limited the effective use of PDT to tumors close to the surface, such as skin cancer, or to areas that can be accessed with an endoscope, such as the esophagus and upper bronchi of the lungs.

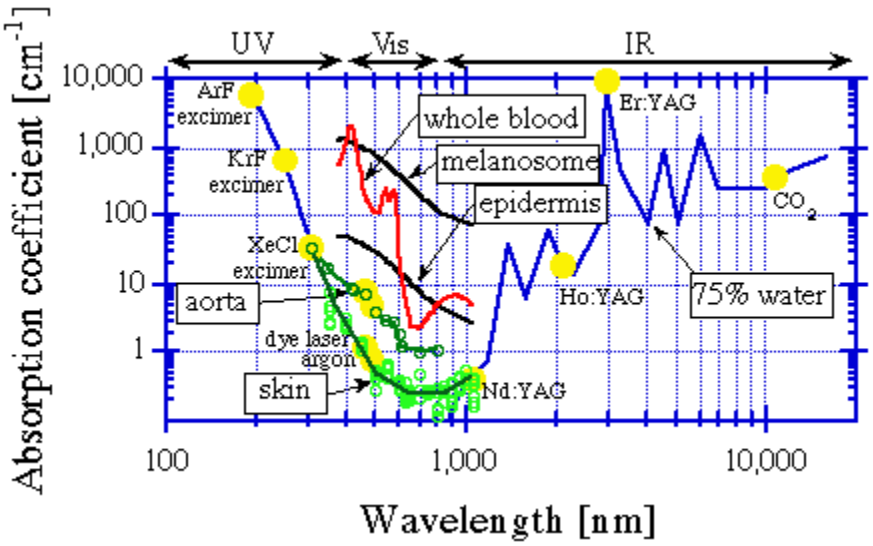

Figure 2. Absorption of biological tissue.[13]

The ability to access longer wavelengths beyond 700 nm would allow for deeper penetration into tissue, and the lower energy of these wavelengths may result in less photobleaching of the PS. Despite the benefit of using longer excitation wavelengths, there remains a significant problem that is inherent with the selectivity of the PS's used today. Many of the commercial PS's available exhibit increased selectivity for particular types of tumors, but

they are not 100 % selective.[14-16] Typically, the PS is administered to the patient and is not activated until the systemic PS concentration in a patient has dropped to a level that will not cause significant damage to healthy tissue. Additionally, there is a limited timeframe in which the concentration of the PS is adequate to destroy the tumor. Typical linear excitation of the PS can lead to some out of focus activation due to the inherent nature of linear (one-photon) excitation. In addition to scattering and absorption loss, out of focus excitation of the PS greatly limits the effective treatment of tumors by PDT.

The use of PS's that can undergo excitation by two-photon absorption (2PA) promises to greatly improve the use of PDT. First proposed by physicist Maria Göppert-Mayer in 1931, the process of 2PA by a molecule is described as the near simultaneous absorption of two photons producing an electronic transition corresponding to the combined energy of the photons involved.[17] To produce an electronic transition under 2PA, high irradiation intensities are required to increase the possibility that two photons will combine at the same time and at the same point in space. The combined energies of the two photons are equivalent to the energy of one-photon for the particular electronic transition.

The nonlinear process of 2PA results in excitation of a molecule in the focal volume of the excitation beam. Unlike 1PA, the probability that a molecule will absorb two photons simultaneously to produce an electronic transition is nonlinearly dependent on the incident intensity of the excitation source. Whereas the probability of the same molecule will undergo an electronic transition under 1PA is linearly dependent. This is clearly evident in Figure 3, where the emission intensity from the sample under two-photon excitation is tightly confined to the focal volume, but out-of-focus emission is clearly visible under one-photon excitation where the emission is linearly dependent on the incident intensity. The quadratic dependence of 2PA on

the incident intensity, I^2, allows one to obtain increased three dimensional (3D) resolution when exciting a molecule. This is a tremendous advantage over linear 1PA.

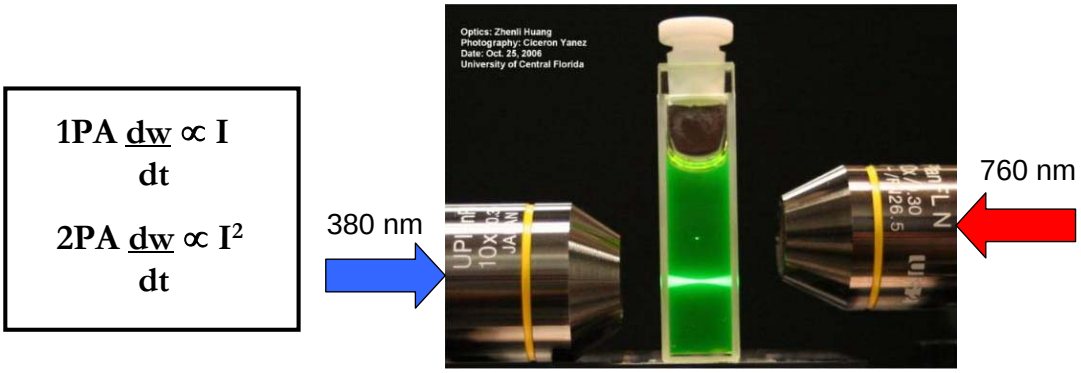

Figure 3. Comparison of 1PA at 380 nm vs. 2PA at 760 nm.

The precision of PDT may be greatly enhanced with the use of PS's that can generate $^1O_2$ under 2PA. This will reduce the need to synthesize PS's that have a high degree of selectivity for tumors. Moreover, the longer wavelengths that are typically used will result in deeper penetration into tissue due to less scattering and absorption. Lastly, the longer wavelengths (NIR) will translate into a lower possibility of photodamage to tissue. As a result, less PS will be required if the chance of excitation is maximized and exposure is tightly controlled. Due to better resolution, activation of the PS can be accomplished early after administration while its concentration is high in the patient, leading to better treatment with PDT.

1.2 Dissertation Statement

The purpose of this dissertation is to prepare and characterize the photophysical properties of new hydrophilic fluorene-based singlet oxygen sensitizers under one- and two-

photon absorption. The decision to use fluorene was based on extensive studies with various derivatives demonstrating good nonlinear optical properties, thermal and photostability, and capacity to photosensitize $^1O_2$.[18-20] Furthermore, the fluorene architecture lends itself well to be easily derivatized to modulate the photophysical properties and solubility of the compound. The use of heavy atoms and nitro groups will be incorporated into the molecular architecture to help promote $^1O_2$ sensitization. Strong electron withdrawing groups will also be included to increase the π-conjugation length and enhance 2PA. The photophysical properties of these novel compounds will be assessed under one- and two-photon excitation at room temperature and 77 K. Emphasis will focus on the direct determination of $^1O_2$ quantum yields by 2PA, a rather challenging but essential aspect of this research. Singlet oxygen quantum yields (QY) will be determined to assess the potential of the sensitizers for 2PA photodynamic therapy.

1.3 Dissertation Outline

Formation of singlet oxygen and its use in PDT is presented in the first Chapter. Its limitations as a therapeutic cancer treatment are also presented providing the motivation for designing $^1O_2$ sensitizers that can be used under 2PE. A summary of the current state of the art of PDT is presented in Chapter 2 along with an extensive review of $^1O_2$ and current FDA approved sensitizers. The salient features of fluorene derivatives for use as 2PA photosensitizers will be highlighted. Chapter 3 will describe the synthetic methods used to incorporate heavy atoms and nitro groups, extend the π-conjugation with strong electron withdrawing groups, and methods to increase the hydrophilic character of the photosensitizers. The photophysical characterization of the PS candidates will be presented in Chapter 4, including 1PA

spectroscopic data at room temperature and 77 K and the $^1O_2$ quantum yield under 1PE and 2PE. Chapter 5 concludes the dissertation with a synopsis of results and provides a brief discussion for future synthetic work to improve the photophysical properties of the fluorene derivatives for singlet oxygen sensitization and possible experiments to be performed *in vitro* with the PS's.

CHAPTER 2: BACKGROUND

The current status of photodynamic therapy is in its infancy. Although the therapeutic properties of light have been known for thousands of years it has only been in the latter part of the last century that PDT has begun to evolve into a unique treatment modality. It was in the early 1900's that some of the earliest pioneers in the field of PDT realized the combination of light and certain chemicals could be used to induce cell death. Since then numerous investigations have been undertaken to identify new compounds and to understand the mechanisms involved in the formation of singlet oxygen.[21] However, it wasn't until the late 1960's when lasers and instrumentation were beginning to come of age that the photosensitization of $^1O_2$ would begin to be seriously developed into a useful medical treatment for treatment of malignant and non-malignant diseases. Despite the tremendous interest in PDT over the past forty years there have been less than a dozen PS's that have been approved for medical applications using PDT, and many of these compounds possess limited effectiveness in their treatment.

Hence, this chapter will focus on the more recent PS's that have been identified as good $^1O_2$ sensitizers and their clinical use. An alternative class of compounds will also be proposed based on $^1O_2$ sensitization by 2PE. Section 2.1 will introduce and provide a thorough background on $^1O_2$. The following section will present some of the salient features of currently approved PS's that are being used in PDT and their effectiveness. Section 2.3 will discuss the advantages of using compounds that can generate $^1O_2$ under 2PE for PDT and cover basic terms that are used to characterize their photophysical properties. In addition, section 2.3 will discuss

general trends of the 2PA properties for fluorene derivatives and the motivation for using this class of compounds as new $^1O_2$ photosensitizers.

2.1 Overview of Singlet Oxygen

2.1.1 Introduction of Singlet Oxygen

The chemistry and physical properties of oxygen have been studied for hundreds of years. Oxygen was first described by the Polish alchemist and philosopher, Michal Sędziwój, in the late 1500's, and later identified in 1774 as an element by the English scientist Joseph Priestley. Although molecular oxygen has been studied for hundreds of years it was not until the beginning of the twentieth century that the electronic structure and the photophysical properties of oxygen were described. In 1924, Lewis accurately described the paramagnetic behavior of ground state molecular oxygen. At this time it was thought by many that the electronic structure of oxygen was analogous to ethylene and similar analogs. Lewis, accounting for oxygen's paramagnetic behavior, suggested the double bond in oxygen is broken in a symmetrical fashion leaving an odd electron on each oxygen atom.[22] Four years later, Mulliken introduced the electronic configuration of ground state molecular oxygen.[23] The quantum mechanical calculations that he performed predicted the triplet ground state $^3\Sigma_g^-$ and two metastable electronically excited singlet states with the molecular term symbols $^1\Delta_g$ and $^1\Sigma_g^+$. In this paper Mulliken assigns the atmospheric oxygen band at 1.62 eV to the $^1\Sigma_g^+ \leftarrow {}^3\Sigma_g^-$ transition and predicted another weak transition in the infrared at 0.81 eV, attributed to the lower lying transition of $^1\Delta_g \leftarrow {}^3\Sigma_g^-$. In

1933, Ellis and Kneser, using liquid oxygen, demonstrated the $^1\Delta_g \leftarrow {}^3\Sigma_g^-$ transition was in fact from the infrared transition at 0.81 eV.[24]

In 1976, Paul Schaap compiled a series of benchmark papers that describe some of the earliest and significant investigations of singlet oxygen.[25] Perhaps one of the earliest known reports of chemistry involving singlet oxygen was described by Fritzsche in 1867, where he reported the conversion of a solution of naphthacene into a crystalline material on exposure to light and air.[26] He went on to report that the original compound could be regenerated upon heating the crystalline material. It was later confirmed that the crystalline material was the epidioxide of naphthacene. Similar experiments were performed in 1926 by Moureu and co-workers using rubrene, air, and light to produce a dioxide derivative.[27] The earliest example of a dye sensitized reaction was performed in 1928 by Windaus and Brunken where they excited eosin in the presence of oxygen using a 200 watt bulb.[28] The singlet oxygen was generated in the presence of a plant hormone where it consequently converted the hormone, ergosterol, to a dioxide derivative.

Investigations of dye sensitized singlet oxygen formation continued, and in 1931 Kautsky proposed a mechanism for dye sensitized photooxgenation.[25, 29] Up to this point many believed the photooxidation process involved an unstable sensitizer-oxygen complex, but Kautsky contended that diffusible singlet oxygen was formed in an energy transfer process between ground state oxygen and an excited sensitizer. Between the years of 1933-1938, Kautsky and Bruijn devised a series of clever experiments to prove diffusible singlet oxygen, and not a bound oxygen complex, was the mechanism by which dye-sensitized photooxidation reactions occurred.[25] In these experiments, they physically separated the sensitizer and acceptor compounds by absorbing them individually onto silica gel and then coated it onto a glass tube.

Oxidized product formation was monitored by observing a color change of the acceptor compound after exposing the tube with an arc lamp at different oxygen pressures. The results from the experiments unequivocally demonstrated that the dye sensitized photooxidation of the substrate occurred by means of diffusion of oxygen.

Despite the strong evidence, the mechanism of singlet oxygen diffusion was not adopted and many stood by the originally proposed mechanism of a sensitizer-oxygen complex proposed by Schönberg in 1935.[30] In the mid 1960's, singlet oxygen was being generated by chemical and electrical methods, and similar results of a diffusible oxygen species were being observed. During this time, Kautsky's original mechanism began to earn acceptance, and in 1964 Foote and Wexler published a paper supporting the original mechanism proposed by Kautsky where they demonstrated that they could produce oxygenated organic substrates using sodium hypochlorite and hydrogen peroxide.[31, 32] The compounds obtained by Foote and Wexler were identical to dye sensitized photooxygenation reactions. At the same time, Corey and Taylor performed experiments to oxygenate organic substrates using singlet oxygen produced by passing a stream of oxygen through an electric discharge.[33] They demonstrated that the products obtained from the electric discharge process were also identical to products formed from sensitized photooxygenation. The conclusions by these two groups provided significant support for Kautsky's singlet oxygen mechanism.

In the 1940's researchers began to actively investigate the chemistry of singlet oxygen and its use in organic chemistry. Schenck and Ziegler wrote about the first dye sensitized photooxygenation of α–terpinene, using chlorophyll as the sensitizer, to synthesize the naturally occurring trans-annular peroxide, ascaridole.[34] Dufraisse and Ecary did some of the earliest studies with 3-diphenylisobenzofuran (DPBF), demonstrating its efficiency as a singlet oxygen

acceptor.[35] DPBF is commonly used in experiments to study the kinetics and photophysics of singlet oxygen sensitizers. Wilson used it in 1966 as one of several compounds to provide support for Kautsky's singlet oxygen mechanism, and Merkel and Kearns used DPBF in a study to directly the lifetime of singlet oxygen in solution.[36, 37]

The first comprehensive kinetic experiment of a dye-sensitized photooxidation was performed by Schenck in 1951, using α-terpinene and chlorophyll as the singlet oxygen sensitizer.[25] Although Schenck's experiment was very insightful, the results were interpreted in terms of Schönberg's sensitizer-oxygen complex mechanism, and later determined to be invalid. A couple of years later, Schenck reported on the dye-sensitized photooxygenation of substituted alkenes resulting in the formation of allylic hydroperoxides. By the end of the decade, Nickon and Bagli extended the work of Schenck and presented work on the photosensitized oxygenation of mono-olefins using hematoporphyrin as the dye sensitizer.[38] Their investigation looked at the possible mechanism for the olefin-oxygen product formation.

By 1960, singlet oxygen was routinely formed by dye-sensitization, chemically, and by electric discharge. Spectroscopic studies using various methods of singlet oxygen formation allowed for detailed investigations into the photophysical properties and mechanism of its formation. In 1960, while investigating a method to improve the measurement of emission spectra, Seliger reported on a sharp chemiluminescence band at 634 nm from a reaction between sodium hypochlorite and hydrogen peroxide[39]. Intrigued by Seliger's results, Khan and Kasha followed up on this observation, and in 1963 assigned the emission at 634 nm to the $^1\Sigma_g^+ \rightarrow {}^3\Sigma_g^-$ transition by singlet oxygen.[1] A year later, Browne and Ogryzlo expanded the investigation of the sodium hypochlorite and hydrogen peroxide reaction and assigned the $^1\Delta_g \rightarrow {}^3\Sigma_g^-$ transition for singlet oxygen to the emission bands at 1070 and 1270 nm, corresponding to the (1,0) and

(0,0) transitions, respectively.[40] About this same time, Gollnick and Schenck reported a method to determine the triplet state quantum yield of sensitizers using Rose Bengal as an example.[41] In the paper they use an indirect method where all of the singlet oxygen that is produced from the sensitizer in the triplet state is trapped with a highly reactive singlet oxygen acceptor such as acenes, cyclohexadiene derivatives, and olefins among other singlet oxygen acceptors. Up to this point, direct evidence of $^1\Delta_g$ oxygen formation by energy transfer from an excited sensitizer had not been demonstrated. In 1968, Snelling provided the first direct evidence of energy transfer from electronically excited molecules to oxygen.[42] In his experiment, benzene was excited at 254 nm in the presence of oxygen and emission at 1270 nm was observed corresponding to the $^1\Delta_g \rightarrow {}^3\Sigma_g^-$ transition for singlet oxygen.

By the 1970's, the production of singlet oxygen was being generated by laser excitation of a sensitizer, and investigations included the formation of $^1\Sigma_g^+$ oxygen. In 1970, Andrews and Abrahamson reported for the first time the emission of singlet oxygen at 762 nm for the $^1\Sigma_g^+ \rightarrow {}^3\Sigma_g^-$ transition by photosensitization using gaseous O_2 and fluoronaphthalene.[43] Merkel and Kearns reported the first direct measurement of the $^1O_2(^1\Delta_g)$ lifetime in methanol by pulsed laser excitation, and went on to report on solvent effects and radiationless decay of $^1O_2(^1\Delta_g)$ in solution.[36] Using a series of sensitizers and an indirect method to detect singlet oxygen, Adams and Wilkinson determined that the rate constant for singlet oxygen decay $^1\Delta_g \rightarrow {}^3\Sigma_g^-$ was independent of the photosensitizer used.[44]

By the end of the 1970s the first report of direct detection of $^1O_2(^1\Delta_g)$ luminescence was given by A. A. Krasnovsky Jr. In 1976, he reported the detection of $^1\Delta_g \rightarrow {}^3\Sigma_g^-$ luminescence at 1270 nm using a 1000 W Xe lamp, phosphoroscope, and an S-1 photomultiplier tube (PMT) cooled to –60 °C.[45] Air saturated solutions of protoporphyrin and naphthacene in carbon

tetrachloride were analyzed where Krasnovsky reported $^1O_2$ QYs and lifetimes. This set off a flurry of experiments utilizing direct detection of singlet oxygen luminescence in the early 1980s. Hurst and co-workers investigated the solvent dependence of radiative and nonradiative decay of $^1O_2$ in different solutions.[46] Ogilby and Foote investigated solvent deuterium isotope effects on the lifetime of $^1O_2$, where they found an increase in its lifetime in deuterated solvents by an order of magnitude over nondeuterated solvents.[47] Parker *et al.* followed up on Ogilby and Foote's work with an investigation of the collisional lifetime of $^1O_2$ in deuterated and nondeuterated acetone, where they observed similar results.[48] Rogers *et al.* reported the lifetime of singlet oxygen in water by time resolved luminescence measurements. About the same time, Wilkinson, Helman, and Ross published a paper reporting rate constants for singlet oxygen decay in 145 solvents or solvent mixtures, and second order rate constants for interaction of $^1O_2$ with nearly 2000 different compounds.[49] This same group followed up their report of $^1O_2$ rate constants with a compilation of 102 $^1O_2$ QYs for 755 compounds such as aromatic hydrocarbons, dyes, drugs, porphyrins, and related compounds.[50]

In 1994, Schmidt and Bodesheim were the first to report the detection of $^1\Sigma_g^+ \rightarrow {}^3\Sigma_g^-$ emission at room temperature in carbon tetrachloride, in addition to reporting the lifetime (130 ns) and rate constant for quenching by several different compounds.[51] By the end of the 20th century, researchers were actively investigating the mechanism of photosensitized singlet oxygen formation. Schweitzer and Schmidt investigated the physical mechanisms involved in the formation and deactivation of singlet oxygen in solution.[52] In 2001, Ogilby reported $^1O_2$ formation under one -photon excitation of a 2PA sensitizer for in solution.[53] About the same time, Andersen and Ogilby reported the time-resolved detection of $^1\Sigma_g^+ \leftarrow {}^1\Delta_g$ absorption in air saturated polystyrene through a transmission microscope.[54] This was followed up by Ogilby *et*

al., in 2005, where they reported the qualitative detection of singlet oxygen formation in water by two-photon excitation, and a year later his group again reported the qualitative emission of $^1O_2(^1\Delta_g)$ by 2PE in bulk solution through a microscope.[55, 56] In 2006, Belfield et al. reported, for the first time, quantitative determination of singlet oxygen upon 2PE of a PS in solution, using an indirect chemical quenching procedure to calculate the $^1O_2$ quantum yield.[18]

The seminal contributions by some of the early pioneers in the field of singlet oxygen helped to lay the foundation for the rich and diverse chemistry that is available through the use of singlet oxygen. Contributions like Lewis' description of oxygen's paramagnetic behavior and the prediction of a spin-paired electronic state helped Mulliken develop the full electronic structure of oxygen and to predict the two low lying excited states of singlet oxygen. Equally important was Kautsky's work on developing the mechanism of photooxgenation by singlet oxygen. Since this time a vast amount of research has been undertaken to develop the chemistry of singlet oxygen.

2.1.2 Generation of Singlet Oxygen

Over the years there have been numerous methods devised to produce singlet oxygen for investigating its photophysical and chemical properties. Some of the earliest investigations at the beginning of the twentieth century generated $^1O_2$ in a photosensitized process, such as the work by Fritzsche and Moureu where they independently investigated photooxygenation of naphthacene and rubrene respectively.[57, 58] In their investigations they produced singlet oxygen in a photosensitized process by exposing the sensitizer to direct sunlight in the presence of air. In the late 1950's, electric and chemical methods of $^1O_2$ formation were introduced. Foner and

Hudson were the first to produce the lower lying excited state ($^1\Delta_g$) of singlet oxygen by passing a stream of oxygen through an electric discharge, and a few years later Foote and Wexler investigated olefin oxidations with $^1O_2$ using the reaction of sodium hypochlorite and hydrogen peroxide.[1, 59, 60] In 1969, Evans demonstrated $^1O_2$ formation by laser excitation of O_2 under high pressure (2000 psi) and in the presence of an acceptor molecule, 1,3-diphenylisobenzofuran or 9,10-dimethylanthracene.[61] As a result of numerous efforts, there are a variety of different methods to produce singlet oxygen, but the two most common methods of singlet oxygen production are by chemical means and photosensitization.

With the exception of photosensitized production of singlet oxygen, many of the techniques that were just introduced have limited usefulness in the formation of singlet oxygen. Generation of $^1O_2$ by electric discharge has a rather poor yield (10 – 20%) and requires a stream of oxygen. In the past, this method has been used to study the photophysical properties of singlet oxygen. Generating $^1O_2$ with the use of lasers requires high pressures of O_2 and the need for powerful lasers. There are a number of compounds available to generate $^1O_2$ chemically which have been successful for studying the photophysical and synthetic properties of $^1O_2$. As mentioned previously, the reaction of NaOCl and H_2O_2 was used extensively for synthetic and photophysical investigations. The thermal decomposition of triphenylphosphite ozonide at -78 °C was used to yield singlet oxygen.[62] Additionally, some cyclic organic peroxides can be thermally decomposed to produce singlet oxygen. There are a couple drawbacks to generating singlet oxygen chemically. The yield of singlet oxygen is limited by the stoichiometry of the reaction, which can also result in unreacted material or side product.

Singlet oxygen formation by photosensitization of ground state oxygen can be very efficient, and is one of the most commonly used methods to generate $^1O_2$. Currently, there is a

plethora of photosensitizers (PS) that are used in $^1O_2$ formation, and new sensitizers are continuously being introduced. PS are commonly used to produce $^1O_2$ in organic synthesis, water purification and disinfection, in photodynamic therapy, and in photophysical investigations of $^1O_2$. Singlet oxygen is also easily produced naturally in living organisms and plants, and is a problem in the photodegradation of polymers.[63, 64] The remainder of this dissertation will focus on photosensitized formation of singlet oxygen.

2.1.3 Singlet Oxygen Sensitizers

There are several different groups of PS comprising aromatic hydrocarbons, dyes, porphyrins, and transition metal complexes among others. As a group, these compounds provide the ability to produce $^1O_2$ with high efficiency and the ability to be excited at wavelengths in the UV to near IR spectral region. These compounds have numerous applications in materials science, and have found use in nonlinear optics, electrochromic devices, probes, sensors, liquid crystals, and photosensitizers.[65-70] Many hydrocarbons and dyes are utilized for investigative photophysical studies, organic synthesis, and may serve as $^1O_2$ standards. They are characterized by good singlet oxygen QYs, and usually absorb up to ~600 nm. Porphyrins have been utilized as $^1O_2$ sensitizers nearly as long as the hydrocarbon and dye sensitizers. Sometimes referred to as first generation sensitizers, porphyrins are frequently used in PDT, and typically have absorption maxima at longer wavelengths (500-650 nm) than the other hydrocarbon and dye sensitizers. Phthalocyanine and texaphyrin sensitizers are similar in structure to porphyrins but were designed to have longer absorption wavelengths (680-750 nm), possessing a larger central ring that can complex metals more strongly than their related porphyrin derivatives. Some

transition metal complexes have been developed for $^1O_2$ sensitization. Ruthenium (II) complexes, for example, have very good $^1O_2$ QYs, and numerous other metals such as Cr, Pt, and Pd have found use as sensitizers. One drawback is that many of these compounds absorb at relatively short wavelengths (< 400 nm), and there are many more transition metal complexes that are quenchers of $^1O_2$ than sensitizerss.[71-73]

Aromatic hydrocarbons were some of the earliest compounds investigated for $^1O_2$ sensitization. Typically they are comprised of multiple fused ring structures and often form unstable cyclic peroxides upon reaction with singlet oxygen (Figure 4). Some aromatic hydrocarbons are very efficient sensitizers such as naphthalene, anthracene, and biphenyl derivatives. Naphthalene absorbs at short wavelengths and has a low molar absorptivity (275 nm, 6 x 10^3 M^{-1} cm^{-1}), but the singlet oxygen quantum yield (0.62) in benzene is relatively large. There have been a number of studies utilizing biphenyl and naphthalene derivatives to investigate the mechanism of photosensitized $^1O_2$ formation.[74-77] 9,10-Diphenylanthracene has three absorption bands in the longwavelength region of the UV spectrum (360-400 nm), and is reported to have a singlet oxygen quantum yield of 0.75 in chloroform.[50] Reactions of anthracene with singlet oxygen produce a cyclic peroxide. Wasserman investigated the peroxides of 9,10-diphenylanthracene and rubrene as potential sources of singlet oxygen under thermal decomposition for photooxygenation reactions.[78] The anthracene derivative generated molecular oxygen in 96% yield, and was reported to be much more efficient than the rubrene derivative as a photooxygenation reagent.

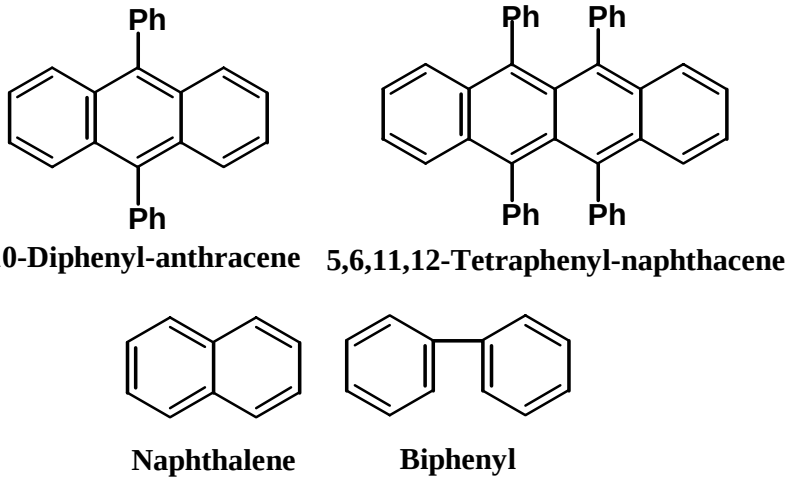

Figure 4. Chemical structures of common aromatic hydrocarbon $^1O_2$ sensitizers.

Dyes represent a large portion of the singlet oxygen sensitizers and have been investigated for many years for a number of applications including organic synthesis, photophysical studies of $^1O_2$, and photodynamic therapy.[79-81] Many dyes absorb in the UV or visible spectrum and often have large singlet oxygen quantum yields. Dye sensitizers are typically highly conjugated aromatic compounds and often contain one or more halogens to increase $^1O_2$ formation by the heavy-atom effect (Figure 5).[82] Eosin and acridine are two early examples of dyes that were used for PDT at the beginning of the twentieth century and are currently used in organic synthesis and as $^1O_2$ standards.[21] Methylene blue and rose bengal are some other examples of commonly utilized dye sensitizers. These compounds are characterized by good water solubility and absorption in the far visible spectrum. Methylene blue has two strong absorption bands at 609 and 668 nm. This dye has a large molar absorptivity (73,000 M^{-1} cm^{-1}) at 668 nm and a singlet oxygen quantum yield of 0.52 in acetonitrile. Rose bengal has been used in polymer bound supports for synthetic purposes, reducing quenching and eliminating the need to remove the sensitizer after it is used.[83] Excitation occurs at 559 nm where rose

bengal has a molar absorptivity of 90,400 M^{-1} cm^{-1} and a $^1O_2$ QY of 0.54 in acetonitrile. Wilkinson and co-workers have published a large compilation of rate constants and singlet oxygen quantum yields for a number of dyes, porphyrins, and drugs.[49, 50] Wilkinson's papers should be consulted for a comprehensive review of sensitizer photophysical data in different solvents.

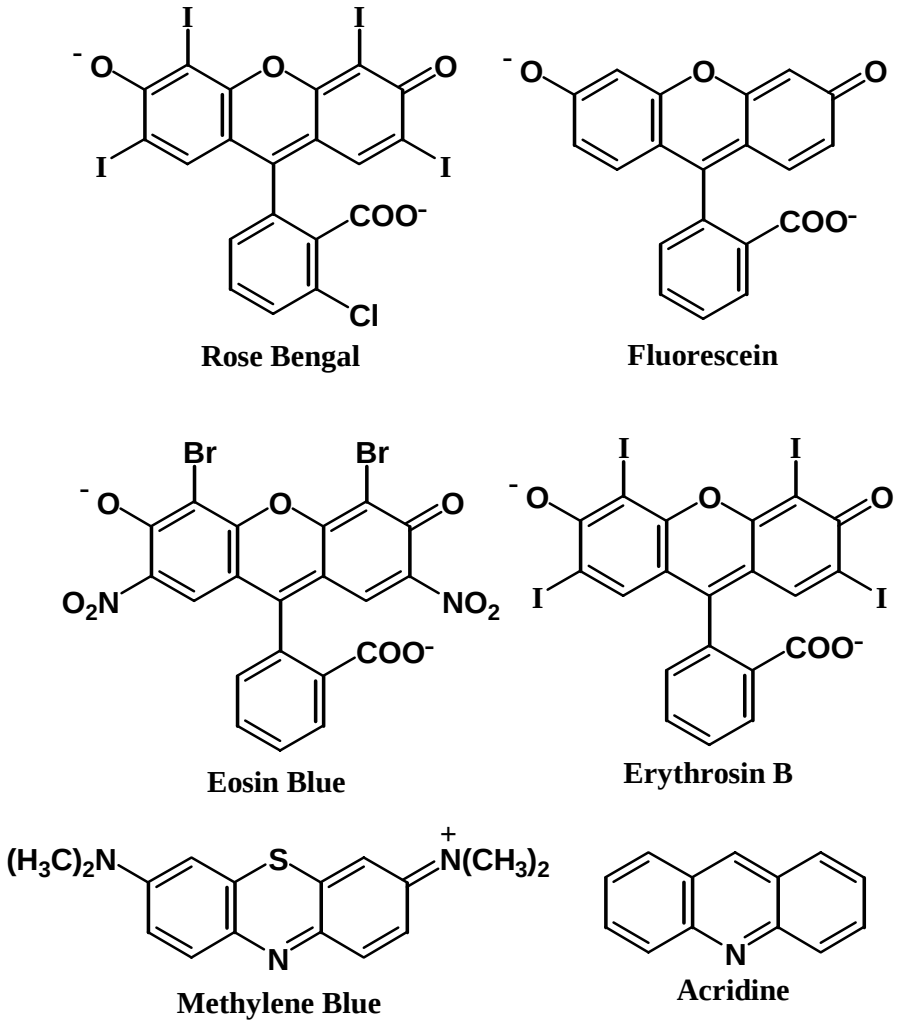

Figure 5. Common singlet oxygen dye sensitizers.

Porphyrins are widely used and have found great success in PDT due to their absorption in the visible, efficient $^1O_2$ QY's, and ability to be taken up readily by tumors. These compounds

will be discussed briefly to complement a more detailed discussion about porphyrin sensitizers for PDT in section 2.2. Porphyrins are highly conjugated macrocyclic rings consisting of four pyrrole-like subunits connected by a methine carbon α to each subunit. The simplest unsubstituted porphyrin ring is known as porphine (Figure 6). Porphyrins are commonly found in nature and can readily be found in plants and red blood cells. Additionally, porphyrin derivatives typically exhibit low cytotoxicity in the absence of light, making them very attractive for therapeutic use. Many different metals with a +2 or +3 charge can bind to the central ring porphyrin structure to modulate the photophysical properties of the sensitizer.

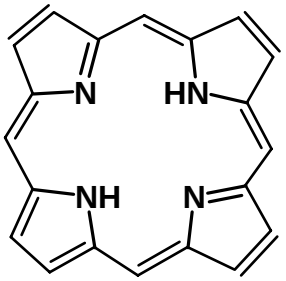

Figure 6. Chemical structure of porphine.

Porphyrins are utilized for a number of applications such as commercial dyes, nonlinear optics, and solar energy production.[84] Consequently, there have been a number of investigations to modulate the photophysical properties of porphyrins.[85-89] Rogers and co-workers investigated the photophysical properties for a series of meso-tetraphenyl, tetrabenzo, and tetranaphtho annulated metalloporphyrins (Figure 7).[90] They were able to increase the intensity and shift the main absorption band by as much as 150 nm by extending the conjugation of the central porphyrin ring. Additionally, the choice of the metal ion had an effect on shifting the absorption maxima, but heavy atom effects were more dominant and resulted in a significant increase in the

phosphorescence QY and rate constant. Other common modifications are performed to effect solubility, includeing alkylation, sulfonation, or carboxylation of the porphyrin.[91]

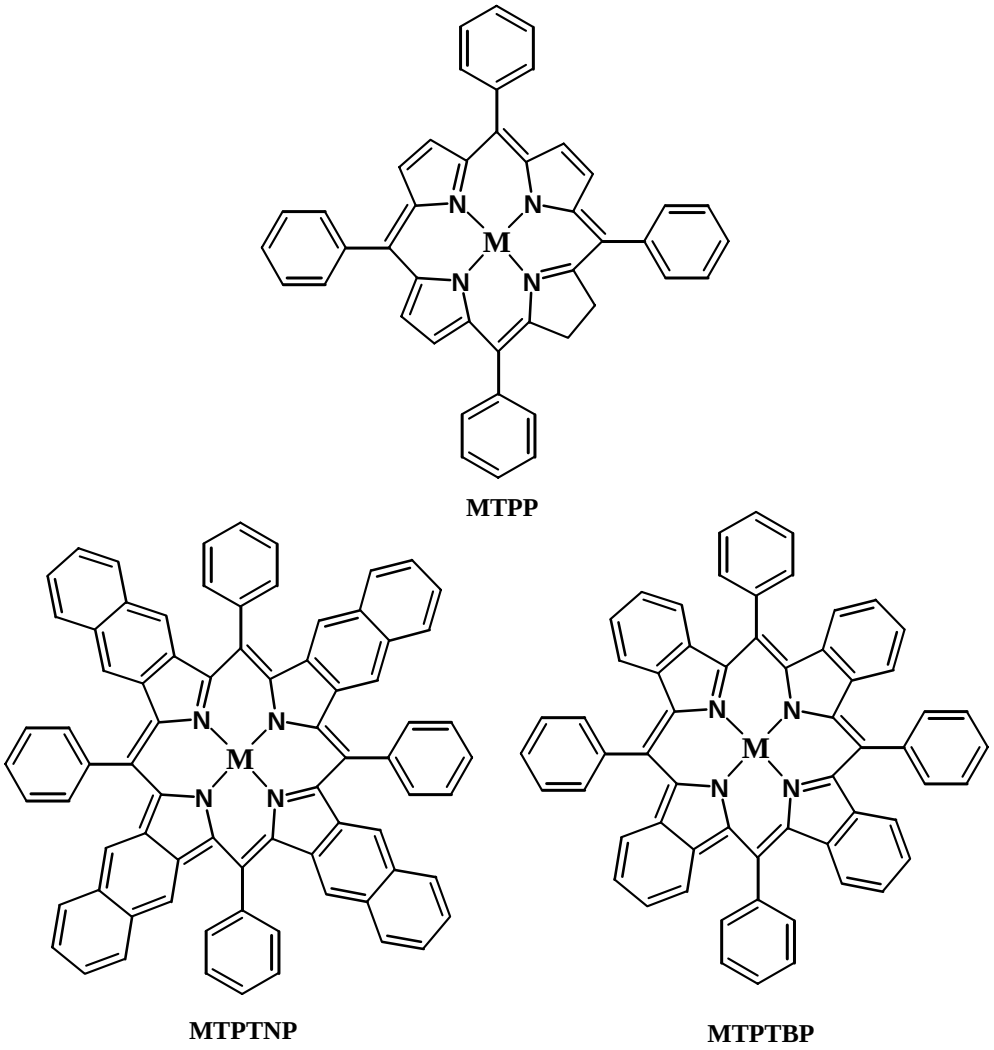

Figure 7. Structures of porphyrin derivatives investigated by Rogers and co-workers. M = Zn or Pd, MTPP (*meso*-tetraphenylporphyrin), MTPTNP (*meso*-tetraphenyltetranaphthoporphyrin), MTPTBP (*meso*-tetraphenyltetrabenzoporphyrin).

Another group closely related to porphyrins consists of phthalocyanines and metalophthalocyanines. The macrocyclic ring of the phthalocyanine consists of four pyrrole-like

subunits connected by a tertiary nitrogen α to each subunit rather than a methine carbon atom. These compounds can coordinate a number of different diamagnetic and paramagnetic metals such as Al^{+3}, Zn^{+2}, Cu^{+2}, and Co^{+2} (Figure 8). Complexes of diamagnetic ions such as Al^{+3} and Zn^{+2} demonstrate better photophysical properties than paramagnetic ions like Cu^{+2} and Co^{+2}. Zinc phthalocyanine tetrasulfonate, for example, has a triplet lifetime of 245 μs and a $^1O_2$ QY of 0.45.[92] Whereas copper phthalocyanine tetrasulfonate has a triplet lifetime of 0.06 μs and a $^1O_2$ QY of 0. For the diamagnetic ions, heavy atom effects contribute to the deactivation of the excited singlet state and enhance the rate constant for triplet state formation, but the paramagnetic ions are less affected by heavy atoms, and deactivation of the singlet state appears to be through nonradiative internal conversion.[71, 93] As with the porphyrins, the photophysical properties and solubility of the phthalocyanines can be tailored by extending the conjugation and inclusion of axial ligands. Soncin and co-workers synthesized Si-naphthalocyanine derivatives that were particularly affective for PDT.[94] The absorption of these compounds were at longer wavelengths (780-800 nm), and cellular uptake by melanoma tissue was increased by the addition of long aliphatic axial groups on the ligand.

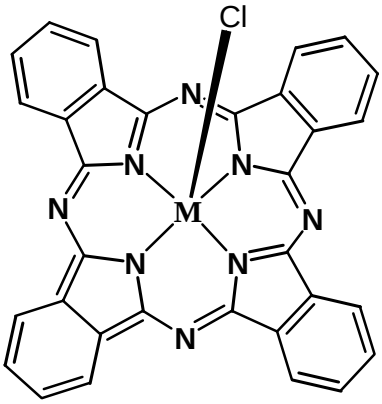

Figure 8. Chemical structure of metallophthalocyanine.

Texaphyrins are similar in structure to the porphyrins, however, they contain an extra nitrogen atom that is able to coordinate with metals with a much greater kinetic stability over the porphyrin derivatives, and they act as monoanionic rather than dianionic ligands (Figure 9). The central ring is 20% larger and can accommodate larger cations. Additionally, the texaphyrins are more conjugated (22 π electrons) than the porphyrins with 18 π electrons, and the greater aromatic delocalization results in longer absorption and emission bands. Guldi and co-workers investigated a series of lanthanide coordinated texaphyrins.[93] It was observed that the intrinsic decay rates were significantly affected by the choice of the metal, and the energies of the singlet or triplet states did not change significantly. Heavy atom effects dominated for diamagnetic ions and resulted in shorter fluorescent lifetimes. The paramagnetic ions produced fluorescent lifetimes that were about an order of magnitude less than the diamagnetic species and was accompanied by smaller intersystem rate constants and triplet lifetimes.

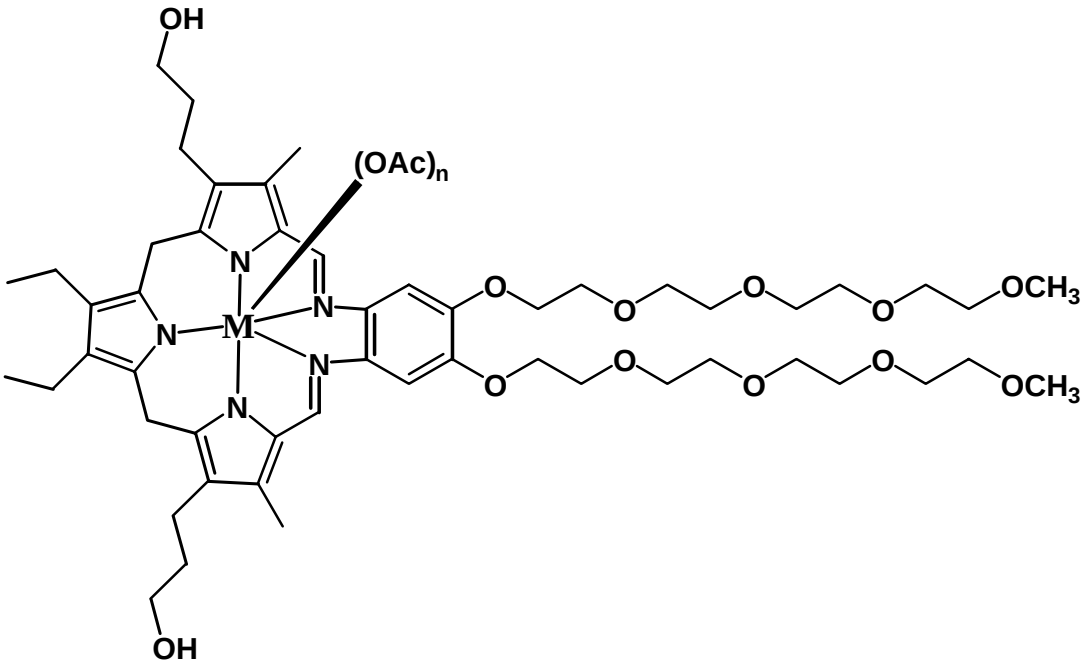

Figure 9. Typical chemical structure of a metallotexaphyrin.

Transition metal coordination complexes represent a very small minority of $^1O_2$ sensitizers and typically absorb in the UV-visible region. Ruthenium (II) bipyridyl complexes are the most common $^1O_2$ sensitizers with impressive $^1O_2$ QY's near unity. These complexes are characterized by long triplet state lifetimes that allow for efficient quenching by oxygen of the triplet metal to ligand charge transfer state. Demas *et al.* were the first to report $^1O_2$ production from quenching of triplet state bipyridyl ruthenium (II) osmium (II), and iridium (III) complexes with $^1O_2$ QY's of (0.68-0.85) in methanol.[95] Abdel-Shafi and co-workers investigated the photophysical properties of a series of vinyl linked benzo-crown ether bipyridyl ruthenium (II) complexes in acetonitrile.[71] The conjugation of the complex was extended by the use of benzo-crown ether ligands, affording complexes with absorption maxima in the range of 460-485 nm. However, the shorter wavelength absorbing bipyridyl complex had a much better $^1O_2$ QY of 0.57 compared to 0.19 for the crown ether complex. Bis-cyclometalated iridium (III) complexes were investigated by Gao and co-workers.[96] Iridium complexes have been reported to quench singlet oxygen, but Gao reported high QY's of 0.6-1.0 for a series of naphtha-benzothiazole derivatives.[97]

The use of singlet oxygen sensitizers for photodynamic therapy has spawned a new class of sensitizers that are capable of producing $^1O_2$ by two-photon excitation. The benefit of using longer wavelengths in combination with 2PE was described in Chapter 1. Around the time of Ogilby's first report on using compounds with relatively high 2PA as $^1O_2$ PS, there have been a number of investigations that have looked at the possibility of exciting known sensitizers by 2PA or modifying them to be more efficient at forming $^1O_2$ under these conditions.[53] Porphyrins are one of the most utilized sensitizers for PDT due to their efficiency of $^1O_2$ production and ability to be taken up by tumors. However, early investigations indicated that the 2PA cross sections (δ)

of these compounds were insufficient to be utilized as 2PA sensitizers. Goyan and Cramb measured a maximum δ value of 2 GM at 790 nm for protoporphyrin IX in methanol.[98] In fact, many of the $^1O_2$ sensitizers that are commercially available for PDT at this time have δ values << 10 GM, rendering them virtually useless as two-photon $^1O_2$ sensitizers for PDT.

Modified porphyrin derivatives make up a large portion of 2PA $^1O_2$ sensitizers. Many of the derivatives were designed to have extended conjugation and included 2PA active motifs in an attempt to shift the main absorption band to longer wavelengths and to increase the 2PA cross section. Karotki and co-workers were able to increase δ based on work by Albota, Cumptson, and Spangler.[99-102] In Karotki's investigation, the conjugation of the porphyrin ring was increased using diphenylaminostilbene and dichlorophenyl substituents (Figure 10, I-III). They reported a δ of 80 GM at 780 nm and the detection of $^1O_2$ under 2PA for their stilbene derivative but did not report any quantitative $^1O_2$ QY's. Drobizhev, Karotki, *et al.* extended this work for a series of tetrapyrrol derivatives, where they reported high δ values for two symmetrical tetraazaporhphines of 380 GM and 900 GM at 800 nm for octakis(4-bromophenyl)-tetraazaporphyrazine and octakis(4-nitrophenyl)-tetraazaporphyrazine respectively (Figure 10, IV).[103-105] Recently, Ishi-i and co-workers investigated tetra substituted porphyrin derivatives containing diphenylamino benzothiadiazole units to increase the δ (Figure 11).[106] The charge transfer character of the porphyrin derivative was increased due to the electron donating diphenylamino and electron withdrawing effect of the benzothiadiazole unit, and increased conjugation lead to larger values of δ without affecting the $^1O_2$ QY. A slight increase of nearly 30 GM was observed for the Zn chelated porphyrin derivative of R^2 over the unchelated ring.

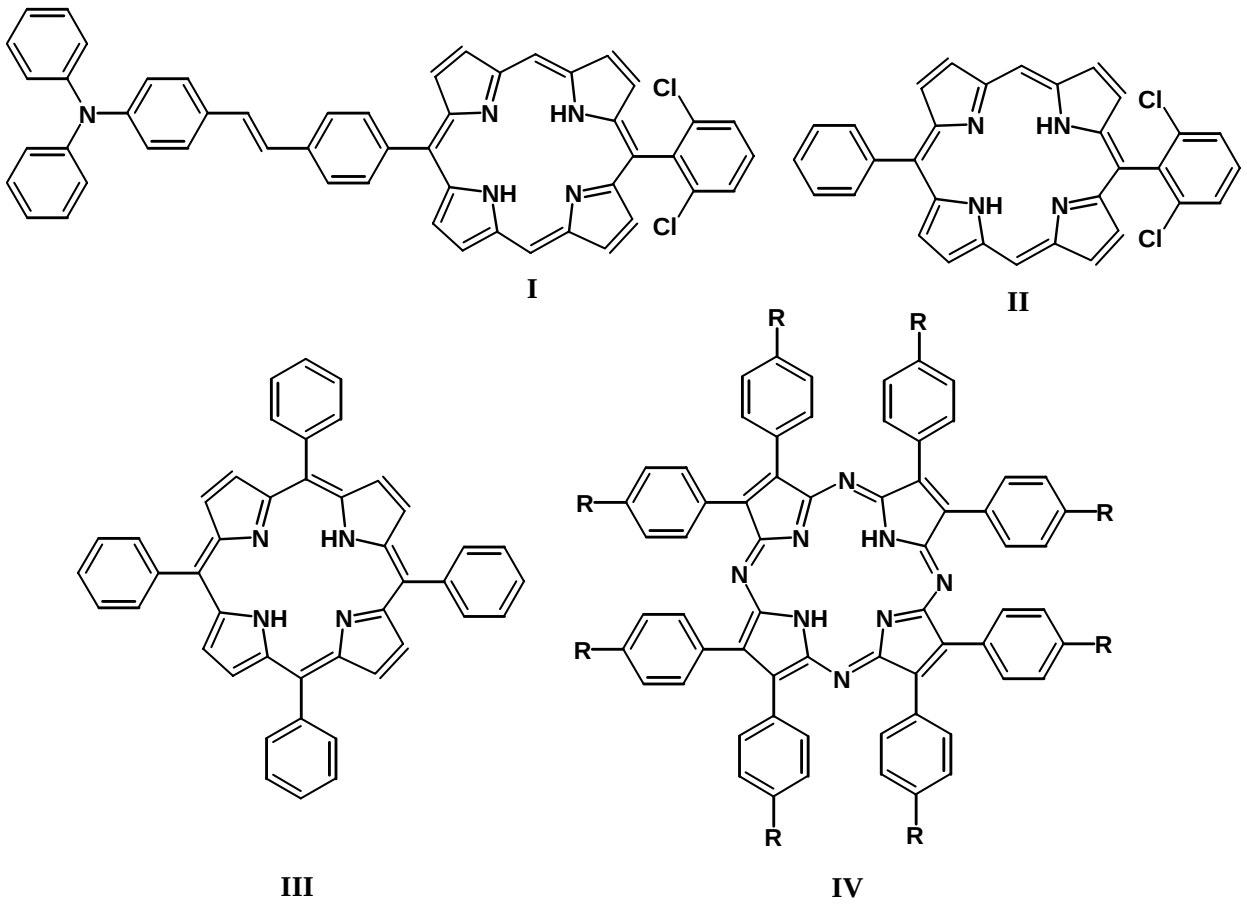

Figure 10. Porphyrin derivatives investigated by Karotki *et al.* with improved δ. (I) 5-(4-diphenylaminostilbene), 15-(2,6-dichlorophenyl)-21H, 23H-porphine (80GM), (II) 5-phenyl, 15-(2,6-dichlorophenyl)-21H, 23H-porphine (11 GM), (III) 5,10,15,20-tetraphenyl-21H, 23H-porphine (25 GM), (IV) Octakis(4-R phenyl)-tetraazoporphine where R = NO_2 (900 GM) or R= Br (380 GM).

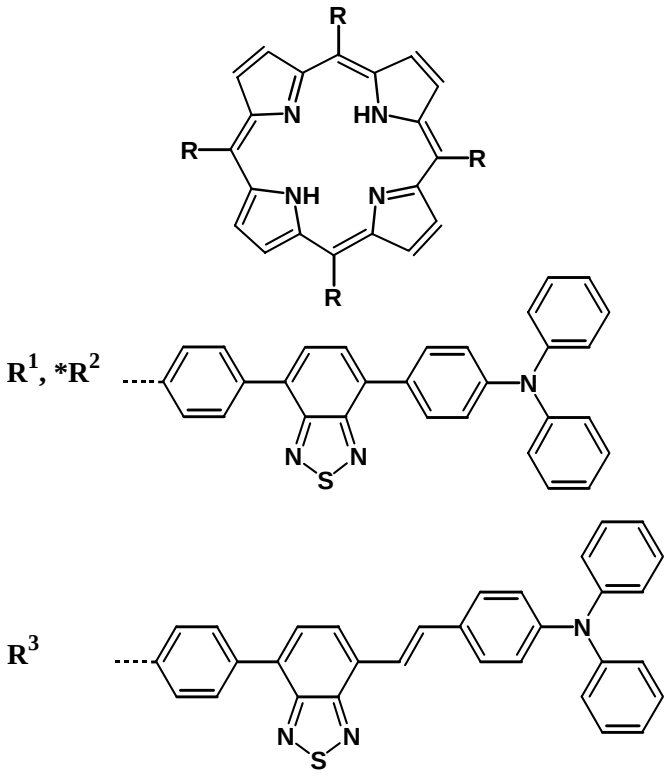

Figure 11. 2PA porphyrin $^1O_2$ sensitizers investigated by Ishi-i with reported δ and $^1O_2$ QY. The porphyrin ring of R^1 and R^3 is in the free-base form, $*R^2$ the porphyrin is chelated with Zn. R^1: 441 GM, QY_Δ 0.68, $*R^2$: 469 GM, QY_Δ 0.62, R^3: 735 GM, QY_Δ 0.65. δ was measured at 800 nm in chloroform and $^1O_2$ QY was measured under 1PE.

Fréchet's group took a slightly different approach to modifying porphyrin derivatives by using fluorescence resonance energy transfer (FRET) from a chromophore that can undergo 2PA and indirectly excite the porphyrin by energy transfer. Once energy transfer to the porphyrin core occurred, intersystem crossing from the singlet to the triplet state can result in the formation of $^1O_2$. Efficient FRET is accomplished by carefully selecting 2PA chromophores that have emission spectra that overlap with the absorption spectra of the porphyrin. In Fréchet's work, they attached fluorene derivatives of diphenylamino benzothiazole as the 2PA chromophore

(Figure 12).[107-110] These compounds have bee reported to have very large δ, reaching upwards around 8000 GM.[111] Using an excitation wavelength of 780 nm, Fréchet's group was able to detect $^1O_2$ emission at 1270 nm due to 2PE of the porphyrin derivative by FRET. In another investigation the same group used FRET with a porphyrin core surrounded by dendrimers composed of one or more types of chromophores.[108] Efficient energy transfer to a porphyrin derivative was accomplished using a dendrimer composed of naphthopyranone and coumarin dyes. The use of multichromophore dendrimers expands the usable excitation range of the sensitizer making them more useful.

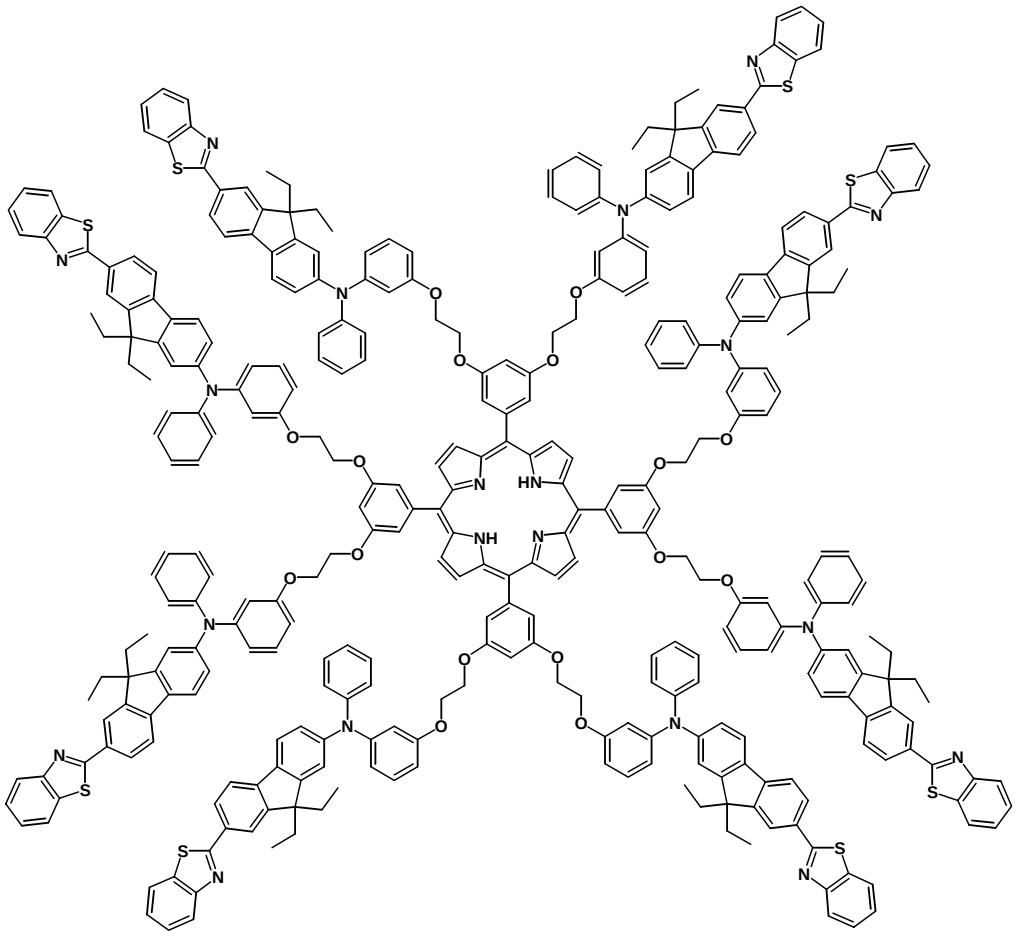

Figure 12. 2PA-FRET based $^1O_2$ sensitizer investigated by Fréchet *et al.*

Up to this point, the investigations that have been presented on new 2PA $^1O_2$ sensitizers have been very limited in their scope, and a number of key issues have not been addressed such as the difficulty of sensitizer synthesis, solubility, or the lack of thorough chemical and photophysical characterization. Ogilby and co-workers have made some strides integrating the field of 2PA compounds and photosensitized singlet oxygen. They have made good progress in theoretical modeling of structure property relationships for predicting δ.[112-114] Additionally, a number of comprehensive investigations into the synthesis of hydrophobic and hydrophilic 2PA $^1O_2$ sensitizers have been reported where solubility, chemical stability, and maximization of δ and $^1O_2$ QY have been addressed.[53, 113, 115-118] The ability to synthesize a 2PA $^1O_2$ sensitizer with good chemical and photophysical properties is challenging.

One apparent trend that has emerged from the work of Ogilby is that the features of a compound which give it good two-photon absorption characteristics often are counter productive to qualities of a good singlet oxygen sensitizer, and often a balance between the two needs to be obtained. Larger 2PA cross sections can be obtained by increasing the polarizability of the chromophore. This can be accomplished by extending the conjugation and/or utilizing functional groups that can impart greater charge transfer character into the chromophore. There are a number of different methods to promote $^1O_2$ formation, but increasing the charge transfer character results in lower efficiency of singlet oxygen formation. Consequently, it is quite challenging to develop a 2PA singlet oxygen sensitizer that can meet or exceed all requirements of an efficient sensitizer.

Ogilby's investigation into a series of toluene soluble difuranonaphthalenes and styrylbenzenes resulted in the identification of key functional groups that can lead to improved 2PA cross sections, and computational tools were presented that can be used to predict potential

two-photon singlet oxygen sensitizers. Their computational method produced δ values that were substantially smaller than experimental values, however, for relative comparison their computational methods proved useful. Increased 2PA cross sections were obtained when the central chromophore was extended through the use of styrylbenzene moieties (Figure 13), giving δ at 618 nm that were nearly four times greater (205 GM vs. 780 GM) than the parent difuranonaphthalene derivative.[113] In addition to extending the conjugation, larger 2PA values were accomplished by increasing the polarizability of the chromophore using electron donating or withdrawing groups in the meta or para position of the conjugated system. For example, cyano, aldehyde, or a carboxylic acid were utilized as electron withdrawing groups, whereas diphenylamino and methoxy groups were used as electron donating substituents. Larger $^1O_2$ QY and δ were obtained for the aldehyde difuranonaphthalene derivative (R = CHO, 0.49, 205 GM) in comparison to no electron withdrawing group (R = H, 0.36, 8 GM). The 2PA cross section increased to 780 GM at 618 nm when the conjugation of the aldehyde containing difuranonaphthalene was extended with two styrylbenzene units (R = CHO), but the $^1O_2$ QY dropped dramatically (0.13), emphasizing the difficulty in maintaining both $^1O_2$ and δ parameters. Unfortunately, it is well known that increasing the charge transfer character of the sensitizer reduces the efficiency of $^1O_2$ formation. A detailed discussion of this phenomenon will be discussed later in the mechanism of singlet oxygen formation.

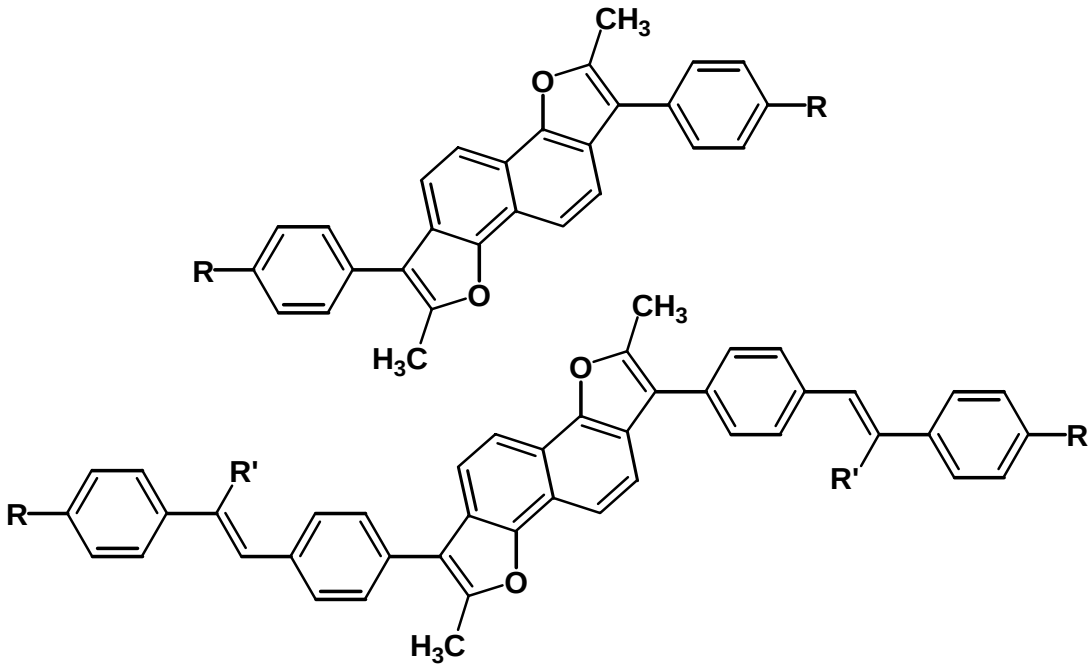

Figure 13. Difuranonaphthalene 2PA $^1O_2$ sensitizers investigated by Ogilby *et al.* R = H, CN, CHO, Br, COOH, OCH_3: R' = H, or CN.

One problem of having vinyl groups present, such as styrylbenzene, is that they are susceptible to photooxidation by singlet oxygen. It was also demonstrated that attachment of a vinyl-substituted cyano group to the styryl bridge can impart improved photochemical stability without affecting the 2PA properties of the sensitizer. Another method that has been proposed is to replace the vinyl group with an alkyne. The photostability of the alkyne group was demonstrated in a study of 2PA phenylene-ethynylene-based chromophores, where oxidation was nearly eliminated by substituting a styryl alkene with an alkyne without significantly affecting the photophysical properties.[117]

Water solubility is necessary for a sensitizer if it is to be used as a PDT agent. Many of the sensitizers that have been investigated and optimized for PDT have been characterized in organic solvents. Most often these compounds have poor water solubility and/or they have small

$^1O_2$ QYs. In fact, the solvent has a significant impact on photosensitized singlet oxygen formation, and, in general, the $^1O_2$ QY in polar solvents like water is about half of what it would be in a nonpolar solvent like toluene. As a result, one needs to question the validity of a sensitizer that has a $^1O_2$ QY < 0.3 in nonpolar solvents if it is to be a potential PDT agent.

In two other investigations by Ogilby's group they looked at increasing the solubility for a series of porphyrins, porphyrazines, difuranonaphthalenes, and phenylene-vinylene 2PA $^1O_2$ sensitizers. In their studies they were particularly interested in photophysical changes that might occur due to modifying the sensitizer for increased water solubility. Charge transfer is enhanced in polar solvents, and as a result, additional deactivation pathways exist that can compete with energy transfer from the excited state of the sensitizer to triplet oxygen, leading to lower $^1O_2$ formation. Many of their compounds had very small $^1O_2$ QYs in water, but a number of important conclusions were made providing valuable insight into the synthesis of efficient 2PA water soluble $^1O_2$ sensitizers.

Several different functional groups were investigated to increase the solubility of a series of porphyrins, vinyl benzenes, and phenylene-vinylene 2PA $^1O_2$ sensitizers. Ionic and nonionic substituents were attached in two different configurations where the substituent was directly attached to the chromophore π system, and in the other configuration the substituent was not an integral part of the chromophore. Aryl sulfonic acid derivatives and salts of methylated benzothiazole, piperazine, and pyridine were utilized as ionic functional groups. Nonionic solvation was accomplished by appending one or more triethyleneglycol units to the sensitizer. When the ionic group was an integral part of the π conjugation $^1O_2$ was formed in very low yield due to rapid charge transfer mediated deactivation of these sensitizers. This was most readily observed in the styrylbenzenes and phenylene-vinylene derivatives where the ionic group was an

integral part of the π conjugation. For example, a very low singlet oxygen quantum yield (0.03) was obtained for the ionic *N*-methylpyridinium phenylene-vinylene derivative (Figure 14 I), and similar results were obtained for other ionic derivatives where the π conjugation was perturbed.[55] Contrary to this observation, when either the ionic or nonionic substituent was attached in a way that it no longer interacted with the π conjugation, larger $^1O_2$ QYs were observed. For an *N*-methylpyridinium porphyrin derivative a rather large 2PA cross section and $^1O_2$ quantum yield (1890 GM, 0.77) were observed when the ionic substituent was placed on the phenyl ring in the meso position of the porphyrin (Figure 14 III). The values were relatively large and comparable to other porphyrin derivatives. It was assumed that the ionic group did not interact strongly with the conjugated system and only provided enhanced solubility. The reduced $^1O_2$ QYs are the result of the ionic substituents imparting an electron withdrawing effect to the chromophore system. The water solubility of the sensitizer could be increased by the addition of nonionic ethyleneoxy groups. A slight increase in the δ and $^1O_2$ QY were observed when the substituent was attached directly to the π conjugation and appeared strongest when placed in the ortho or para position. The tetra substituted ethyleneoxy derivative of phenylene-vinylene (Figure 14 II) had good water solubility and a reported $^1O_2$ QY of 0.20 in water.[118]

The findings by Ogilby's group indicate charged ionic species will have an adverse effect on singlet oxygen production if the group is an integral part of the conjugation. On the other hand, hydrophilic electron donating groups like an alkoxy chain can enhance $^1O_2$ formation while imparting solubility to the sensitizer. The charge transfer character of the sensitizer is not significantly altered when the solvating group is separated from the chromophore system. This was most readily seen when comparing the phenylene-vinylene and vinylbenzene derivatives to the porphyrins. As a result of these studies, several different synthetic strategies have been

investigated, highlighting important features that can be utilized to impart water solubility and maintain or enhance singlet oxygen formation.

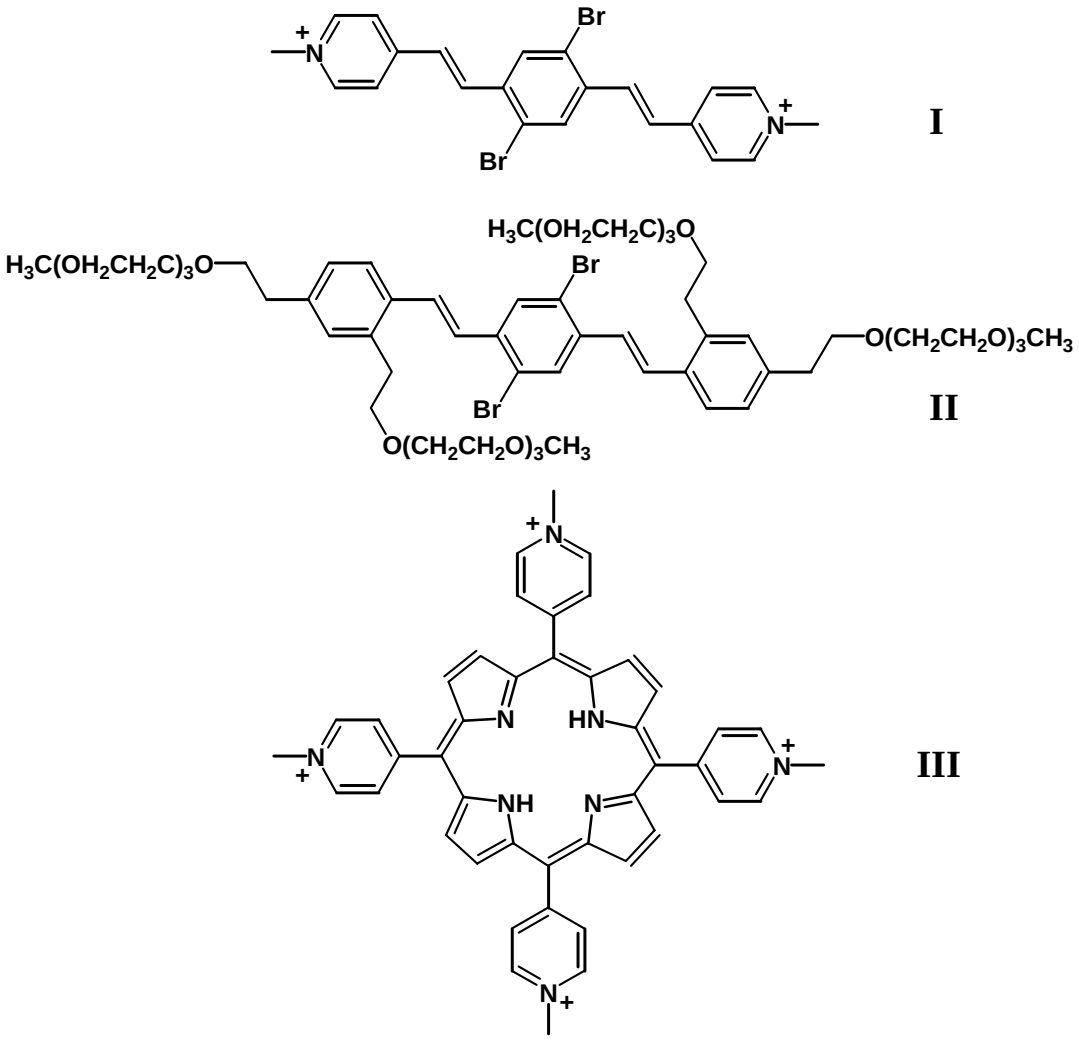

Figure 14. Water soluble $^1O_2$ sensitizers investigated by Ogilby *et al.*

2.1.4 Chemistry of Singlet Oxygen

Although singlet oxygen can be generated by various methods such as chemical and electrical means, its use in synthetic organic chemistry is typically formed in a photosensitized process using a sensitizer in low to near catalytic amounts. Many different sensitizers have been used effectively. The choice of the sensitizer is dictated by the reaction conditions such as solubility, efficiency of $^1O_2$ formation, wavelength of excitation, as well as other conditions.

Photosensitized oxidations involving a sensitizer and oxygen can occur by two competing processes known as Type I and Type II reactions.[119] Both processes involve the photo excitation of a sensitizer (sens*) into the singlet or triplet state, but reactions involving the triplet state are more common. In Type I reactions, transfer of a hydrogen atom or electron between sens* and a substrate or solvent can result in radicals and radical ions. Most commonly, the sensitizer is the reduced species. Once formed, the sensitizer then reacts with molecular oxygen to regenerate the sensitizer, while substrate radicals can initiate free radical chain reactions. In Type II reactions singlet oxygen is formed in an energy transfer process between sens* and ground state triplet oxygen. The overall reaction produces singlet oxygen and ground state (S_0) sensitizer. The sens* can also be oxidized by triplet state oxygen in an electron transfer process to form the superoxide ion O_2^-. Even though the formation of the superoxide ion is an electron transfer process, it is considered by some to be a Type II reaction because the sensitizer is reacting directly with oxygen.[119]

It has been demonstrated that the higher excited state $^1\Sigma_g^+$ of singlet oxygen has a very short lifetime and quickly decays to the lower $^1\Delta_g$ excited singlet state. Consequently, all photochemistry originates from the lower excited singlet state of oxygen. The ene and [4 + 2]

cycloaddition reactions were some of the earliest reactions identified. More recently, [2 + 2] cycloaddition and oxidation of heteroatoms like sulfur, selenium, phosphorus, and nitrogen-containing compounds were identified. Heterocyclic photooxygenations of furans, pyrroles, thiophenes, and imidazoles, among others, are also well represented in the chemistry of singlet oxygen. Some of the photooxygenation reactions lead to mixtures of products or have low yields of product formation. Thus, the discussion on the chemistry of singlet oxygen will focus on some of the more useful synthetic reactions and those that posses significant biological applications such as those that are relevant to photodynamic therapy.

The majority of synthetic organic chemistry using singlet oxygen involves Type II reactions. The ene, [2 + 2], and [4 + 2] reactions (Figure 15) are useful routs for the addition of molecular oxygen to organic substrates. Allylic hydroperoxides can be generated with the ene reaction. The [2 + 2] cycloaddition reaction occurs readily with electron rich alkenes, and in the absence of allylic hydrogens, resulting in the formation of isolable dioxetanes that are thermally unstable and can decompose into carbonyl compounds. The products of the ene and [2 + 2] reactions can be reduced to obtain the alcohol or diol, respectively. The [4 + 2] cycloaddition forms an endoperoxide which can also serve as a valuable intermediate for other oxygenated products.

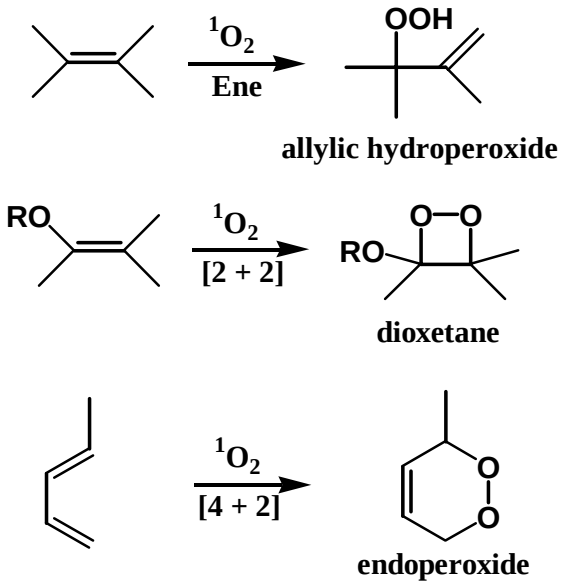

Figure 15. Ene, [2 + 2], and [4 + 2] photooxidation reactions with singlet oxygen.

Singlet oxygen will react with heteroatoms often resulting in physical and chemical quenching. Chemical quenching of singlet oxygen will lead to covalent adducts resulting in the transfer of one or two oxygen atoms to the heteroatom substrate. Organosulfur compounds containing an α–hydrogen will undergo photooxidation with singlet oxygen to form sulfoxides and sulfones. The reaction proceeds through a hydroperoxy sulfonium ylide intermediate (Figure 16).

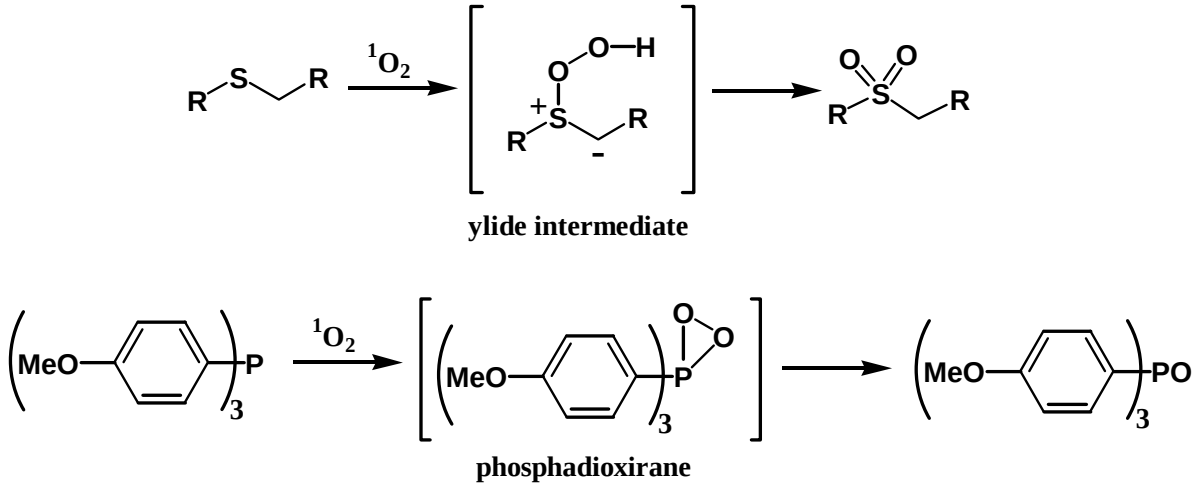

Figure 16. Sulfide photooxidation showing ylide intermediate (top), and oxidation of an organophosphorus compound by singlet oxygen (bottom).

Amines have also been proven to be very useful substrates in cycloaddition reactions. Cheng and Shi have reported a method to synthesize substituted pyrrolidine derivatives (Figure 17). In the reaction, singlet oxygen can be sensitized using C60. The nitrogen is then oxidized by singlet oxygen, followed by abstraction of two α-protons, resulting in the loss of hydrogen peroxide and the formation of an azomethine ylide. The final step involves the cycloaddition of the ylide to the maleimide.

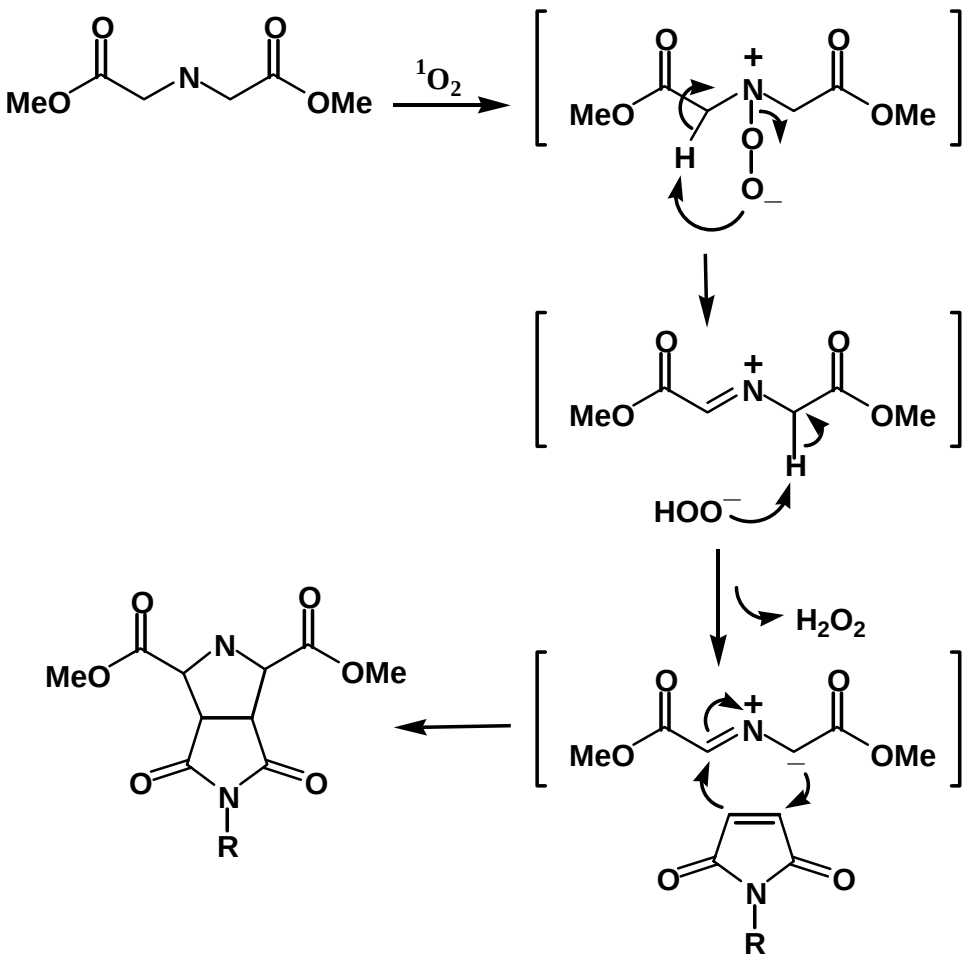

Figure 17. General mechanism for the cycloaddition of a maleimide with an amine to form the pyrrolidine derivative.

Five membered rings comprise a large group of heterocyclic photooxygenation reactions with singlet oxygen and are important in biological and heterocyclic chemistry. The following examples are only a small sampling of some of the more relevant reactions of this class involving furans, pyrroles, and imidazoles. Furans are important due to their widespread occurrence in biological and pharmaceutical applications. Singlet oxygen will react with these substrates to form reactive 2,5-endoperoxide intermediates. The peroxide is formed through a [4 + 2] cycloaddition of singlet oxygen via the 2,5-position of the furan (Figure 18). The endoperoxide

can be reduced *in situ* by cleavage of the peroxide and elimination of oxygen. Solvolysis of the endoperoxide can generate a cyclic lactone containing an ether group. Another useful reaction is the decomposition of the endoperoxide intermediate to form an epoxide.

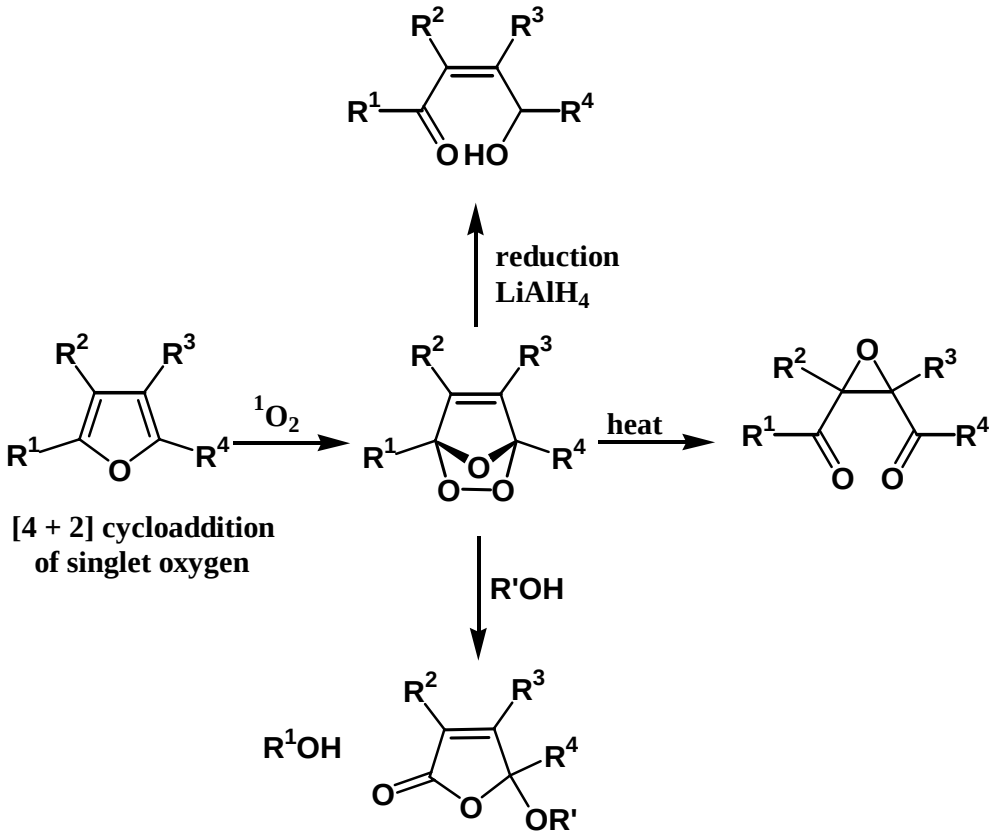

Figure 18. Reaction of a furan derivative with $^1O_2$ to for the endoperoxide intermediate through a [4 + 2] cycloaddition followed by reduction, solvolysis, or thermal decomposition of the intermediate peroxide.

Reactions of singlet oxygen with pyrroles are of particular interest in phototheraputics and serve as model compounds for important biological substrates such as tryptophan. The pyrroles undergo [4 + 2] cycloaddition with singlet oxygen to form endoperoxide, dioxetane, and

hydroperoxide intermediates (Figure 19). Although similar to the chemistry of furans, pyrroles typically do not undergo ring opening at the N(1)-C(2) or N(1)-C(5) bond positions. The reactions of pyrroles are very sensitive to the structure of the substrate, solvent, and temperature of the reaction, and often lead to a mixture of different products. Maleimides can be produced by homolytic bond cleavage of the endoperoxide, whereas the dioxetane can undergo bond cleavage at the C(2)-C(3) position or form the endoperoxide through rearrangement.

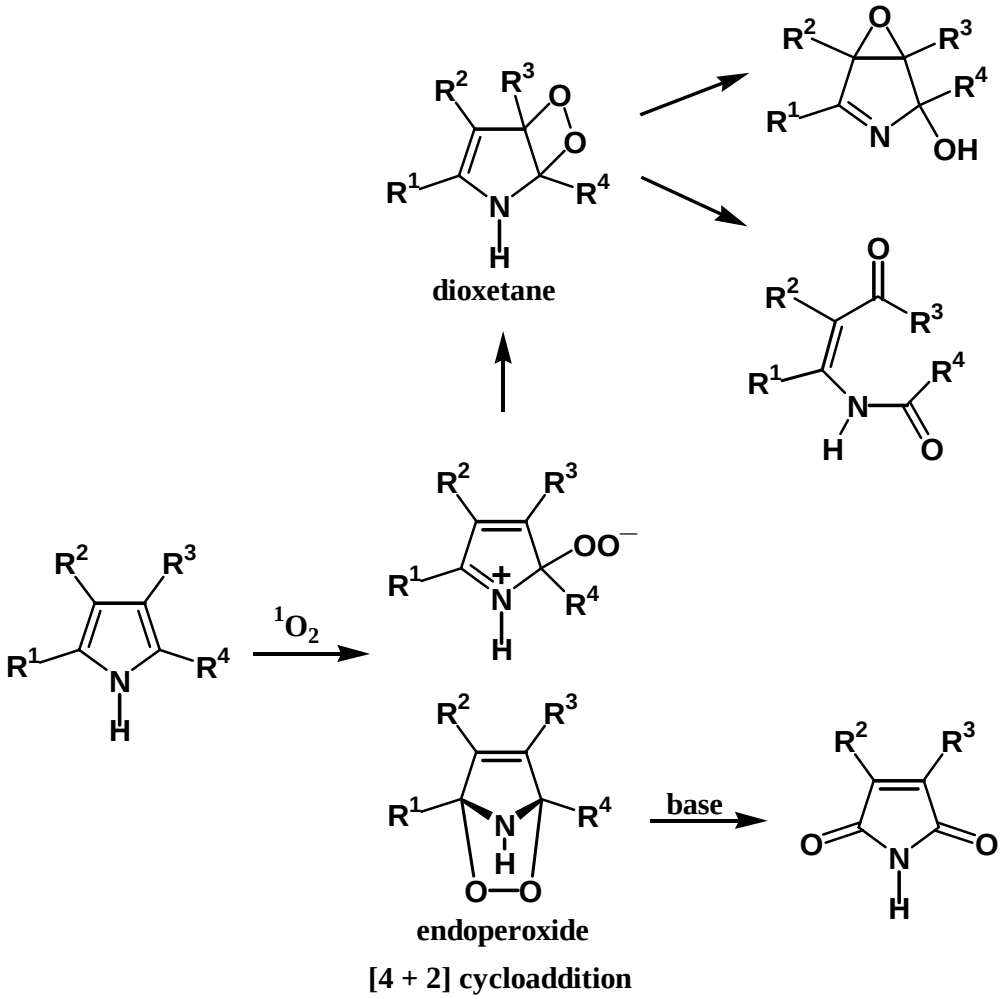

Figure 19. Reaction of pyrrole derivative with $^1O_2$ by a [4 + 2] cycloaddition to form the endoperoxide or dioxetane intermediate and their corresponding products.

Imidazoles are limited in their scope of synthetic use, but the understanding of their mechanistic behavior is of great interest in photodynamic therapy since the imidazole ring plays a key role in reactions of singlet oxygen with nucleic acids and proteins. Reaction of imidazoles with singlet oxygen leads to the formation of endoperoxide intermediates (Figure 20). Substitution around the ring plays a key role in effecting the final outcome of the reaction product. The hydroperoxide is formed when R^1 contains a hydrogen atom. Additionally, if R^2 or R^5 is a hydrogen atom water is eliminated, resulting in the corresponding amide or urea. George and Bhat demonstrated the synthesis of methoxy imidazolones by addition of methanol to the endoperoxide using methylene blue as a singlet oxygen sensitizer. Formation of the dioxetane from hydroperoxide **A** can result in the formation of diacylamidines. Guanine is particularly important in biological applications because the residue may be decomposed in the presence of singlet oxygen during photodynamic therapy. Low temperature NMR investigations have shown the imidazole ring undergoes a [4 + 2] cycloaddition of singlet oxygen to form the endoperoxide. Additional studies using N-benzoylhistidine have been used to explain crosslinking of the imidazole ring in proteins during photodynamic therapy. The studies demonstrated the formation of dimeric products from the photooxygenation of the histidine residue.

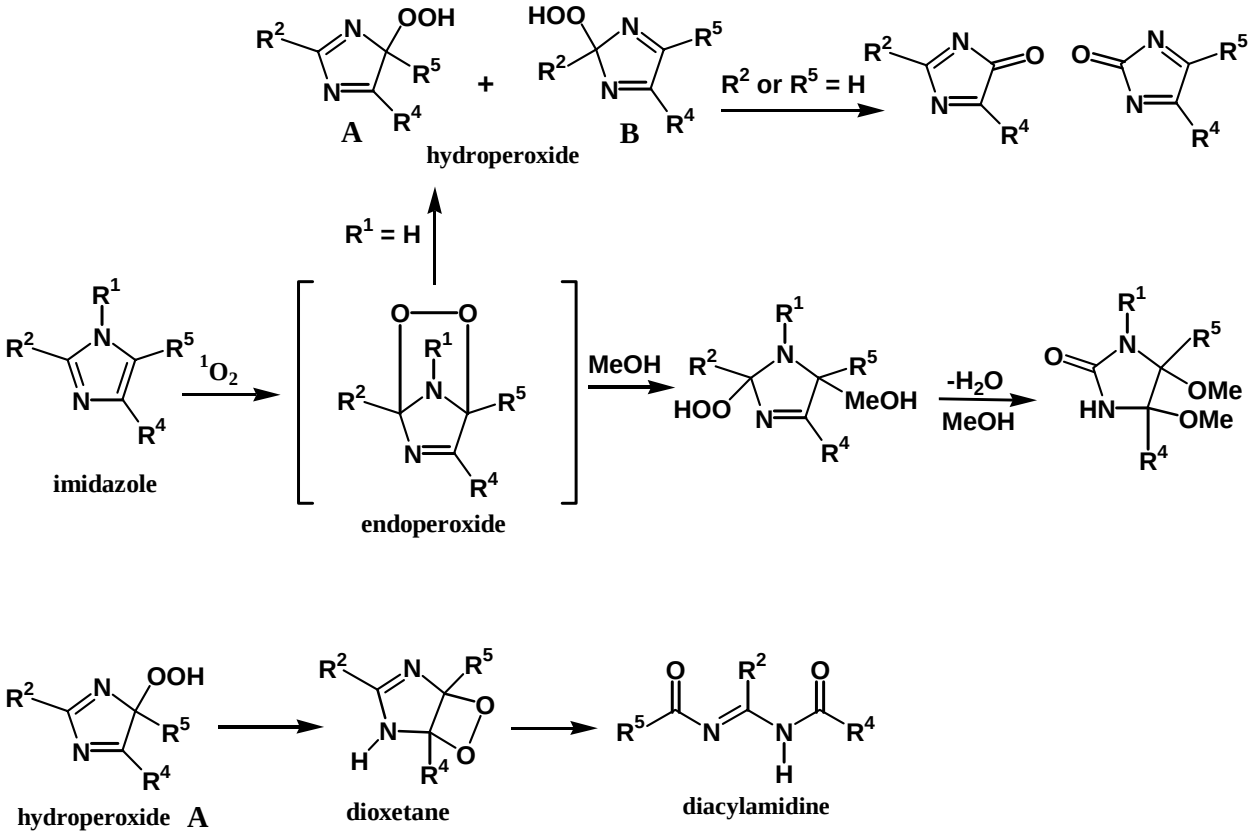

Figure 20. Reaction of imidazole with singlet oxygen leading to the formation of the endoperoxide intermediate followed by elimination of water from the hydroperoxide A and B to form the corresponding amide and urea.

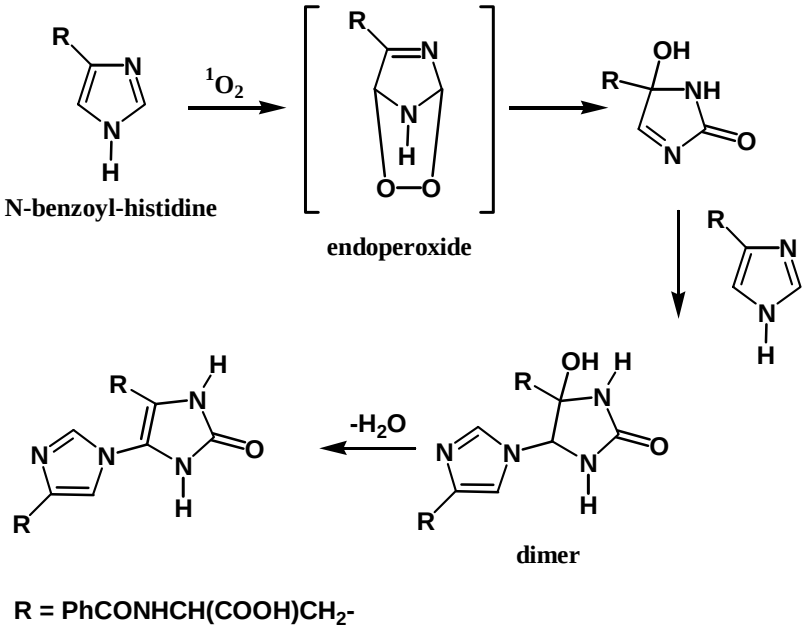

Figure 21. Dimer formation during the reaction of N-benzoylhistidine with $^1O_2$ to explain crosslinking of the imidazole ring in proteins during photodynamic therapy.

2.1.5 Detection and Characterization of Singlet Oxygen

There are a number of methods to detect photosensitized singlet oxygen formation in solution for kinetic analysis, determination of sensitizer singlet oxygen quantum yields, and other photophysical properties. Direct detection of singlet oxygen is the most efficient method to use for analysis, but its phosphorescence is a highly forbidden process, making its detection difficult. Currently, time resolved direct detection of $^1O_2$ emission at 1270 nm is accomplished through the use of low temperature photodiode detectors such as germanium or indium gallium arsenide diodes. These detectors typically operate around –70 °C, which reduces the signal to noise level significantly, and are equipped with wide band amplifiers. There are numerous indirect

detection methods, some of which have been used for many years. One method is to monitor the photooxidation of a substrate by observing its appearance or disappearance using absorption or fluorescence emission spectroscopy as a function of time. The photooxidized substrate can be the sensitizer or some other species that is known to react with singlet oxygen and undergoes a change in its spectral properties as it reacts. Some additional examples to indirectly detect singlet oxygen utilize advanced optical techniques such as thermal lensing of a laser pulse due to $^1O_2$ formation, photocalorimetry, and laser induced photoacoustics.

Direct detection of $^1O_2$ luminescence provides increased precision and simplification of experimental procedures. Germanium detectors that can operate in the infrared region were first introduced in the early 1980s and have become the method of choice for detection of singlet oxygen. In 1976, Krasnovsky *et al.* were the first to directly measure sensitized singlet oxygen phosphorescence in air saturated solutions using a set-up that included a cooled PMT (-60 °C) and a phosphoroscope.[120] They were able to measure excitation and emission spectra, quantum yields, and phosphorescence lifetimes that exceeded 500 μs. Time resolved and steady state measurements are simplified without the need to add and detect singlet oxygen quenchers or other reagents to study the photophysics of singlet oxygen. Measurement of the $^1O_2$ phosphorescence intensity as a function of time allows the determination of the rate constant for singlet oxygen deactivation (k_D) by the substrate or any other molecule that quenches by physical or chemical means. This is accomplished by plotting the logarithm of the phosphorescence intensity as a function of time, where the slope is equal to the decay constant k_D. The first order decay rate of singlet oxygen (k_Δ) is typically determined by measuring k_D as a function of sensitizer concentration and extrapolating to zero concentration. This type of experiment also allows for the determination of the bimolecular rate constant (k_S). Additional experimental

information can be found in Wilkinson's paper where he describes in detail methods for kinetic analysis of $^1O_2$ in solution.[49] Time resolved and steady state $^1O_2$ emission can also be used to determine $^1O_2$ quantum yields.

There are several methods that can be used to indirectly detect photosensitized singlet oxygen for kinetic analysis. One method requires determining the concentration of a substrate or quencher that can react chemically or physically with $^1O_2$. A relative $^1O_2$ QY (Φ_Δ) can be obtained from a double reciprocal Stern-Volmer plot ($1/\Phi_M$) versus ($1/[M]$), where Φ_M is the photooxidative product quantum yield and [M] is the concentration of the substrate or quencher.[49, 50, 121] The Stern-Volmer plot should be linear with a slope equal to (k_D/k_M) and a (y) intercept of Φ_Δ^{-1}. Some of the earliest investigations used chemical quenchers such as 1,3-diphenylisobenzofuran (DPBF), p-nitrosodimethylaniline (NMA), or a physical quencher such as β-carotene.[44, 122] DPBF reacts directly with $^1O_2$ and can be monitored by changes in absorption or by a decrease in fluorescence emission as it is oxidized to the diketone. NMA has been used in a manor similar to DPBF for the investigation of histidine or imidizole protein residues that have been oxidized by singlet oxygen in biological systems.[123] The photobleaching of NMA occurs secondary to oxidation of histidine or imidizole by $^1O_2$, and it is monitored by observing changes in its absorption as it is oxidized by the trans-annular peroxide of histidine or imidizole. β-Carotene can quench singlet oxygen by energy transfer. Farmilo and Wilkinson developed a method to investigate the kinetics of $^1O_2$ by monitoring the absorption decay of β-carotene at 520 nm in solution.[72]

Some additional examples to indirectly detect singlet oxygen utilize advanced optical techniques such as thermal lensing of a laser pulse due to temperature changes during $^1O_2$ formation, photocalorimetric studies, and laser induced photoacoustics.[49, 50] The lifetime, decay

constant, and singlet oxygen quantum yield can be determined by thermal lensing. During pulsed excitation of photosensitized $^1O_2$ part of the energy from the pulse is absorbed resulting in local temperature changes in the solution. The increased temperature is the result of decaying excited states causing the density and refractive index of the solution to change and act as a diverging lens. A separate continuous laser beam can be used as a probe to monitor the magnitude of the thermal lensing due to the nonradiative processes. Hence, relative rate constant and $^1O_2$ quantum yield values can be obtained for sensitizers. Photocalorimetric methods can be utilized to determine sensitizer triplet quantum yields and overall $^1O_2$ quantum yields by measuring the rate of heating in the solution upon $^1O_2$ formation. The measurement is performed in the presence and absence of a $^1O_2$ acceptor such as DPBF. When measured over a short time interval, the Φ_M is proportional to the change in temperature $(\Delta T - \Delta T_{DPBF})/ \Delta T$. Kinetic data can also be obtained by laser induced photoacoustic changes. As with thermal lensing, the local temperature changes that occur during pulsed excitation of a sensitizer in solution can also cause a pressure wave that can be detected at the surface of the solution. A microphone can be used to detect the photoacoustic wave and convert it into an absorption spectrum.

2.1.6 Mechanism of Photosensitized Singlet Oxygen Formation

Photosensitized formation of singlet oxygen is one of the most commonly used and efficient methods to form singlet oxygen. There are numerous sensitizers available that can fulfill a number of needs such as excitation wavelength, solubility, and efficiency of $^1O_2$ formation. The indirect generation of $^1O_2$ by a sensitizer is necessary because the probability of directly exciting ground state oxygen does not produce $^1O_2$ in a considerable amount. The transition

from ground triplet state to the lowest excited singlet state is a spin forbidden, parity forbidden, and angular momentum forbidden process. However, ground state triplet oxygen can be promoted to the excited singlet state in a photosensitized triplet-triplet transition between a sensitizer in the excited triplet state and ground state oxygen. Therefore, a thorough explanation of the sensitizer triplet state will be given to explain its formation and factors that can effect triplet state population.

A simplified Jablonski diagram is presented in Figure 22 in an attempt to illustrate the various intramolecular processes initiated by photon absorption by a sensitizer. The ground singlet state (S_0), lowest excited singlet (S_1), and triplet (T_1) states are the three most important electronic states of the sensitizer for singlet oxygen formation. These states are important because direct excitation to the triplet state ($T_1 \leftarrow S_0$) of the sensitizer is a very weak process and it is much more efficient to indirectly populate the triplet state through absorption from the lowest excited singlet state ($S_1 \leftarrow S_0$). Photon absorption by a sensitizer results in population of a higher excited state (S_n) and is followed by internal conversion and vibrational relaxation to the lowest excited state S_1. In organic molecules there are many different absorption processes that may occur, but there are primarily two emission processes, from the S_1 or T_1 electronic states, that result in fluorescence or phosphorescence, respectively. According to Kasha's rule, all subsequent photophysics and photochemistry originate from these lowest excited states of a given multiplicity. Population of the S_1 state can lead to intersystem crossing followed by internal conversion to populate the triplet state, T_1.

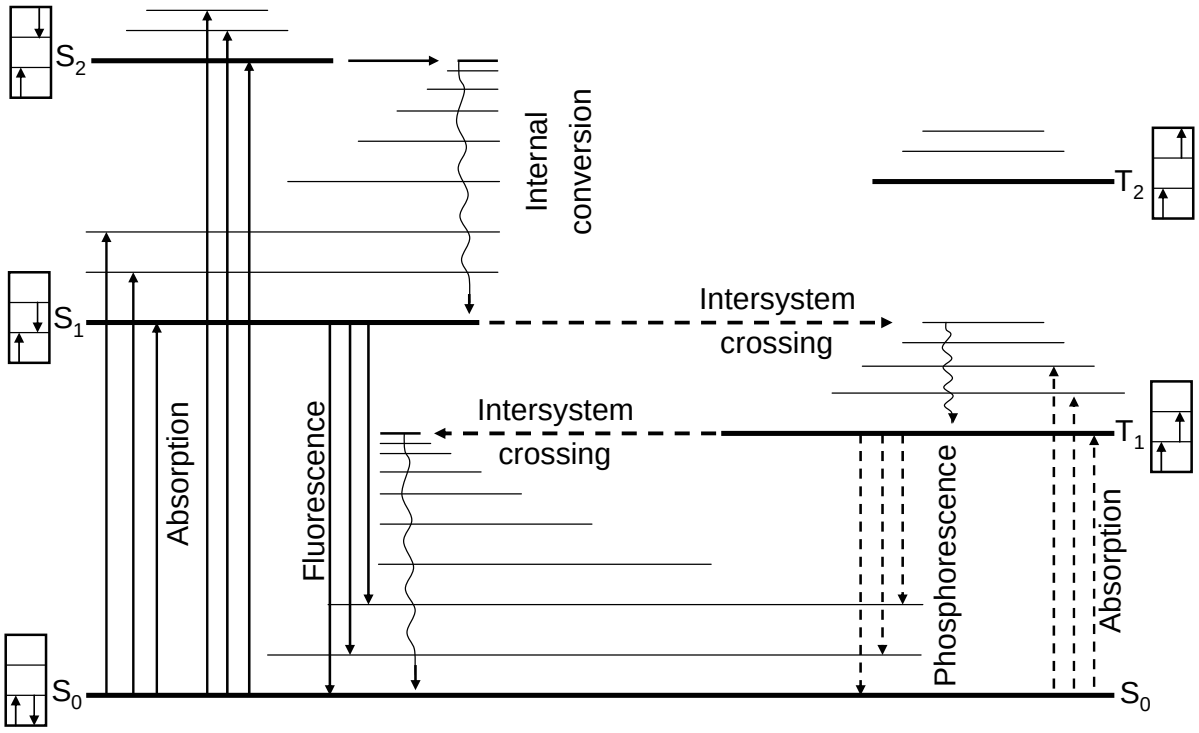

Figure 22. Simplified Jablonski diagram showing the major photophysical processes that occur during excitation of an organic molecule.

The left hand side of the Jablonski diagram represents a manifold of singlet states, and the right side constitutes the triplet state manifold. The heavy horizontal lines represent the electronic energy levels, and the lighter horizontal lines represent the vibrational-electronic energy states. Absorption and emission processes are represented by solid vertical lines and nonradiative (NR) events as wavy lines. Phosphoresce and direct absorption to the triplet state are represented by dashed vertical lines.

Absorption of a photon by a molecule to populate a higher excited state (S_n) is a very rapid process with a rate constant of $10^{15} - 10^{16}$ s^{-1} and is considered to be an instantaneous event. The excited state S_n is followed by radiationless internal conversion which is a passage between two different electronic states $(S_n \rightarrow S_1)_{NR}$ of the same multiplicity to a vibrationally excited S_1 state. This state must then undergo intramolecular vibrational relaxation to a thermally equilibrated S_1 state. The final internal conversion event results in a state with the same multiplicity but lower energy by a NR process. The three most likely transitions that can occur after internal conversion are NR transition to S_0, radiative decay to S_0, or NR intersystem crossing to a triplet state, T_n. A radiative transition to the ground state is observed as fluorescence, whereas intersystem crossing can lead to phosphorescence and NR events from the triplet state. Relaxation directly to the ground state from S_1 by radiative and NR pathways results in a lower quantum yield of sensitizer triplet state population.

In general, fluorescence emission arises from transitions between levels of the same multiplicity and, with a few exceptions, results from the $(S_1 \rightarrow S_0)$ transition. The fluorescence lifetime for most molecules is about 10^{-6} s or less. In addition, the shape of the fluorescence emission spectrum is independent of the excitation wavelength, since all photophysics occurs after internal conversion from the lowest vibrationally relaxed excited state. The emission will be at lower energies and will be approximately a mirror image of the $S_1 \leftarrow S_0$ transition. If the sensitizer singlet state is long lived and the excitation energy exceeds 157 kJ mol^{-1}, quenching of the lowest excited sensitizer singlet (S_1) state by ground state oxygen can lead to the formation of singlet ($^1\Sigma_g^+$ and $^1\Delta_g$) and triplet ($^3\Sigma_g^-$) state oxygen.[45] The higher electronically excited singlet state ($^1\Sigma_g^+$) of oxygen rapidly undergoes electronic-vibrational relaxation to form the lower

metastable singlet state ($^1\Delta_g$) with excitation energy E_Δ = 94 kJ mol^{-1}. Quenching of the sensitizer S_1 state by O_2 can lead to the following products according to Equation 1 a-c.

$$S_1 + O_2(^3\Sigma_g^-) \rightarrow T_1 + O_2(^1\Delta_g) \qquad (1\mathbf{a})$$

$$S_1 + O_2(^3\Sigma_g^-) \rightarrow T_1 + O_2(^3\Sigma_g^+) \qquad (1\mathbf{b})$$

$$T_1 + O_2(^3\Sigma_g^-) \rightarrow T_1 + O_2(^1\Delta_g) \qquad (1\mathbf{c})$$

Equation 1. Quenching of the S_1 state by $O_2(^3\Sigma_g^-)$.

If the energy gap ΔE_{ST} between the sensitizer singlet and triplet state is larger than E_Δ, equation **a** leads to the formation of excited triplet state sensitizer and singlet oxygen and equation **c** becomes equally important in singlet oxygen formation. In this event the singlet oxygen quantum yield can be as large as 2. When the energy gap ΔE_{ST} < 94 kJ mol^{-1}, equations **b** and **c** become important in the formation of singlet oxygen and $^1O_2$ quantum yields are usually ≤ 1. When the possibility of fluorescence emission and NR relaxation to the ground state is low the possibility of intersystem crossing to the triplet state increases. Intersystem crossing is typically observed in organic aromatic compounds containing carbonyls, nitro groups, and heavy atoms such as halogens.

Intersystem crossing is a radiationless transition between the singlet and triplet manifolds of an excited molecule. Population of the S_1 state followed by intersystem crossing is the primary route to populating the triplet state $(S_1 \rightarrow T_1)_{NR}$, which is also capable of going in the reverse direction to depopulate the triplet state $(T_1 \rightarrow S_0)_{NR}$. Internal conversion and intersystem crossing are very similar processes, but the distinguishing characteristic that differentiates the two transitions is in the crossover process between the two-quasi-degenerate states of ($S_n \rightarrow$

$S_1)_{NR}$ and $(S_1 \rightarrow T_1)_{NR}$, respectively. Intersystem crossing connects states of different multiplicities and requires a reorientation of the electron spin-axis, whereas internal conversion does not require a spin-axis reorientation. Depopulation of the triplet state can result from intersystem crossing by $(T_1 \rightarrow S_0)_{NR}$ transitions to a higher vibrationally excited state of S_0. Despite the fact the two intersystem crossing pathways appear to be comparable and would possess similar probabilities in either direction, the rate constant for the $(S_1 \rightarrow T_1)_{NR}$ transition is typically three to four orders of magnitude greater than the rate constant for the $(T_1 \rightarrow S_0)_{NR}$ transition. The difference in the rate constants is related to the energy gap between the $(S_1 \rightarrow T_1)_{NR}$ and $(T_1 \rightarrow S_0)_{NR}$ transitions. The energy gap of the $(T_1 \rightarrow S_0)_{NR}$ transition is typically much larger than the $(S_1 \rightarrow T_1)_{NR}$ transition, and it has been suggested that the transition probability increases as the energy gap decreases.

Intersystem crossing by radiative and nonradiative transitions requires a change in spin multiplicity which is a quantum mechanically forbidden event. In molecules that do not contain heavy atoms the spin angular momenta and orbital angular momenta of the electrons are not coupled and there is no interaction between the two momenta. Consequently, the electric dipole transition moment operator is dependent on the spatial coordinates of the electrons and nuclei and will have a zero probability for a transition between states with different spin functions. Hence, a transition between states of different spin multiplicity $(S_1 \rightarrow T_n)_{NR}$ are forbidden. The quantum mechanic selection rules can be relaxed by the interaction between the magnetic dipole generated by the spin of the electron and the magnetic dipole resulting from the orbital motion of the electron around the nucleus. The sum of these two interactions can be described as the total angular momentum of the electron. This interaction, which leads to a relaxation of the selection rules, is termed spin-orbit coupling, and the larger the interaction the higher the probability of

intersystem crossing between singlet and triplet states. The contribution of spin-orbit coupling in light atoms, and molecules containing them, is minimal because the spin angular momenta and orbital momenta of the electrons are not coupled. One would expect that there would be no relaxation of the selection rules, and transitions between states of different spin multiplicity would not be observed. Nonetheless, some spin-orbit coupling is present and transitions where there is a change in the spin quantum number are observed.

Spin-orbit coupling can be enhanced, thus increasing the probability of intersystem crossing, by incorporating heavy atoms into the molecule in the region were the transition is localized. This is termed the internal heavy-atom effect, and it can result in a significant increase in spin-orbit coupling of an electron. Enhancement can also be achieved using a solvent matrix that contains heavy atoms, giving the term external heavy-atom effect. As a result, the possibility of a forbidden transition ($S \leftrightarrow T$) that is only weakly allowed may be increased by the heavy atom effect. In heavy atoms, those with a large atomic number Z, the nuclear charge is larger resulting in a greater magnetic field as the electrons orbit the nucleus. Accordingly, the spin-orbit coupling will increase as the magnetic field is increased. The distance of the electron from the nucleus plays a significant role as well. The angular momentum of the electron must also increase as it gets closer to the nucleus to counteract the attractive coulombic force that is applied to the electron by its interaction with the nucleus. As a result, the spin-orbit coupling will increase as the electron orbits closer to the nucleus. Hence, the spin-orbit coupling can be maximized by incorporating atoms that possess a large atomic number and have filled or nearly filled outer shell orbitals. It turns out that the atomic number has a significant impact on spin-orbit coupling and takes on a Z^4 dependence. Therefore, the greatest spin-orbit coupling is

observed in molecules that contain atoms from the right hand side of the periodic table, such as the halogens, whose atomic numbers are large and have nearly full outer shell electronic orbitals.

Phosphorescence emission ($T_1 \rightarrow S_0$) can result following intersystem crossing ($S_1 \rightarrow T_1)_{NR}$. The forbidden emissive transition is between two different states of multiplicity, resulting in very long phosphorescence (excited state) lifetimes of about 10^2 to 10^{-4} s. Similar to fluorescence, phosphorescence emission usually occurs at lower energies than the excitation wavelength or fluorescence emission and is independent of the excitation wavelength. A number of events can occur during the very long lifetime of phosphorescence; some of the most likely events are nonradiative intersystem crossing to the singlet state S_1 or S_0 and quenching from intermolecular interactions. Intersystem crossing back to S_1 can result in delayed thermal fluorescence ($S_1 \rightarrow S_0$) following thermal excitation and ($S_1 \leftarrow T_1)_{NR}$. Eosin and fluorescein are two examples where delayed fluorescence has been observed in deoxygenated solutions. Delayed fluorescence is more common in molecules where there is a small difference in the energy of the S_1 and T_1 states or compounds that have a long phosphorescence lifetime. Intermolecular energy transfer between solvent, ground state sensitizer molecules, and other quenchers such as oxygen can lead to deactivation of the triplet state. Quenching of the sensitizer triplet state by molecular oxygen can occur if the triplet state energy is > 157 kJ mol^{-1}. Sensitized formation of singlet oxygen is typically performed in dilute solutions ($\leq 10^{-6}$ M) of sensitizer, where bimolecular interactions involving the sensitizer do not have a significant contribution to triplet state quenching in comparison to oxygen. On the other hand, ground state oxygen can diffuse very rapidly through solution and is usually present in relatively high concentration (1-3 x 10^{-3} M) in air saturated organic solvents at room temperature. The

concentration of oxygen in polar solvents like water, ethylene glycol, and glycerol is about an order of magnitude less than some of the more common organic solvents.[50]

As mentioned previously, ground state oxygen ($^3\Sigma_g^-$) can quench both the sensitizer singlet and triplet states resulting in singlet oxygen quantum yields as high as 2. Conditions that can produce two molecules of singlet oxygen per photon absorbed are very rare. According to Schweitzer and Schmidt, five conditions must be met simultaneously in order to achieve a $^1O_2$ QY = 2.[52] The difference in energy between the sensitizer singlet and triplet state must be > 94 kJ mol^{-1}. The lowest excited triplet state (T_1) should be the only triplet below S_1. Quantitative quenching of the singlet state (S_1) by oxygen should also quantitatively lead to the formation of the triplet state T_1. Finally, the singlet and triplet states should quantitatively lead to the formation of singlet oxygen. In the event that all necessary criteria are met, the overall singlet oxygen quantum yield, QY_Δ,

$$QY_\Delta = P_S \cdot f_S + Q_T \cdot P_T \cdot f_\Delta \qquad (2)$$

Equation 2. Determination of $^1O_2$ QY for quenching of the sensitizer singlet and triplet state by $O_2(^3\Sigma_g^-)$.

where P_S and P_T are the fractions of the singlet and triplet state quenched by oxygen, respectively, f_S is the efficiency of $^1O_2$ production during quenching of the singlet state, and Q_T is the quantum yield of the triplet state. When the lifetime of the S_1 state is short-lived and the difference in energy of the singlet and triplet states ($E_{S1} - E_{T1} << E_\Delta$) is much less than the energy of $^1O_2(^1\Delta_g)$, the rate of S_1 quenching by oxygen goes to zero and the first term can be ignored. The efficiencies of $^1\Sigma_g^+$ and $^1\Delta_g$ production during O_2 quenching of the triplet state are given by the term, f_Δ, to describe the overall efficiency of singlet oxygen production from the triplet state.

The triplet state is typically long lived, and in air saturated solutions quenching of the triplet state by oxygen is very efficient with values of P_T approaching 1. When quenching of the S_1 state is ignored, the singlet oxygen quantum yield can be simplified even further to give Equation 3.

$$QY_{\Delta}, = Q_T \cdot f_{\Delta} \quad (3)$$

Equation 3. Determination of $^1O_2$ QY for quenching of the sensitizer triplet state by $O_2(^3\Sigma_g^-)$.

Schmidt, Schweitzer, Wilkinson, and co-workers have performed a great deal of research investigating the mechanism of direct photosensitized singlet oxygen formation.[2, 76, 77, 124-127] Schmidt recently published a paper describing the mechanism of photosensitized production of singlet oxygen where he developed a model to quantitatively predict the rate constants and efficiencies of different competing processes in the formation of singlet oxygen by quenching of sensitizer ππ* excited triplet states.[128] The model, which is based on more than 40 different ππ* triplet sensitizers, ties in previous investigations on nπ* quenching of phenyl ketone sensitizers.[74, 77, 129] Quenching of triplet state ππ* and nπ* sensitizers both proceed through two different pathways by internal conversion of excited non-charge transfer (nCT) encounter complexes and partial charge transfer (pCT) exciplexes of the sensitizer and oxygen. The mechanism of singlet oxygen production does not occur by direct energy transfer between individual molecules but rather by internal conversion of excited complexes of triplet state sensitizer and ground state oxygen ($^3\Sigma_g^-$). The nCT and pCT pathways operate with different singlet oxygen efficiencies. Formation by ππ* transitions are heavily dependent on the triplet state energy and oxidation potential of the sensitizer, and to some extent on solvent polarity.

Transitions involving nπ* are less understood and exhibit a much smaller dependence relative to ππ* transitions (as discussed below).

The rate of singlet oxygen production by the nCT pathway for ππ* transitions is heavily dependent on the sensitizer triplet state energy E_T. Energy transfer occurs upon sensitizer-oxygen complex ($T_1{}^3\Sigma$) formation followed by internal conversion (IC) to form complexes of ($S_0{}^1\Sigma$), ($S_0{}^1\Delta$), and ($S_0{}^3\Sigma$). Following IC, the complexes will dissociate to form ground state sensitizer S_0, $O_2(^1\Sigma_g^+)$, $O_2(^1\Delta_g)$, and $O_2(^3\Sigma_g^-)$. The energies (E_Σ, E_Δ, and zero) associated with the three complexes are used to determine the excess energy ΔE, where $\Delta E = E_T - E_\Sigma$, $E_T - E_\Delta$. The excess vibrational energy, ΔE, for each of the complexes needs to be dissipated by the sensitizer as heat. Hence, the rate constant, k_{IC}, for internal conversion of the complex will decrease as more vibrational energy needs to be dissipated. It has been demonstrated that the rate constants for triplet state quenching by oxygen will decrease with increasing excess energy ΔE for the nCT pathway.[130] Schmidt demonstrated a common dependence for the multiplicity normalized rate constants ($k_T{}^{1\Sigma}$, $k_T{}^{1\Delta}$, and $k_T{}^{3\Sigma}/3$), and excess energy ΔE in the region $\Delta E \leq 220$ kJ mol^{-1}.[128] The data from 11 different ππ* triplet sensitizers was used to devise an empirical curve, $\log(k^P_{\Delta E}/m = f(\Delta E)$, describing the rate constant dependence on the excess energy ΔE. The curve decreases rapidly in a nonlinear fashion as E_T is increased. For nCT transitions involving ππ*sensitizers, the rate and efficiency of singlet oxygen formation will increase rapidly as ΔE is decreased. Thus, IC is restricted by an empirical energy-gap relation and is the rate limiting step in the formation of singlet oxygen by the nCT pathway.

For ππ* sensitizers possessing large triplet state energies CT interactions between the sensitizer and oxygen cannot be ignored. In the region where $\Delta E > 240$ kJ mol^{-1}, the rate and efficiency of singlet oxygen formation is strongly influenced by CT interactions. Exciplex

formation between sensitizer and oxygen is the dominant species rather than encounter complexes. As a result, the oxidation potential (E_{ox}) of the sensitizer is a key parameter that determines the amount of CT character of the exciplex, best described as pCT. The rate constants of singlet oxygen formation ($k_T^{1\Sigma}$, $k_T^{1\Delta}$, and $k_T^{3\Sigma}/3$) rapidly increase with larger values of ΔE and deviate from the empirical curve $\log(k^P_{\Delta E}/m = f(\Delta E)$. The deviation is because the empirical curve describes the energy-gap relation for IC of nCT encounter complexes without charge transfer stabilization. Consequently, singlet oxygen formation in the pCT pathway is accomplished by exciplex formation and is favored by smaller E_{ox} values, thus increasing the strength of CT interactions and larger rate constants for quenching of the sensitizer by oxygen.Schmidt correlated the strength of the CT interaction for $\pi\pi^*$ sensitizers with the free-energy change (ΔG_{CET}) for complete electron transfer where

$$\Delta G_{CET.} = F(E_{ox} - E_{red}) - E_T + C \qquad (4)$$

Equation 4. Free energy dependence for complete electron transfer during sensitizer quenching by $O_2(^3\Sigma_g^-)$ for pCT complexes.

F, E_{ox}, E_{red}, and C are the Faraday constant, sensitizer oxidation potential, reduction potential of O_2, and electrostatic interaction energy, respectively. Typically, the CT interactions are best described as pCT and complete electron transfer between triplet state sensitizer and oxygen does not occur. A linear relation was obtained for the multiplicity normalized rate constant $\log(k^P_{\Delta E}/m)$ as a function of the free-energy change ΔG_{CET} for sensitizers with $\Delta E \geq 240$ kJ mol^{-1}. The nCT pathway is dominant in the region where $\Delta G_{CET} \geq 40$ kJ mol^{-1}, whereas the pCT pathway is dominant for sensitizers that posses $\Delta G_{CET} \leq -25$ kJ mol^{-1}. Hence, large sensitizer triplet energy and small sensitizer oxidation potential will favor the pCT pathway,

where the singlet oxygen rate constant increases as the free energy change becomes more exergonic. In the pCT pathway the overall efficiency of singlet oxygen, $O_2(^1\Sigma_g^+)$ and $O_2(^1\Delta_g)$, decreases as the rate constants of formation are increased. This is in stark contrast to the nCT pathway where the efficiency of singlet oxygen increased with the rate of formation of $^1O_2$.

Triplet state quenching of nπ* sensitizers is similar to ππ* sensitizers and occurs by the nCT and CT pathways. Mehrdad *et al.* investigated a series of nπ* benzophenone sensitizers, where the triplet state energy, E_T, was nearly the same for the series and the rate constant for triplet state quenching by oxygen was evaluated as a function of sensitizer oxidation energy, E_{ox}.[129] The data was then compared to similar ππ* biphenyls investigated by Schmidt *et al.* All nπ*and ππ* sensitizers operated through the nCT and pCT pathways and were capable of producing $O_2(^1\Sigma_g^+)$, $O_2(^1\Delta_g)$, and $O_2(^3\Sigma_g^-)$. Unlike the ππ* sensitizers, the nπ* sensitizers did not exhibit such a strong dependence of E_T and E_{ox}. The rate constants for the nπ* sensitizers increased with smaller E_{ox} values as did the ππ* sensitizers, but the change was much smaller. Additionally, nπ* sensitizers with a very large E_{ox}, where CT interactions are minimal, exhibited a significant deviation from the empirical curve $f(\Delta E)$ that was formulated for the ππ* sensitizers.

The significant deviation of the data for nπ* benzophenones is attributed to the electronic and steric interactions of the intermediate sensitizer-oxygen complexes $^{1,3}(T_1(n\pi^*)^3\Sigma)$. It is believed that the intermediate for the similar $^{1,3}(T_1(\pi\pi^*)^3\Sigma)$ biphenyl complex is a supra-supra structure where oxygen interacts directly with the aromatic ring (Figure 23 A). In this configuration it is expected that there are no significant changes in bond lengths between the O-O bond and complex during IC and deactivation of the complex. In the $^{1,3}(T_1(n\pi^*)^3\Sigma)$ benzophenone complex a four-center structure is formed (Figure 23 B), where O_2 and the

carbonyl group take on a parallel arrangement. Consequently, the excitation energy of the complex is localized on the carbonyl group, and large changes in the bond lengths of the $^{1,3}(T_1(n\pi^*)^3\Sigma)$ complex are expected. The excess energy is dissipated by displaced potential energy during IC and deactivation of the complex, and a smaller excess-energy dependence of the rate constant of IC is expected during deactivation. As a result of the different electronic configuration, deactivation of nπ* complexes do not exhibit such a strong dependence on the excess energy or oxidation potential for nCT and pCT pathways, respectively.

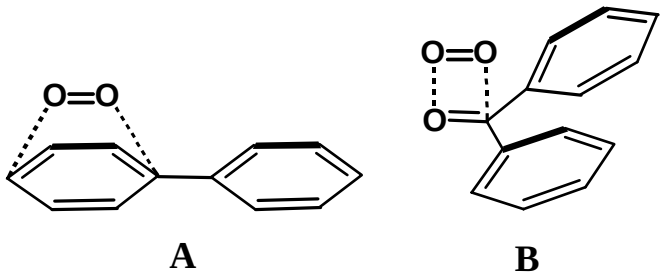

Figure 23. Structures of ππ* and nπ* sensitizer-oxygen exciplex formation of A) biphenyl $^{1,3}(T_1(\pi\pi^*)^3\Sigma)$ and B) benzophenone $^{1,3}(T_1(n\pi^*)^3\Sigma)$.

The solvent polarity surrounding the sensitizer-oxygen complex has a stronger effect on pCT exciplexes than on the nCT encounter complexes. In particular, the effects of solvent polarity on ππ* exciplexes is most profound, resulting in a significant increase in the overall rate constant for quenching of the triplet state by oxygen. The polarity of the solvent helps to stabilize the exciplex during IC and appears to have a larger stabilizing effect as the CT character of the complex is increased. Additionally, the efficiency of singlet oxygen formation decreases despite an increase in the quenching of the triplet state. The effects of solvent polarity on nCT ππ* encounter complexes is minimal and does not produce any significant changes in the rate of

triplet state quenching. For nπ* complexes there is no measurable effect from solvent polarity in regard to nCT or the pCT pathways.

2.1.7 Optimization of Singlet Oxygen Photosensitizers

The maximum singlet oxygen quantum yields are obtained when both the sensitizer singlet and triplet states are quenched by oxygen to give an upper singlet oxygen quantum yield of 2. In this situation, absorption of one photon will produce two molecules of singlet oxygen. This event is quite rare for reasons mentioned previously. Briefly, the difference of the S_1-T_1 energy gap must exceed 94 kJ mol^{-1}, and T_1 must be the only triplet level below the S_1 state. Quantitative quenching of the S_1 and T_1 states must be achieved, resulting in the quantitative formation of singlet oxygen. Quenching of the singlet state is usually observed in compounds that exhibit moderate to strong CT interactions. This poses a problem since it is known that the efficiency of triplet state quenching decreases as the CT character of the sensitizer is increased. Quenching of S_1 for nCT sensitizers requires high O_2 partial pressures, making it unpractical for most applications.

Under typical conditions, singlet oxygen formation by quenching of the sensitizer triplet state is the most efficient pathway, and methods to optimize the formation of the triplet state and efficiency of its quenching appear to be the best approaches to photosensitized singlet oxygen. The energy of the triplet state is an extremely important parameter and should be > 157 kJ mol^{-1} to produce $O_2(^1\Sigma_g^+)$ and $O_2(^1\Delta_g)$, and at a minimum T_1 should not be less than 94 kJ mol^{-1} to produce the lower energy $O_2(^1\Delta_g)$ species. This will require shorter excitation wavelengths, since T_1 is typically obtained by populating a higher S_n state. Large triplet energies should be

avoided to minimize the excess energy (ΔE) between the sensitizer and the energy of the two $^1O_2$ states. The most common $^1O_2$ sensitizers are of the $\pi\pi^*$ type and proceed through the nCT and pCT pathways. As ΔE is increased the rate and efficiency of triplet state quenching rapidly decreases.

The effects of the excess energy can be minimized by incorporating electron withdrawing groups into the molecular architecture in an attempt to increase the E_{ox} and minimize the CT character of the sensitizer. There are numerous electron withdrawing groups that can be placed into the sensitizer such as nitro, cyano, and benzothiazole groups, which are often included to modulate the properties of the sensitizer. Unfortunately, one often wants a moderate to large amount of charge transfer in the sensitizer for other photophysical properties. Some nonlinear optical effects, such as two-photon absorption, are heavily dependent on the amount of charge transfer within the chromophore system.

Maximizing the formation of the triplet state sensitizer by ISC is one method to increase the probability of $^1O_2$ formation. Incorporation of heavy atoms into the region of the sensitizer that is responsible for the electronic transition can increase spin-orbit coupling (SOC) in the molecule, thus increasing the probability of ISC. The amount of SOC is strongly affected by the atomic number of the heavy atom and takes on a Z^4 dependence. As a result, halogens are frequently incorporated as the heavy atom constituents. In conjugated systems it has been observed that placement of the heavy atom in the ortho-position rather than directly in line with the conjugation leads to better SOC, allowing additional modifications of the conjugated system.

2.2 Current Progress in PDT

Some of the earliest PS studies, dating back to the early 1900's, were on compounds like acridine, eosin, and hematoporphyrin.[21, 131-133] In fact, porphyrin derivatives are one of the most thoroughly studied PS's and represent a good portion of the compounds that are commercially available. In the early 1960's, Lipson and Schwartz separately investigated the use of hematoporphyrin derivatives (HpD) to treat neoplastic tissue, and found that the compound had a high affinity for tumors with a strong phototoxicity and a low affinity for healthy tissue.[134] Interest in HpD continued through the 1970's, and a few years later Dougherty introduced the first drug grade hematoporphyrin. After extensive studies, the PS known as Photofrin® (Axcan Pharma, Inc.) was used in Canada in 1993, and later approved by the FDA in 1995 to become the first clinically used PS for use in PDT.[12]

Since the introduction of Photofrin® there have been several new PS's approved by the FDA or that are in clinical trials. These sensitizers fit into three main families; porphyrins, chlorin or chlorophyll-based, and dye-based photosensitizers (Table 1). With the exception of 5-aminolevulinic acid (ALA) derivatives, all of the currently FDA approved compounds fit into the porphyrins or chlorine-based families. ALA is a metabolic precursor in the biosynthesis of protoporphyrin IX (PpIX), a naturally occurring heme that can function as a photosensitizer. Even though ALA is not a porphyrin, the prodrug is classified under the porphyrin-based family. All currently approved PS's have absorption maxima below 730 nm. Some of the PS's are very specific in the types of tumors they can treat whereas others can be used on a broad range of tumors. The $^1O_2$ QY in phosphate buffered saline (PBS) of these PS range from 0.80 down to 0.06.[50, 135-137]

Table 1. $^1O_2$ Sensitizers for PDT

Trade Name	Indication	λ nm	ε $M^{-1}cm^{-1}$	QY	Year Approved by FDA
Photochlor	Basal cell carcinoma	665	—	—	CT
Talaporfin	Solid tumors from diverse origins	664	15,800	0.56	CT
Levulan**	Basal-cell carcinoma, head and neck, gynecological tumors	635	10,000	0.42	1999
Benzvix**	Gastrointestinal cancer	635	10,000	—	CT
Metvix**	Basal-cell carcinoma	635	10,000	—	2004
Hexvix**	Diagnosis of bladder tumors	400	10,000	—	EU
Photofrin	Cervical, endobronchial, esophageal, bladder, gastric cancers, brain tumors	630	1,170	0.06-0.12	1995
BOPP	Brain tumors	630	—	—	—
Visudyne	Neovascularization of retina secondary to macular degeneration	689	35,000	0.80	2000
Foscan*	Head and neck, prostate, pancreatic tumors	660	30,000	0.58	2001
Pc 4	Cutaneous/ subcutaneous lesions	675	84,000	0.38	—
Purlytin	Cutaneous metastatic breast cancer, basal cell carcinoma, Kaposi's sarcoma, prostate cancer	664	30,347	0.71	CT

(*) Seeking FDA approval, (**) derivatives of 5-aminolevulinic acid, (—) data is not available. (CT) in clinical trial, (EU) approved for use in Europe

The porphyrin-based PS Photofrin® can be used to treat a large number of conditions and is one of the most frequently utilized PS's. It is difficult to purify during synthesis and contains a mixture of mono-, di-, and oligomeric ether- and ester-linked porphyrins (Figure 24), and the purified PS contains about 85% oligomeric material. This fraction of the PS is most readily taken up by tumors and is responsible for its activity. The PS is only delivered systemically by intravenous (IV) injection and is activated after clearance from healthy tissue 40-50 h later on illumination at 630 nm. Clearance of the sensitizer is slower from tumors and some healthy

tissue such as skin, liver, and the spleen. It is most commonly used to treat cancers of the head and neck, Barrett's esophagus, other esophageal, endobronchial, and bladder cancer, although some clinical trials have also used Photofrin® on brain tumors such as glioblastoma and some types of breast tumors.[21]

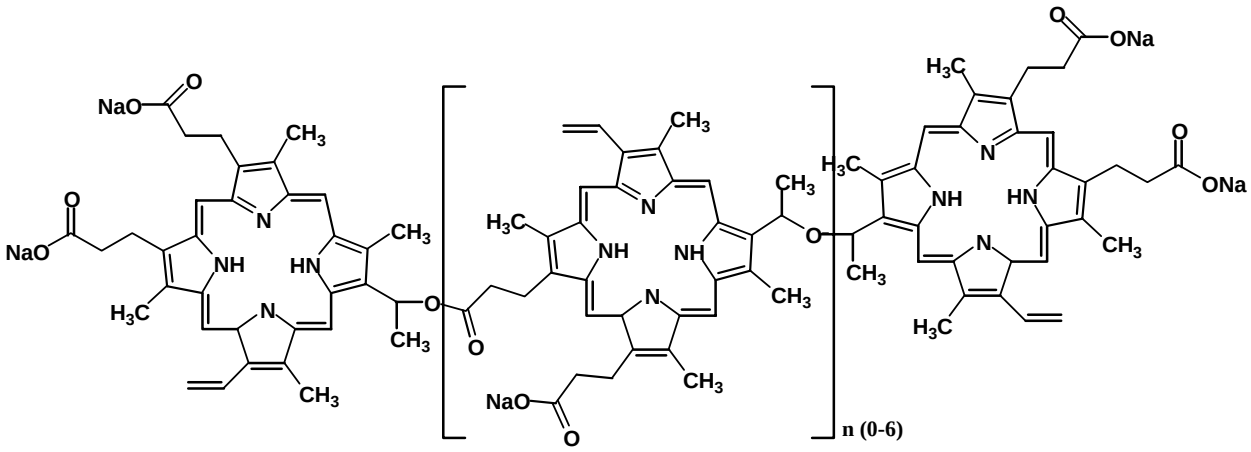

Figure 24. Chemical structure of Photofrin®

In general, there is no one single characteristic of a photosensitizer that determines its success, but rather a collective group of characteristics when combined, contribute to the overall effectiveness of the PS. Photofrin® is one example. Its photophysical properties are certainly not stellar. The PS absorbs at relatively short wavelength (630 nm) and has a very low absorption coefficient (1,170 $M^{-1}cm^{-1}$). The $^1O_2$ QY is rather low in PBS (0.06-0.12). As a result, large concentrations of the PS and high light intensities are required for clinical use.[136] The relatively high concentrations result in increased photosensitivity for extended periods of time (4-6 wks) due to an elevated systemic uptake of the PS in the patient. Nonetheless,

Photofrin® has been successfully used to treat a large number of neoplastic diseases due to the PS's efficient uptake by cancerous tumors and good photocytotoxicity.

There are four derivatives of the prodrug 5-aminolevulinic acid (Figure 25). Three of the derivatives, Levulan®, Metvix®, and Hexvix®, are approved for use in the U.S. and elsewhere. Benzvix® is in clinical trials in Europe to treat gastrointestinal cancer. Levulan® and Metvix® are used topically in an ointment to treat precancerous and skin cancers such as actinic keratosis, Bowen's disease, and basal cell carcinoma. Hexvix® is used as a bladder tumor imaging agent delivered in a solution to the bladder cavity where it forms fluorescent PpIX in cancerous tissue.

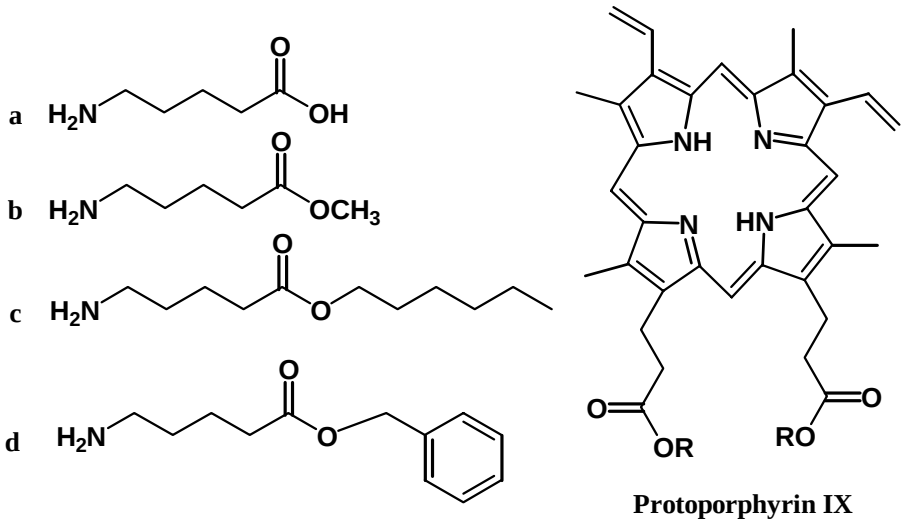

Figure 25. Chemical structures of a) Levulan®, b) Metvix®, c) Hexvix®, d) Benzvix®, and PpIX.

ALA is applied topically and is taken up by active transport into the cells. Once in the cells it is metabolized through the haem biosynthetic pathway to protoporphyrin IX. The rate of uptake of ALA is higher in malignant tissue than normal tissue by about 10:1.[138] One drawback to using these compounds is that they are not taken deep into the tissue (< 1 cm), limiting their

use to mostly skin cancers.[139] Nevertheless, ALA is rapidly taken up by the cells, and treatment can begin within 3-4 h of being administered. Systemic clearance is rapid and is usually complete within 24 h. The photophysical properties of ALA are only slightly better than Photofrin®. Excitation of ALA biosynthetic adducts occur at 635 nm, and its absorption coefficient is about 10,000 $M^{-1}cm^{-1}$. These derivatives have a good $^1O_2$ QY (0.42) adding to their efficiency as an effective PS. The greatest advantage of the ALA derivatives is their rapid uptake and systemic removal from the body along with an efficient $^1O_2$ QY.

Visudyne® is from the chlorin-based family of PS's and is an equal mixture of two regioisomers that differ in the acid and methyl ester groups on the C and D pyrrole rings (Figure 26). This PS is hydrophobic and is solubilized as a liposomal formulation for intravenous delivery. Also known as verteporfin or benzoporphyrin derivative monoacid ring A (BPD-MA), it is used to prevent the loss of visual sight due to subfoveal choroidal neovascularization secondary to age-related macular degeneration or progressive myopia.[137]

The PS is activated 15 minutes after administration by passing a beam of light at 689 nm through the front of the eye for 83 seconds. The procedure is typically performed once a month for a total of three doses. Visudyne® has a high affinity for plasma low-density lipoproteins (LDL) and is taken up by cells that express a high level of LDL receptors. Once taken up by the cells, the PS generates $^1O_2$ on excitation, destroying the area of neovasularization within the eye while leaving nearby healthy vasculature undamaged.[140] The PS is very selective in its action and exhibits about a 15-fold greater affinity for diseased tissue when compared to Photofrin®.[140]

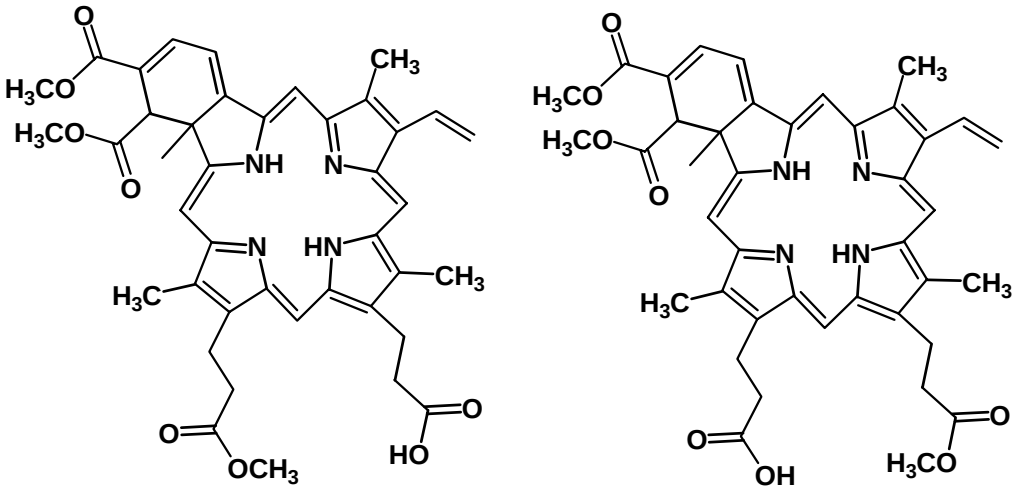

Figure 26. Chemical structure of Visudyne

Visudyne® is very similar to the other porphyrin based PS's in its macrocycle ring structure but with one of its four pyrrol rings reduced making it a chlorin. These ring structures typically exhibit a 30-50 nm shift to longer wavelengths in its absorption spectrum when compared to similar porphyrin ring structures. The molar absorptivity of Visudyne® is about 3 times greater (30,000 $M^{-1}cm^{-1}$ at 689 nm) than the ALA porphyrins, and has a higher $^1O_2$ QY (0.80). This sensitizer has been very successfully used and is available in over 70 countries including the U.S. and Europe.

Foscan® is another chlorin-based PS that has been used in clinical trials to treat head and neck, prostate, and pancreatic tumors and is similar in its use to Photofrin®. Biolitec AG, based in Germany, is actively seeking FDA approval for this sensitizer. Also known as Temoporfin and meta-tetra hydroxyphenyl chlorin (m-THPC), it has increased solubility due to the phenol rings (Figure 27) and is delivered intravenously in a mixed solvent solution of polyethylene glycol, ethanol, and water (3:2:5). It has a larger molar absorptivity (30,000 $M^{-1}cm^{-1}$) and is excited at slightly longer wavelength (660 nm). When compared to Photofrin®, m-THPC

exhibits a higher selectivity for cancerous tissue over healthy tissue and has a considerably larger $^1O_2$ QY (0.58).

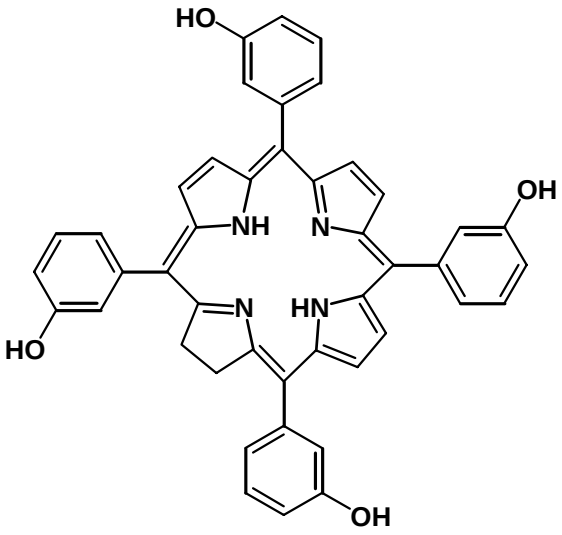

Figure 27. Chemical structure of Foscan®

In general, the commercial PS's currently available have demonstrated their usefulness in PDT, although their full potential as a therapeutic treatment for neoplastic disease has yet to be accomplished. At the moment, all PS's have excitation wavelengths (λ_{max}) at the very edge or below the transmission window for biological tissue (700-1000 nm). Limited progress has been accomplished in moving further into this transmission window with the porphyrin-based PS's. A reduction in one of the four pyrrol rings leads to the chlorin-based PS's. These compounds have longer excitation wavelengths (660–700 nm) and slightly larger $^1O_2$ QY's. Another subclass of the porphyrins is being developed with pentadentate metalloporphyrins. Commonly called texaphyrins, these compounds have longer λ_{max}, around 700-760 nm. Phthalocyanines and

purpurins with extended conjugation are also being developed, but these compounds do not appear to absorb at significantly longer wavelengths than the porphyrins.

One method that has been recently investigated to access longer wavelengths is the use of PS's that can generate $^1O_2$ under 2PA. Investigations have been done on Photofrin® PpIX, tetrapyrrolic, and stibene-based PS's to investigate the possibility of using these compounds for $^1O_2$ sensitization under 2PA.[53, 98, 101, 141-143] This will be discussed further in the next section.

Another aspect of $^1O_2$ PS's is their specificity for neoplastic tissue. The commercial PS's rely heavily on the hydrophilicity of the compounds to direct the uptake of the PS by cancerous tissue. Research is being conducted on improving the tumor specificity of PS's. Bioconjugation techniques using antibodies and proteins have shown to be promising in clinical studies, but there are some drawbacks to using these compounds, such as synthesis, transport barriers, and the potential of serious toxicity in the host.[144, 145] Targeting of cell surface receptors and cellular transport using short oligopeptides and small molecules has also shown to be hopeful in the delivery of drugs to tumors. Cyclic peptides have been used to target cell-surface receptors for fluorescence and MRI imaging of cancerous brain and breast tumors in vivo.[146-150] The future of photodynamic therapy will become even more promising as the photophysical properties and ability to accurately target tumors improves with $^1O_2$ sensitizers. The PS's that are in commercial use today demonstrate the great potential that PDT holds for the treatment of various diseases.

2.3 Fluorene Derivatives for Two-Photon Sensitization of $^1O_2$

2.3.1 Singlet Oxygen Sensitization by 2PE

The nonlinear two-photon absorption (2PA) process provides an alternative pathway to singlet oxygen sensitization, and, in particular, is a promising alternative for photodynamic therapy applications. The tissue transparency window of 700–1000 nm is ideally situated for 2PE, and the longer wavelengths reduce scattering by tissue. As explained in section 1.1, the quadratic dependence of 2PE provides one with the opportunity of 3D resolution that can not be obtained under linear 1PE.

Singlet oxygen formation by sensitization occurs by populating an excited singlet state of a photosensitizer under one- or two-photon excitation. It is usually assumed that all photophysical processes occur from the lowest vibrationally relaxed excited state and is independent of the type of excitation. For centrosymmetric molecules the excited state initially populated by 2PA is not usually the same as 1PA. For this reason one can't simply assume that a doubling of the 1PA λ_{max} will result in a high probability of populating the excited state. The quantum mechanical selection rules are essentially relaxed for noncentrosymmetric molecules, and, in general, 2PE can be used to directly access 1PE allowed electronic transitions, though the 2PA-allowed transitions will be stronger and more favorable.

A simplified Jablonski diagram is presented in Figure 28, depicting the formation of $^1O_2$ under 1PA and 2PA of a sensitizer. The formation of $^1O_2$ begins by populating an excited singlet state of the photosensitizer under 1PA or 2PA. Under 2PA, two photons are absorbed to make an electronic transition corresponding to the combined energy of the photons involved. The two

photons combine at the same point in space and at the same point in time, passing through a short lived virtual state that is a superposition of the real states of the molecule.[151, 152] Population of a higher excited state, S_n, is followed by internal conversion and vibrational relaxation to the lowest excited state S_1, as outlined in section 2.1. According to Kasha's rule, all subsequent photophysics and photochemistry originate from this lowest excited state, regardless of whether it was populated under 1PA or 2PA. Intersystem crossing from the S_1 state, followed by internal conversion, leads to population of the first excited triplet state, T_1. Ground state triplet oxygen can then quench the triplet state sensitizer producing $^1O_2$ and ground state sensitizer. $^1O_2$ can either undergo photochemical reactions, return back to the ground state by phosphorescence emission at 1270 nm, or decay to the ground state by nonradiative pathways.

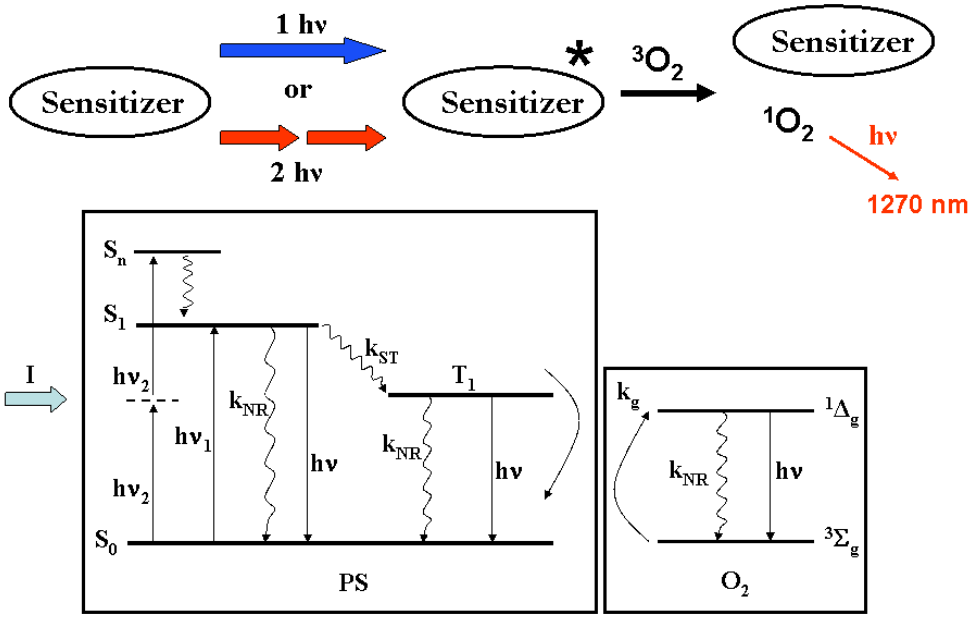

Figure 28. Jablonski diagram illustrating the production of singlet oxygen by irradiating a sensitizer under one- and two-photon excitation.

Ground state oxygen can also quench the sensitizer singlet state, so it is theoretically possible to have a singlet oxygen quantum yield with an upper limit of 2. However, this is unusual because the sensitizer S_1 state has a very short lifetime, but it is observed for some compounds such as fullerenes.[153, 154] Additional pathways that can lead to a lower population of the sensitizer triplet state will result in lower $^1O_2$ QY's. Nonradiative decay of the sensitizer S_1 or T_1 states and radiative decay such as fluorescence and phosphorescence have a significant impact on $^1O_2$ QY. For a full review of possible mechanisms for the generation and deactivation of $^1O_2$ see Schweitzer and Wilkinson's references.[50, 52] As a result, compounds with low or no luminescence emission are desirable for $^1O_2$ sensitization. Incorporation of functional groups that can promote intersystem crossing to the triplet state is one method to increase the $^1O_2$ QY. Inclusion of heavy atoms such as halogens and heterocyclic compounds with non-bonding π electrons have been found to promote intersystem crossing efficiently.[2]

The 2PA cross section (δ) is an important parameter of the sensitizer and is a measure of the sensitizer's ability to absorb two photons. The cross-section is used to determine the wavelength at which maximum absorption will be obtained for optimal excitation of the sensitizer. Given the SI unit Göppert-Mayer, (GM) in honor of Maria Göppert-Mayer, it is expressed in the units of 1×10^{-50} cm^4 sec $molecule^{-1}$ $photon^{-1}$. As mentioned previously, one cannot rely on the one-photon absorption spectrum to quantitatively predict where 2PA will occur. For fluorescent molecules, whose fluorescent QY has been previously determined, the 2PA cross-section can be determined from the fluorescence emitted under 2PA.[155] However, most good $^1O_2$ sensitizers exhibit no fluorescence or very low fluorescence, making this method difficult.

The nonlinear 2PA cross-section can be determined directly by the open aperture Z-scan method.[156] The experimental set up is shown in Figure 29. In the experiment, a focused Gaussian monochromatic beam is passed through a thin sample (< 2 mm) and the transmittance is measured as the sample is passed through the propagation path of the beam. The trace is expected to be symmetric with respect to the focus where there will be a minimum transmittance due to nonlinear absorption. The 2PA cross section can be determined from a fitting of the normalized transmittance as a function of position (z). Since the two-photon absorption cross section is a measure of how well the molecule will undergo 2PA, there has been considerable effort to increase this parameter. In general, compounds containing an electron rich aromatic central core such as fluorenes, distyryl benzenes, and naphthalene compounds have the ability to exhibit large 2PA cross sections.[19, 20, 53, 155, 157, 158] Increased conjugation length coupled to strong donor and acceptor groups have also been used to increase the intramolecular charge transfer character of molecules. The use of a rigid central π-conjugated system also helps to keep the conjugation in one plane, maintaining the conjugation through out the molecule. All of these approaches help to increase the 2PA cross section, but it should be noted that modifications to the molecular architecture often lead to manifestations of other properties such as fluorescence, changes in absorption wavelength, and, most critically, changes in $^1O_2$ QY.

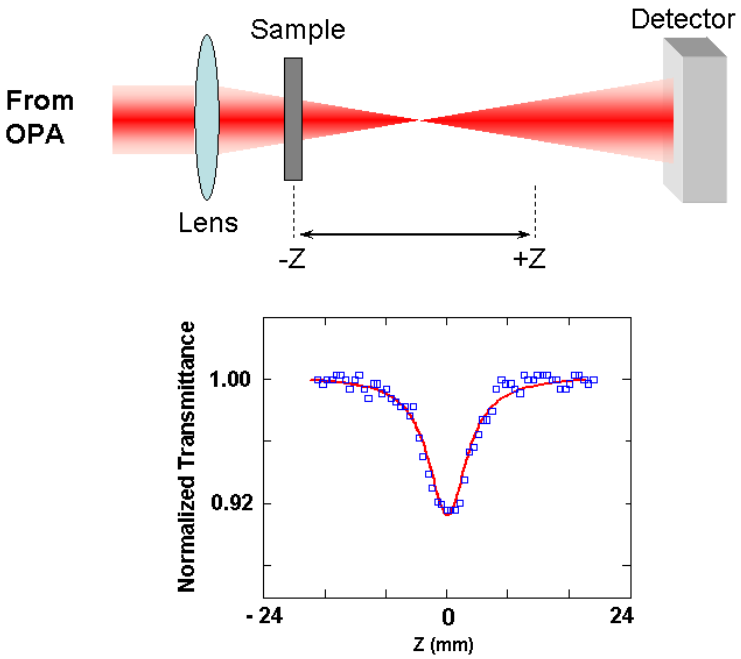

Figure 29. Z-scan experimental set up and plot of transmittance dependence on position z.

There have been a number of studies evaluating the 2PA cross section and $^1O_2$ QY of the PS's currently being used in PDT.[98, 101, 159] Protoporphyrin IX and Photofrin® have been reported to have very low 2PA cross sections of about 1 to 10 GM at 800 nm under femtosecond excitation. Additionally, chlorophyls, porphyrins, and phthalocyanines, have been reported to have 2PA cross-sections of several GM or less. Methods to increase the 2PA cross-section of these PS's have been investigated, and much larger values have been reported in the range of several hundred up towards several thousand GM.[101, 160] Modification of the porphyrin ring with polarizable groups, such as diphenylaminostilbene substituents and other conjugated electron donor/acceptor groups, have been attempted with promising results.

2.3.2 Fluorene Based 2PA $^1O_2$ Sensitizers

Fluorene derivatives for nonlinear applications have been actively investigated in our laboratory for a number of years. Synthetic efforts and photophysical characterization of these compounds have been undertaken to better understand the nonlinear photophysical properties of various fluorene derivatives and to improve on these properties. Fluorene was originally chosen to serve as the central chromophore because it is a rigid, highly π-conjugated, ring system with high thermal stability. Synthetic derivatives are easily afforded by functionalization of the rings 2, 4, 7, and 9 positions (Figure 30). The 2, 4, and 7 positions are ideal locations for electron donor/acceptor substituents, and the hydrophilic nature of the derivatives can be controlled through the 9 position of fluorine, since this position can easily be made nucleophilic and modification typically does not perturb the electronic structure of the π conjugated system.

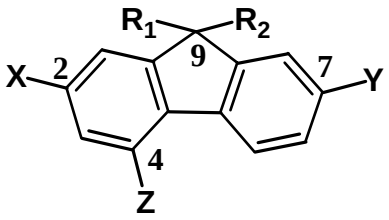

Figure 30. Chemical structure of fluorene chromophore showing the positions for synthetic modification by introducing various groups X, Y, Z, R_1, and R_2.

Investigations into the synthesis and characterization of the nonlinear absorption properties of fluorene derivatives have lead to a better understanding of these compounds. These investigations were intended to correlate the nonlinear absorptivity as a function of molecular structure. The systematic investigation has been pursued by examining the effects of different electron donating (D) and electron withdrawing (A) groups attached to fluorene in the 2 and 7

positions. These derivatives included symmetrical A-π-A, D-π-D, and unsymmetrical A-π-D structures. Furthermore, the π-conjugation length between the donor and acceptor groups was varied in an effort to increase the nonlinear absorption properties of the fluorene-based derivatives. A 4-fold increase in 2PA cross-section was observed over similar unsymmetrical fluorene derivatives utilizing benzothiazole accepting groups.[19] The effects of increased conjugation using styryl and vinylene moieties also resulted in higher 2PA cross sections and shifted the 2PA band from 600 to 800 nm. High 2PA cross sections (> 1000 GM, 800 nm) were observed for unsymmetrical fluorene derivatives with extended conjugation.[19, 157, 161] As a result of these studies, it is not uncommon to see large 2PA cross sections (500 to >1000 GM) at wavelengths in the near IR region.

In addition to large 2PA cross sections, fluorene derivatives have been of some interest due to a number of nonlinear applications such as optical data storage, optical power limiting, 3-D microfabrication, and nondestructive fluorescence imaging.[162-164] Since Ogilby's report of two-photon sensitized formation of $^1O_2$ there have been a number of investigations to develop new two-photon activated sensitizers. Gollnick *et al.* reported singlet oxygen formation from fluorene derivatives in the 1970s, and recently Mehrdad *et al.* investigated the mechanism of $^1O_2$ formation with a series of fluorene derivatives.[74, 165] Mehrdad reported overall rate constants, T_1 state energies (E_T), oxidation potentials, and overall efficiencies of $^1O_2$ formation (S_Δ) for the fluorene derivatives. Impressive triplet state energies (270-285 kJ mol^{-1}) and overall efficiencies (~ 0.3-0.7) were reported. Recently, investigations of nonfluorescent, hydrophobic fluorene derivatives in our laboratory lead to the formation of singlet oxygen under 1PA and 2PA, providing the motivation for this dissertation.[18, 166]

The synthetic approach that was taken was to synthesize water soluble or hydrophilic fluorene derivatives that are capable of photosensitizing the formation of singlet oxygen under two-photon excitation. Hydrophilicity or water solubility was accomplished by utilizing alkyl carboxylic acid or short (3 repeat units) ethoxy chains in the 9 position of fluorene. The possibility of populating the sensitizer triplet state was accomplished by synthesizing fluorene derivatives containing heavy atoms and functional groups such as iodide and nitro groups in position 2 and 7. Benzothiazole derivatives were also synthesized in an effort to increase the conjugation and enhance the 2PA cross section of the sensitizer. A detailed discussion of the synthesis and motivation of our approach will be presented in chapter 3.

CHAPTER 3: SYNTHESIS OF FLUORENE-BASED SINGLET OXYGEN SENSITIZERS

The synthesis of several hydrophilic singlet oxygen photosensitizers will be discussed in this chapter. All solvents and reagents were purified prior to use, and commercially available reagents were used as received unless otherwise noted. Reactions were carried out under nitrogen or argon atmospheres. ^{1}H NMR spectra were recorded on Varian Mercury-300 (300 MHz) or Varian Innova-500 NMR (500 MHz) spectrometers using TMS as the internal standard where the chemical shift was reported in parts per million (ppm). ^{13}C NMR spectra were recorded on Varian Mercury-300 (75 MHz) NMR spectrometer. High resolution mass spectrometry analysis were performed in the Department of Chemistry at the University of Florida. Elemental analyses were performed by Atlantic Microlabs.

3.1.1 Synthesis of Photosensitizer 1

The synthesis 3,3'-(2-iodo-7-nitro-9*H*-fluorene-9,9-diyl)dipropanoic acid (PS **1**) began from fluorene after recrystallization from hexanes (Scheme 1). The synthesis involved the acid-catalyzed nitration of fluorene in the 2 position. Fluorene (20.0 g, 120 mmol) was placed in a three-neck flask equipped with a condenser and dissolved in 180 mL acetic acid. The solution was degassed under argon and heated to 50 °C. HNO_3 (28 mL, 70%) was then added dropwise through an addition funnel over 30 min while maintaining constant temperature, during which time a yellow precipitate formed. After HNO_3 addition, the reaction was slowly heated to 60-65 °C over 20-30 min. Once the precipitate was dissolved, the temperature was increased to 80 °C for 5 min. TLC (5:1 hexanes/ethyl acetate) indicated no starting material, at which point the

reaction was slowly cooled to room temperature. The reaction mixture was filtered through a Büchner funnel, affording a bright yellow precipitate. The crude product was placed in a beaker and washed twice with ice cold water and filtered each time resulting in the isolation of a pale yellow solid. The product was dried under vacuum to give 19.8 g (78% yd) of product (mp = 161-163 °C), was determined to be pure after TLC and ^{1}H NMR analysis, and used without further purification.

Scheme 1. Synthesis of fluorene based $^1O_2$ photosensitizer **1** (PS **1**).

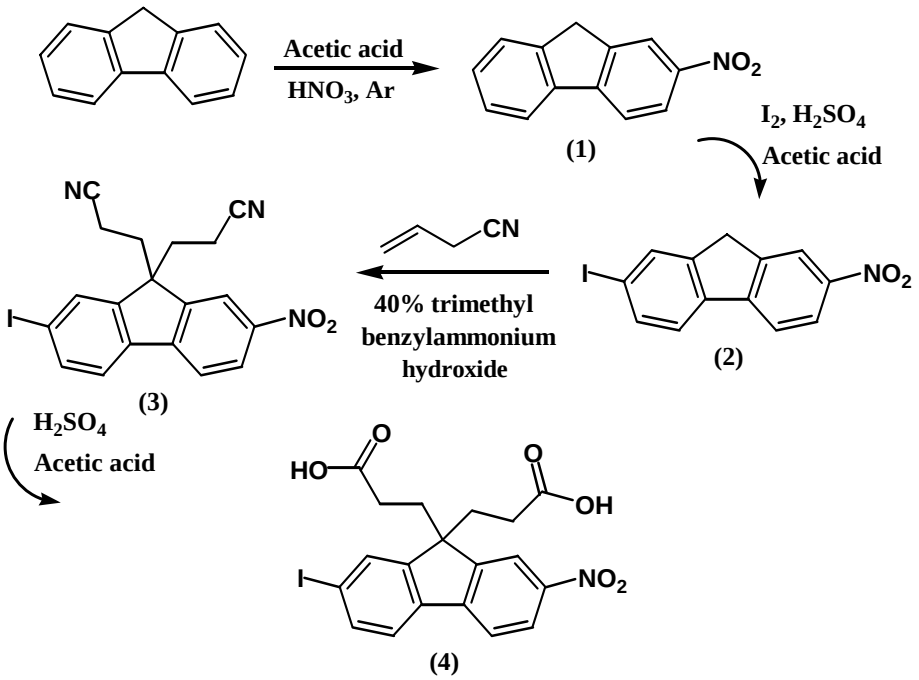

2-Nitrofluorene (intermediate **1**) was then converted to the iodo nitro intermediate **2** by placing 19.0 g (90 mmol) intermediate **1** into a three neck flask and dissolving it in 600 mL acetic acid and degasseing under argon. I_2 (11.4 g, 90 mmol) was then added to the solution at

room temperature and allowed to stir for 20 min, after which time an orange-brown mixture with undissolved material was observed. $NaNO_2$ (6.58 g, 95 mmol) was added, followed by the slow addition of 62 mL (98%) H_2SO_4. The reaction was slowly heated to 115-120 °C and maintained at this temperature for 1 h while monitoring by TLC (5:1 hexanes/ethyl acetate). The reaction was stopped, cooled to room temperature, and isolated by filtration. The crude cake was washed with three small portions of cold water. The filtrate was added to 500 mL ice, and the precipitate was filtered and combined with the crude product. The product was dried and recrystallized from acetic acid, yielding 28.5 g (94% yd) of bright yellow needle like crystals (mp = 248-249.5 °C).

Intermediate **2** (2-iodo-7-nitrofluorene) was converted to the nitrile derivative (intermediate **3**) by Triton B (benzyltrimethylammonium hydroxide)-catalyzed addition of acrylonitrile to fluorene in the 9 position. Intermediate **2** (2.4 g, 7.1 mmol) was dissolved in dioxane (12 mL) and degassed for ~ 20 min. under N_2 atmosphere. Triton B (40%, 0.11 mL) in water was added slowly through a syringe resulting in a brown mixture. Acrylonitrile (0.80 g, 15 mmol) was slowly added while maintaining a near constant temperature (40–45 °C). The greenish-brown solution was stirred at room temperature for 21 h while monitoring by TLC (7:3 hexanes/ethyl acetate). The reaction was neutralized with ~ 7 mL 10% HCL followed by the addition of 20 mL distilled water. The crude product was extracted with CH_2Cl_2, dried over anhydrous $MgSO_4$, and the solvent was removed at reduced pressure. A brown oil was obtained (56% yield) after purification by recrystallization from dioxane to give 1.8 g intermediate **3**. M.p. 312-313°C. ^{1}H NMR (500 MHz, DMSO-d_6) δ 8.59 (s, 1H, Ph), 8.33(d, J=8.0 Hz, 1H, Ph), 8.15(m, 2H, Ph), 7.87(m, 2H, Ph), 2.62(m, 4H, CH_2), 1.66(t, *J*=7.3 Hz, 4H, CH_2). ^{13}C NMR (75 MHz, DMSO-d_6) δ 150.34, 148.13, 147.23, 147.08, 138.91, 138.25, 133.70, 125.19, 124.57,

122.00, 120.65, 120.25, 97.83, 54.92, 33.66, 12.37. Anal. Calcd. for $C_{19}H_{14}IN_3O_2$ (443.24): C, 51.49; H, 3.18; N, 9.48. Found: C, 51.51; H, 3.23; N, 9.32.

The nitrile group of intermediate **3** was hydrolyzed in a 1:1 mixture of H_2SO_4 in acetic acid by refluxing for 24 h. After cooling to room temperature, the precipitate was filtered and recrystallized from isopropanol and hexane, affording 1.6 g (81% yd) of compound **4** (3,3'-(2-iodo-7-nitro-9*H*-fluorene-9,9-diyl)dipropanoic acid , PS **1**). M.p. 292-293 °C. ^{1}H NMR (300 MHz, DMSO-d_6) δ 11.90 (s, 2H, OH), 8.41(s, 1H, Ph), 8.27 (m, 1H, Ph), 8.09(m, 2H, Ph), 7.83(m, 2H, Ph), 2.41(m, 4H, CH_2), 1.34(t, *J*=8.3 Hz, 4H, CH_2). ^{13}C NMR (75 MHz, DMSO-d_6) δ 174.18, 152.72, 149.41, 147.96, 146.93, 138.74, 137.62, 133.18, 124.60, 124.39, 121.74, 119.77, 97.55, 55.13, 33.97, 29.52. ESI-TOF MS: theoretical m/z $[M+Na]^+$ = 503.9914, found 503.9916.

3.1.2 Synthesis of Photosensitizer 2

PS **2** (3,3'-(2-(benzo[d]thiazol-2-yl)-7-nitro-9*H*-fluorene-9,9-diyl)dipropanoic acid) was synthesized starting from intermediate **2** by first converting the iodo group to the nitrile using CuCN. Intermediate **2** (5.0 g, 14.8 mmol) and CuCN (1.4 g, 15.6 mmol) were placed in 41 mL dry DMF, degassed, and brought to reflux under N_2 for 1.5 h. The reaction was monitored by TLC (5:1 hexanes/ethyl acetate). Upon cooling to 85 °C, a solution of $FeCl_3 \cdot 6H_2O$ (5.9 g, 22 mmol), dissolved in 1.4 mL 36% HCl and 9.0 mL distilled water, was added, and the reaction was maintained at 60-70 °C for 1 h. The reaction mixture was cooled to room temperature and precipitate collected by filtration, washed with two small portions of distilled water, and once with 95% ethanol. The crude product was recrystallized from a 1:1 mixture of DMSO/toluene to

afford 2.8 g (79% yd) of a pale yellow solid (mp 280.5-282, lit. 281-282),[167] designated as intermediate **5**. M.p. 280.5 – 282 °C. ^{1}H NMR (300 MHz, DMSO-d_6) δ 8.50(s, 1H, Ph-H), 8.29(m, 3H, Ph-H), 8.14(s, 1H, Ph-H), 7.91(d, *J*=4.5 Hz, 1H, Ph-H), 4.15(s, 2H, CH_2). ^{13}C NMR (75 MHz, DMSO-d_6) 147.74, 146.17, 145.85, 143.85, 131.98, 129.82, 123.58, 123.26, 122.73, 121.26, 119.77, 111.23, 104.92, 37.61.

Intermediate **5** was hydrolyzed to the carboxylic acid derivative by dissolving 2-iodo-9*H*-fluorene-7-carbonitrile, the synthesis of which has been reported elsewhere,[168] (2.5 g, 10.6 mmol) in 10 mL 70% H_2SO_4, and 10 mL acetic acid. The mixture was refluxed for 48 h. After completion, the cooled precipitate was collected by filtration and recrystallized from DMSO twice to afford 1.6 g (58% yd) of intermediate **6**. M.p. 338-340 °C (lit. 334-335 °C). ^{1}H NMR (300 MHz, $CDCl_3$) δ 8.48 (s, 1H, Ph-H), 8.31 (d, *J* = 8.4 Hz, 1H, Ph-H), 8.22 (s+d, 2H, Ph-H), 8.17 (d, *J* = 7.8 Hz, 1H, Ph-H), 8.03 (d, *J* = 8.1 Hz, 1H, Ph-H), 4.15 (s, 2H, CH_2). ^{13}C NMR (75 MHz, $CDCl_3$) 167.73, 147.39, 146.92, 145.97, 145.68, 143.52, 131.28, 129.14, 126.92, 123.53, 122.29, 122.23, 121.17, 37.59. HRMS-ESI theoretical m/z $[M+Na]^+$ = 278.0424, found 278.0441.

The carboxylic acid group of intermediate **6** (1.5 g, 5.9 mmol) was converted to the acid chloride (intermediate **7**) by dissolving it in thionyl chloride (4 mL) and bringing it to reflux for 4 h under N_2. After completion, the excess thionyl chloride was removed under reduced pressure. The dried residue of intermediate **7** was mixed with 2-aminobenzenethiol (0.74 g, 5.9 mmol) in 10 mL *N*-methylpyrrolidone (NMP) and heated to 100 °C for 15 h. The reaction was cooled to room temperature, precipitated with 95 % ethanol, and collected by filtration. The solid material was washed with ethanol followed by hexane, and dried at reduced pressure. The crude product was recrystallized from DMSO to afford 1.5 g (74% yd) of intermediate **8**. M.p.

298-299 °C , ^{1}H NMR (300 MHz, DMF-d_7) δ 8.72(s, 1H, Ph-H), 8.63(s, 1H, Ph-H), 8.57-8.43(m, 4H, Ph-H), 8.38(d, *J*=8.1 Hz, 1H, Ph-H), 8.29(d, *J*=9.0 Hz, 1H, Ph-H), 7.77 (t, *J*=8.1 Hz, 1H, Ph-H), 7.68(t, *J*=7.2 Hz, 1H, Ph-H), 3.67(s, 2H, CH_2). HRMS-EI theoretical m/z $[M]^+$ = 344.0620, found 344.0620. Anal. Calcd. for ($C_{20}H_{12}N_2O_2S$): C, 69.75; H, 3.51; N, 8.13; S, 9.31. Found: C, 69.68; H, 3.53; N, 8.09; S, 9.39.

Scheme 2. Synthesis of fluorene based $^1O_2$ photosensitizer **2** (PS **2**).

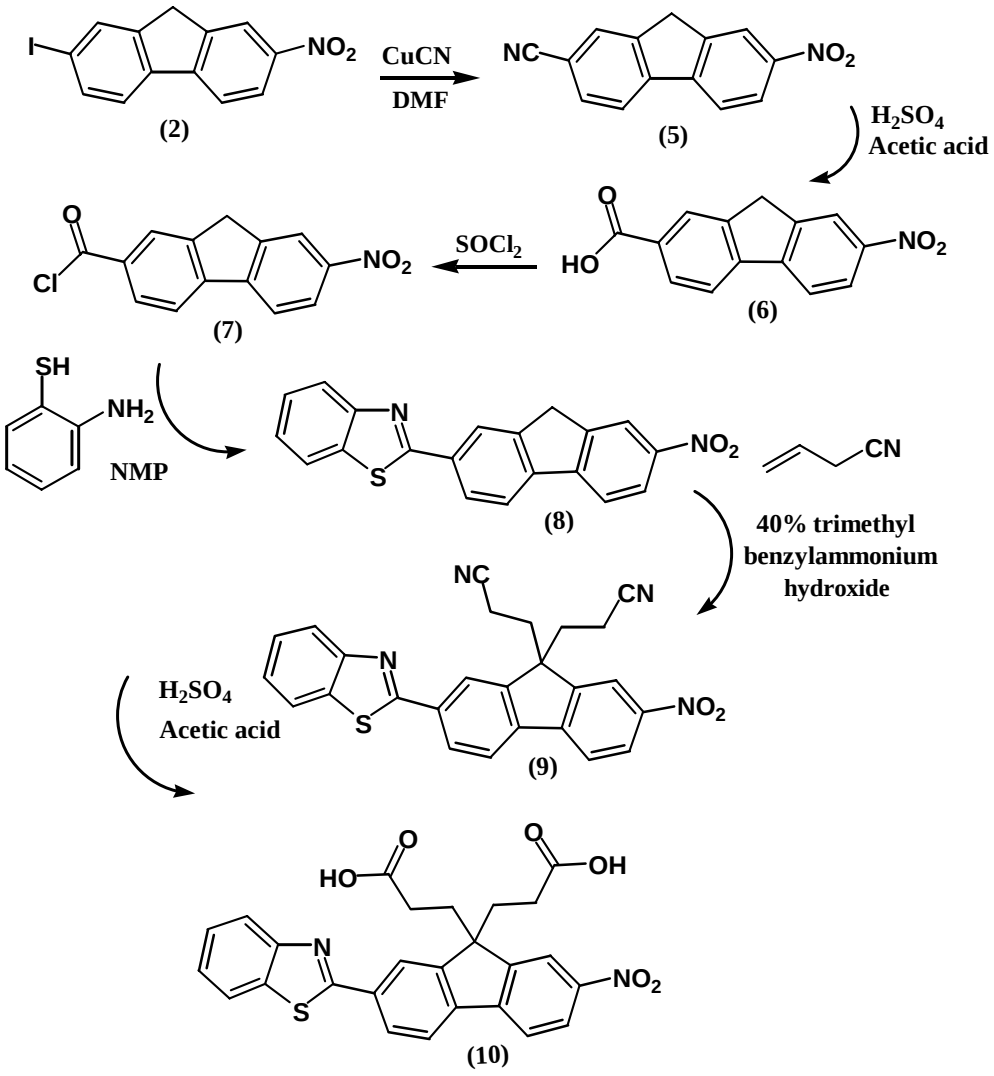

Intermediate **8** was converted to the dinitrile derivative by Triton B-catalyzed addition of acrylonitrile to fluorine, as previously described. Briefly, intermediate **8** (1.5 g, 4.4 mmol) was dissolved in dioxane (8 mL) and degassed under N_2. 40% Triton B (0.07 mL) was added slowly, followed by the addition of acrylonitrile (0.49 g, 9.1 mmol) while maintaining a near constant temperature (40–45 °C). The greenish-brown solution was stirred at room temperature for 23 h, while monitoring by TLC (7:3 hexanes/ethyl acetate), and was neutralized with ~ 5 mL 10% HCL followed by the addition of 13 mL distilled water. The crude product was extracted with CH_2Cl_2, dried over anhydrous $MgSO_4$, and the solvent was removed at reduced pressure. A brown oil was obtained after purification by recrystallization (99:1 CH_2Cl_2/methanol) to afford 1.8 g (91% yd) of intermediate **9**. M.p. 236-237 °C, ^{1}H NMR (500 MHz, $CDCl_3$) δ 8.43 (d, J = 8.5 Hz, 1H, Ph-H), 8.34 (s, 1H, Ph-H), 8.31 (s, 1H, Ph-H), 8.19 (d, J = 7.5 Hz, 1H, Ph-H), 8.13 (d, J = 7.0 Hz, 1H, Ph-H), 7.98 (m, 3H, Ph-H), 7.57 (t, J = 7.5 Hz, 1H, Ph-H), 7.47 (t, J = 7.5 Hz, 1H, Ph-H), 2.65 (m, 4H, CH_2), 1.73 (m, 2H, CH_2), 1.62 (m, 2H, CH_2). ^{13}C NMR (75 MHz, DMSO-d_6) δ 167.58, 154.02, 149.06, 148.35, 148.19, 146.71, 142.02, 135.22, 134.61, 129.00, 127.41, 126.32, 125.18, 123.57, 123.48, 123.24, 123.03, 122.40, 120.68, 120.24, 55.14, 33.80, 12.49. HRMS-EI theoretical m/z $[M]^+$ = 450.1150, found 450.1156. Anal. Calcd. for $C_{26}H_{18}N_4O_2S$·0.38dioxane (determined by ^{1}H NMR) (475.99): C, 69.44; H, 4.46; N, 11.77. Found: C, 69.22; H, 4.56; N, 11.45.

Photosensitizer **2** (compound **10**) was obtained after hydrolysis of intermediate **9** by refluxing 1.7 g (3.8 mmol) in a 1:1 mixture of H_2SO_4 in acetic acid for 24 h. The mixture was cooled to room temperature and the precipitate was collected by filtration. Recrystallization in THF and hexanes produced 1.4 g (78% yd) of PS **2**. M.p. 245-246 °C. ^{1}H NMR (300 MHz, DMSO-d_6) δ 11.88(br, 2H, OH), 8.48(s, 1H, Ph), 8.30(m, 2H, Ph), 8.214-8.07(m, 5H, Ph),

7.55(t, *J*=8.0 Hz, 1H, Ph), 7.48(t, *J*=8.0 Hz, 1H, Ph), 2.54(m, 4H, CH_2), 1.42(t, *J*=8.0 Hz, 4H, CH_2). ^{13}C NMR (75 MHz, DMSO-d_6) δ 174.20, 167.66, 154.15, 151.39, 150.63, 148.12, 146.65, 142.00, 135.29, 134.44, 128.48, 127.42, 126.34, 124.63, 123.58, 123.39, 123.02, 122.55, 122.20, 119.85, 55.31, 34.11, 29.58. HRMS theoretical m/z $[M+H]^+$ = 489.1115, found 489.1112.

3.1.3 Synthesis of Photosensitizer 3

Key intermediate **2** was converted to PS **3** (3,3'-(2-iodo-7-nitro-9*H*-fluorene-9,9-diyl)diethoxy-2-methoxyethane) in one step (Scheme 3). 2-Iodo-7-nitro-9*H*-fluorene (2.5 g, 7.4 mmol) was dissolved in 33 mL DMSO. KI (0.13 g, 0.8 mmol) and KOH (1.7 g, 30.3 mmol) were added and the solution was degassed for 20 min. 1-Bromo-2-(2-methoxyethoxy)ethane (3.3 g, 18 mmol) was added dropwise under Ar. The reaction was monitored by TLC (7:3 cyclohexane/ethyl acetate) and was stopped after 24 h. The reaction was worked up by adding 100 mL brine and extracting the product with five 25 mL portions of CH_2Cl_2. The organic layers were combined and washed with a final 100 mL portion of fresh brine solution. The organic layer was dried over anhydrous $MgSO_4$, filtered, and the CH_2Cl_2. was removed under reduced pressure, affording a dark brown oil. The product (compound **11**) was purified by column chromatography (7:3 cyclohexane/ethyl acetate) to give 3.0 g (74% yd) of a dark amber oil. ^{1}H NMR (300 MHz, $CDCl_3$) δ: 8.26 (s, 1H, ArH), 8.24 (d, 1H, ArH), 7.82 (s, 1H, ArH), 7.76 (d, 1 H, ArH), 7.73 (1H, ArH), 7.51 (d, 1H, ArH), 3.26 (s, 6H, OCH_3), 3.23 (m, 4H, OCH_2), 3.15 (m, 4H, OCH_2), 2.80 (m, 4H, OCH_2), 2.43 (m, 4H, CH_2). ^{13}C NMR (75 MHz, $CDCl_3$) δ: 152.92, 150.11, 147.59, 145.90, 137.85, 137.01, 133.25, 123.79, 122.81, 120.19, 119.22, 95.73, 71.98,

70.28, 67.06, 59.37, 52.61, 39.59. Anal. Calcd. for $C_{23}H_{28}INO_6$: C, 51.03; H, 5.21; N 2.59. Found: C, 50.96; H, 5.23; N, 2.59.

Scheme 3. Reaction of key intermediate 2 with 1-bromo-2-(2-methoxyethoxy)ethane to form PS **3**.

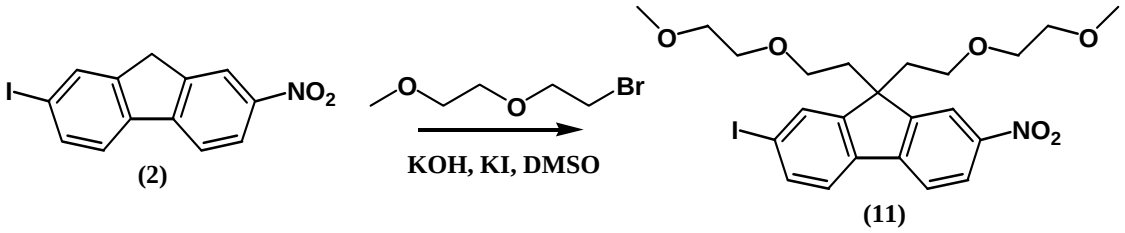

3.1.4 Synthesis of Photosensitizer 4

Key intermediate **8** was converted to PS **4** (3,3'-(2-(benzo[d]thiazol-2-yl)-7-nitro-9*H*-fluorene-9,9-diyl)diethoxy-2-methoxyethane) in one step, as previously described (Scheme 4). Briefly, 2-benzothiazole-7-nitro-9*H*-fluorene (1.3 g, 3.8 mmol) was dissolved in 33 mL DMSO. KI (0.06 g, 0.038 mmol), and KOH (0.85 g, 15.1 mmol) were added and the solution was degassed for 20 min. 1-Bromo-2-(2-methoxyethoxy)ethane (1.7 g, 9.1 mmol) was added dropwise under Ar. The reaction was monitored by TLC (7:3 cyclohexane/ethyl acetate) and was stopped after 24 h. The reaction was worked up by adding 100 mL brine and extracting the product with five 25 mL portions of CH_2Cl_2. The organic layers were combined and washed with a final 100 mL portion of fresh brine solution. The organic layer was dried over anhydrous $MgSO_4$, filtered, and the CH_2Cl_2. was removed under reduced pressure to afford a dark brown oil. The product (compound **12**) was purified by column chromatography (7:3 cyclohexane/ethyl

acetate) to give 1.4 g (69%) of a dark amber oil. ^{1}H NMR (300 MHz, $CDCl_3$) δ: 8.33 (s,1H, ArH), 8.30 (d, 1H, ArH), 8.22 (s, 1H, ArH), 8.15 (d, 1H, ArH), 8.11 (d, 1H, ArH), 7.94, (d, 1H, ArH), 7.88 (d, 1H, ArH), 7.86 (d, 1H, ArH), 7.52 (t, 1H, ArH), 7.41 (t, 1H, ArH), 3.22 (m, 4H, OCH_2), 3.21 (m, 6H, OCH_3), 3.15, (m, 4H, OCH_2), 2.90 and 2.82 (m, 4H, OCH_2), 2.55, (t, 4H, CH_2). ^{13}C NMR (75 MHz, $CDCl_3$) δ: 167.37, 154.17, 151.70, 151.37, 147, 67, 145.78, 140.89, 135.18, 134.59, 127.81, 126.71, 125.66, 123.76, 123.47, 122.60, 121.90, 121.85, 120.60, 119.37, 71.94, 70.25, 67.16, 59.29, 52.77, 39.67. Anal. Calcd. for $C_{30}H_{32}N_2O_6S$: C, 65.67; H, 5.88; N 5.11. Found: C, 65.73; H, 5.98; N, 4.96.

Scheme 4. Reaction of key intermediate 8 with 1-bromo-2-(2-methoxyethoxy)ethane to form PS **4**.

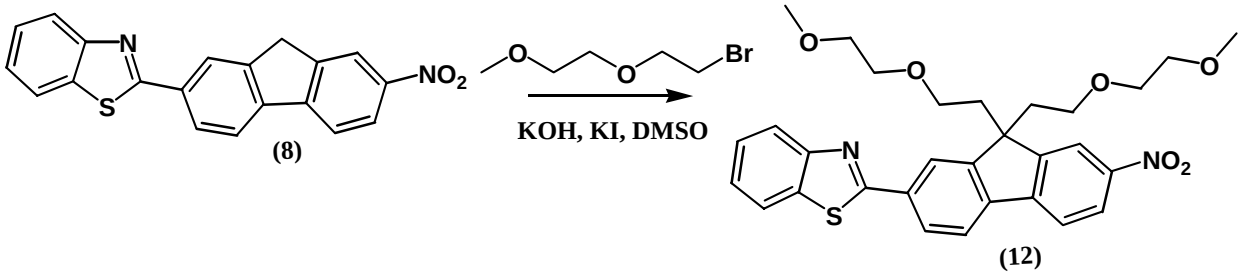

CHAPTER 4: PHOTOPHYSICAL CHARACTERIZATION OF $^1O_2$ SENSITIZERS

This chapter will focus on the linear and nonlinear photophysical properties of the hydrophilic fluorene derivatives described in the previous chapter. Linear spectral properties will be reported in the first section for these derivatives at room temperature and 77 K in organic solvent. A brief comment will be made on the low temperature measurements that were performed to estimate the energies of the lowest triplet state of the sensitizers. In section 4.2, the nonlinear optical parameters will be reported under steady state excitation at room temperature. In addition, the characterization of $^1O_2$ generation under 1PE and results from investigating the spectral dependence of its formation will be described. The final section will conclude with a discussion of $^1O_2$ generation under pulsed 2PE and determination of the corresponding 2PA cross section for each fluorene sensitizer.

4.1.1 Linear Photophysical Characterization at Room Temperature and 77 K

The steady-state linear absorption spectra were obtained with an Agilent UV-visible spectrophotometer. Excitation and luminescence spectra were obtained with a PTI Quantamaster spectrofluorimeter equipped with a PMT and a nitrogen cooled (77 K) Hamamatsu R5509-73 PMT. All luminescence measurements were performed in the photon-counting regime of detectors, using 10 mm path length quartz cuvettes with concentrations of PS, $C \leq 3 \times 10^{-6}$ M. The emission spectra were corrected for the spectral sensitivity of detectors. The optical density of the solutions did not exceed 0.15 at the corresponding excitation wavelengths. The fluorescence quantum yields of PS **1-4** were determined by a standard method relative to 9,10-

diphenylanthracene in cyclohexane using Equation 5.[121] From Equation 5, QY_S and QY_R are the fluorescence quantum yield, I_s and I_R are the integrated fluorescence emission intensity, OD_S and OD_R are the optical density of each solution, and n_S and n_R are the refractive indexes of the sample and reference solvents respectively.

$$QY_S = QY_R\left(\frac{I_S \times OD_R \times n_S^2}{I_R \times OD_S \times n_R^2}\right) \quad (5)$$

Equation 5. Relative fluorescence quantum yield determination.

Time-resolved emission spectra of PS **1**-**4** in ACN were measured at 77 K with a PTI Timemaster spectrofluorimeter (time resolution ~ 0.1 ns) in order to find the energy of their long-lived triplet electronic state that is primarily responsible for singlet oxygen generation. Low temperature measurements were performed in a NMR sample tube with deoxygenated solutions of PS **1**–**4** prepared by repeated freeze-pump-thaw cycles under nitrogen. The efficiency of a photosensitizer to generate singlet oxygen can be estimated by knowing the energy of the sensitizer's triplet state. Typically this energy should be greater than the higher energy orbital of $^1O_2$ ($^1\Sigma^+_g$) 157 kJ/mol. Oxygen was removed from a solution of each PS dissolved in acetonitrile (ACN) to prevent quenching by ground state oxygen and to increase the chances of observing phosphorescence by the sensitizer. Unfortunately, fluorescence emission and not phosphorescence was observed for all oxygen-free low temperature measurements. As a result, the linear spectra that follow contain fluorescence emission at 77 K and zero time delay. The time delay was increased incrementally (0 ~ 1 μs) while attempting to observe phosphorescence. As the delay was increased, the emission intensity decreased maintaining the

same spectral profile. If phosphorescence was present it could not be resolved from the fluorescence emission.

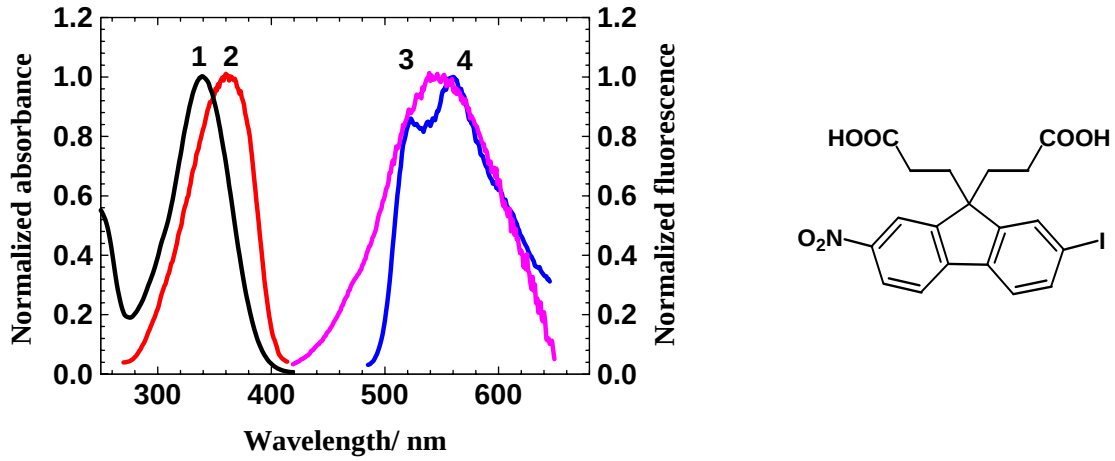

Figure 31. Linear spectral properties for PS 1: (1-black) absorption RT, (2-red) excitation 77 K, (3-magenta) fluorescence emission RT, (4-blue) fluorescence emission 77 K. The chemical structure of PS 1 is on the right.

The normalized linear spectra in ACN are presented in Figure 31 for PS **1**. The room temperature absorption (curve 1) and fluorescence emission (curve 3) are near mirror images of one another with a 206 nm Stokes shift, indicating strong charge-transfer in the S_1 excited state. An absorption maximum for the sensitizer is observed at 340 nm with $\varepsilon = 21{,}000\ M^{-1}\ cm^{-1}$. The low temperature excitation (curve 2) and fluorescence emission spectra (curve 4) exhibit nearly the same Stokes shift (199 nm) compared to the room temperature spectra. This would suggest that the sensitizer is not significantly affected by solvent relaxation of the S_1 excited state or that relaxation occurs very rapidly. Typically, one would observe a blue shift of the low temperature fluorescence emission if solvent relaxation had much of an effect on the S_1 state. This is because solvent molecules cannot rotate as rapidly and reorient around the fluorophore at low

temperature. The solvent dependent reorientation lowers the energy of the fluorophore excited state and can shift the fluorescence emission to longer wavelengths. The low temperature fluorescence emission (curve 4) shows additional vibrational structure than its absorption and excitation spectra which are devoid of fine structure. The fine structure is probably not seen at room temperature because excess vibrational energy is lost to solvent. The fluorescence quantum yield ($< 10^{-4}$) is also impressively low. A summary of the linear photophysical data can be found in Table 2.

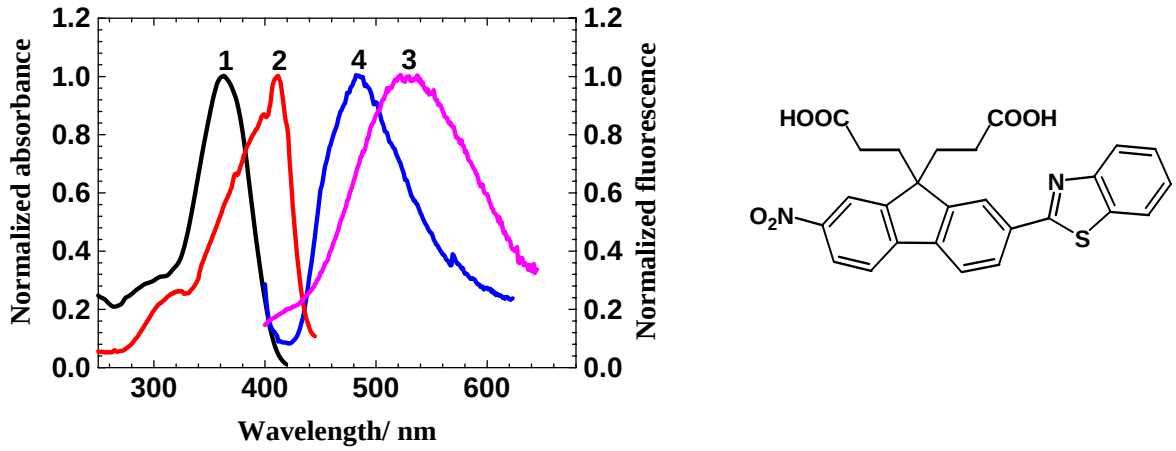

Figure 32. Linear spectral properties for PS 2: (1-black) absorption RT, (2-red) excitation 77 K, (3-magenta) fluorescence emission RT, (4-blue) fluorescence emission 77 K. The chemical structure of PS 2 is on the right.

The spectra for PS **2** obtained at room temperature and 77 K (Figure 32) exhibit less charge transfer character in the excited state compared to PS **1**. This is identified by the smaller Stokes shift (166 nm) between the absorption (curve 1) and fluorescence spectra (curve 3) at room temperature. Substitution of the iodo group with benzothiazole resulted in a small red shift (22 nm) in the main absorption band of curve 1 (362 nm) along with an increase in the molar

absorptivity (ε = 36,000 M^{-1} cm^{-1}) of the sensitizer. The emission spectra (curves 3 and 4) mirror their corresponding absorption (curve 1) and excitation spectra (curve 2) well. Clearly, there is a larger polar dependence on the sensitizer S_1 excited state as seen by the blue shift of the fluorescence emission (484 nm) at 77 K in comparison to the room temperature emission (528 nm), resulting in a 72 nm Stokes shift. The fluorescence QY for PS **2** remained sufficiently low (6 x 10^{-3}) , affording the possibility of efficient intersystem crossing to the triplet state.

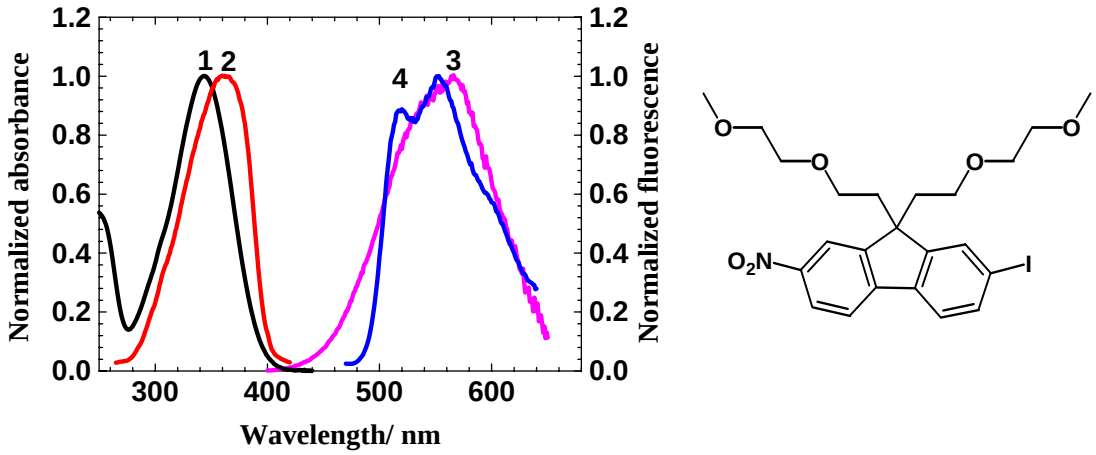

Figure 33. Linear spectral properties for PS **3**: (1-black) absorption RT, (2-red) excitation 77 K, (3-magenta) fluorescence emission RT, (4-blue) fluorescence emission 77 K. The chemical structure of PS **3** is on the right.

The linear spectral data for PS **3** is very similar to that of PS **1**, as expected. The absorption (curve 1) and fluorescence emission (curve 3) maxima were observed at 342 and 564 nm, respectively. Substitution of the two carboxylic acid groups with alkoxy chains in the 9 position of fluorene to affect solubility does not significantly perturb the main π-conjugation of the fluorene ring system. However, a small increase in the molar absorptivity (23,000 M^{-1} cm^{-1})

and a larger Stokes shift (223 nm, curve 3) was observed for PS **3** relative to the similar PS **1** derivative (21,000 M^{-1} cm^{-1}, 206 nm). It would appear that the S_1 state is somewhat affected by changes in the 9 position of fluorene, and substitution of a carboxylic acid with an alkoxy chain slightly increases the charge transfer character of the sensitizer. Comparison of the low temperature Stokes shift for PS **1** (199 nm) and PS **3** (191 nm) indicates that substitution with the alkoxy groups do not appear to change the polar dependence of the sensitizer as seen by their similar Stokes shift.

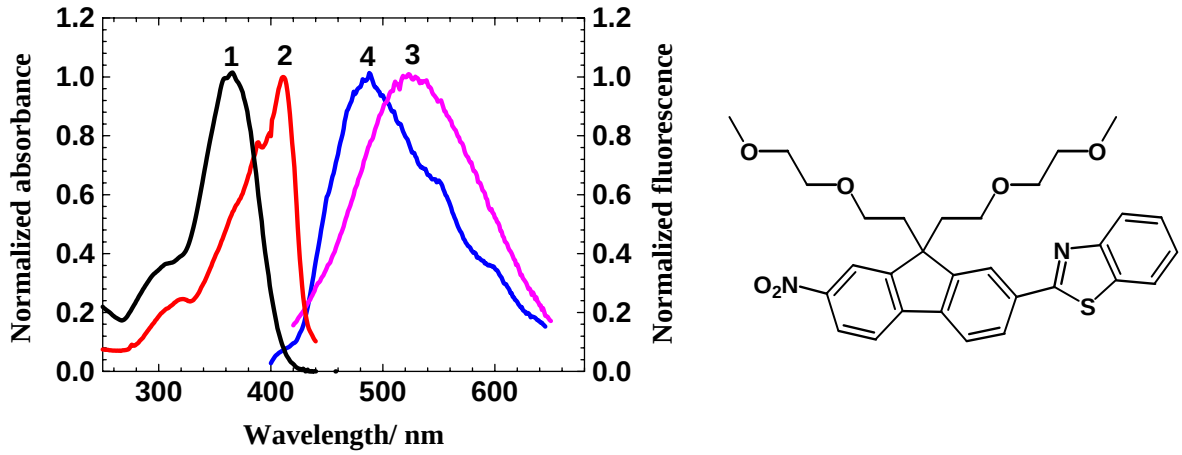

Figure 34. Linear spectral properties for PS **4**: (1-black) absorption RT, (2-red) excitation 77 K, (3-magenta) fluorescence emission RT, (4-blue) fluorescence emission 77 K. The chemical structure of PS **4** is on the right.

The maxima of absorption (curve 1) and emission (curve 3) of PS **4** were observed at 364 and 525 nm, respectively with a Stokes shift of 161 nm at room temperature. The fluorescence QY (7 x 10^{-3}) of PS **4** was determined to be quite small. The charge transfer character of PS **4** is nearly the same as the carboxylic acid derivative PS **2**. A slightly larger change in charge transfer character was observed between the two iodo nitro derivatives (PS **1** and **3**) when the

functional group for solubility was changed from the carboxylic acid to the alkoxy chain. The Stokes shift (75 nm) observed at low temperature (curve 4) is more than half that of the iodo nitro derivative (PS **3**, 191 nm). A similar result was observed for PS **2**, indicating that the two benzothiazole derivatives have a larger solvent dependence than the iodo derivatives. As with PS **2**, the alkoxy nitrobenzothiazole derivative (PS **4**) exhibits less charge transfer character, in addition to some solvent dependence, when compared to the iodo derivatives (PS **1** and **3**). Similar to PS **1** and **3**, the molar absorptivity (40,000 M^{-1} cm^{-1}) of PS **4** was about 10% larger than the carboxylic acid derivative PS **2** (36,000 M^{-1} cm^{-1}).

Table 2. Linear photophysical parameters of PS 1-4 in ACN: absorption, $^{abs}\lambda_{max}$, excitation, $^{exc}\lambda_{max}$, and steady state emission, $^{em}\lambda_{max}$, maxima, steady state Stokes shift, fluorescence quantum yield, Φ_{Fl}, and molar absorptivity, ε.

	PS 1	PS 2	PS 3	PS 4
$^{abs}\lambda_{max}$ nm (298 K)	340	362	342	364
$^{em}\lambda_{max}$ nm (298 K)	546	528	565	525
$^{exc}\lambda_{max}$ nm (77 K)	361	412	362	412
$^{em}\lambda_{max}$ nm (77 K)	560	484	553	487
Stokes shift, nm (298 K)	206	166	223	161
Stokes shift, nm (77 K)	199	72	191	75
Φ_{Fl} (298 K)	$\leq 10^{-4}$	$(6 \pm 2) \times 10^{-3}$	$\leq 1.3 \times 10^{-4}$	$(7 \pm 2) \times 10^{-3}$
ε M^{-1} cm^{-1}	21,000	36,000	23,000	40,000

Modification of the chromophore π conjugation resulted in small changes in spectroscopic properties of the investigated PSs. The iodo nitro derivatives (PS **1** and **3**) exhibited increased charge transfer character and less solvent polarity dependence when compared to the benzothiazole derivatives (PS **2** and **4**). Substitution of the iodo group by

benzothiazole resulted in a small red shift of the main absorption band and a small increase in the fluorescence QY. Modification for solubility increased the molar absorptivity by about 10% when the carboxylic acid group was substituted with an alkoxy chain, and nearly no change in absorption, fluorescence emission, or fluorescence QY was observed.

4.1.2 Singlet Oxygen Generation under One-Photon Excitation

Singlet oxygen luminescence, produced under steady-state excitation of the PS (Xe-lamp irradiation), was measured at room temperature with a PTI Quantamaster spectrofluorimeter using a cooled PMT (77 K) Hamamatsu R5509-73. The spectral resolution of the singlet oxygen phosphorescence spectra was ≈ 8 nm. The quantum yields of O_2 ($^1\Delta_g$) generation under one-photon excitation, Φ_Δ, were obtained for PS **1**-**4** from the relative steady-state measurements of singlet oxygen phosphorescence at ≈ 1270 nm in comparison with acridine in ACN ($\Phi_\Delta \approx 0.82$).[50] The quantum yields of O_2 ($^1\Delta_g$) generation in water was obtained for the two carboxylic acid derivatives (PS **1** and **2**) in phosphate buffered saline (0.1 M, pH 7.2) relative to rose bengal ($\Phi_\Delta \approx 0.76$). The singlet oxygen quantum yield was determined from Equation 6 where, QY_S and QY_R are the singlet oxygen quantum yield of the sample and reference, respectively, I_s and I_R are the integrated phosphorescence emission intensity of the sample and reference, respectively, P_S and P_R are the excitation power of the sample and reference, respectively, OD_S and OD_R are the optical density from the sample and reference, respectively. No photochemical decomposition of PS **1**-**4** was observed during these experiments.

$$QY_S = QY_R\left(\frac{I_S \times P_R \times OD_R}{I_R \times P_S \times OD_S}\right) \quad (6)$$

Equation 6. Relative singlet oxygen quantum yield determination.

The spectral dependence of the singlet oxygen quantum yield was determined for each PS over a broad spectral range (270 – 420 nm). A representative spectrum from PS **4** is presented in Figure 35. The spectral range investigated covers several possible electronic transitions of the PS. It is evident from the data that higher excited states (S_n) do not contribute to the production of singlet oxygen, and the most efficient singlet-triplet transitions of the fluorene-based PS occur from the lowest excited singlet electronic state (S_1). Hence, the quantum yield of singlet oxygen photosensitization is independent of excitation wavelength over the spectral region of PS absorption.

The values of Φ_Δ obtained from relative phosphorescence measurements are presented in Table 3. All PS's investigated were very efficient in producing singlet oxygen, especially the two nitro benzothiazole derivatives (PS **2** and **4**) with their Φ_Δ approaching unity. The iodo nitro derivatives had Φ_Δ values that were slightly smaller than the nitro benzothiazole derivatives. This is not surprising since it is known that the efficiency of $^1O_2$ production decreases as the charge transfer character of the sensitizer increases. The carboxylic acid derivatives (PS **1-2**) were water soluble, enabling their quantum yields of O_2 ($^1\Delta_g$) generation in PBS to be measured. These two derivatives had fairly large Φ_Δ values (≈ 0.4) in water, which are at least twice that of many of the water soluble $^1O_2$ sensitizers that are being developed by other groups.[55] Most water soluble sensitizers that have been developed for 1PE or 2PE have $^1O_2$ QYs < 0.20 and are typically closer to 0.05.

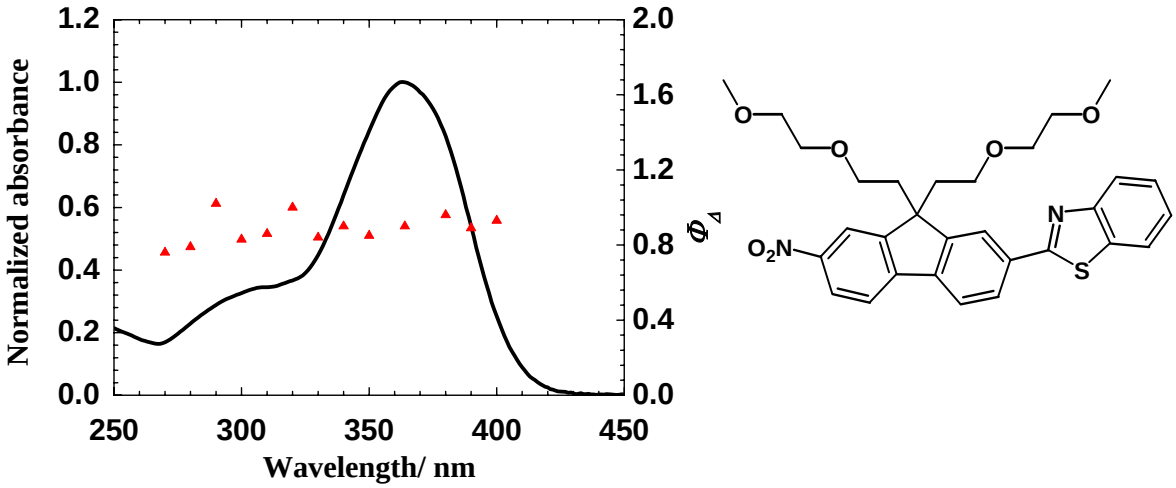

Figure 35. Spectral dependence of singlet oxygen quantum yield generation, Φ_Δ (red triangles), for PS 4 in ACN under one-photon excitation along with its corresponding one-photon absorption spectrum (black line).

Table 3. Quantum yields of singlet oxygen generation, Φ_Δ, under one-photon excitation of PS **1-4**, and molar absorptivity, ε, measured at $^{abs}\lambda_{max}$ in ACN.

	PS 1	PS 2	PS 3	PS 4
Φ_Δ (ACN)	0.65 ± 0.07	0.93 ± 0.10	0.74 ± 0.08	0.92 ± 0.10
Φ_Δ (H_2O)*	0.43 ± 0.10	0.34 ± 0.02	NA	NA
ε M^{-1} cm^{-1}	21,000	36,000	23,000	40,000

* Measured in phosphate buffered saline 0.1 M, pH 7.2. (NA) sensitizer was not measured due to poor solubility.

The irradiance dependence on excitation power was investigated to determine if there were any nonlinear processes occurring under 1PE of the investigated PS's. All compounds exhibited a linear response with a slope of nearly 1 (Figure 36). Accordingly, no nonlinear, quenching, or photodecomposition processes were observed during analysis.

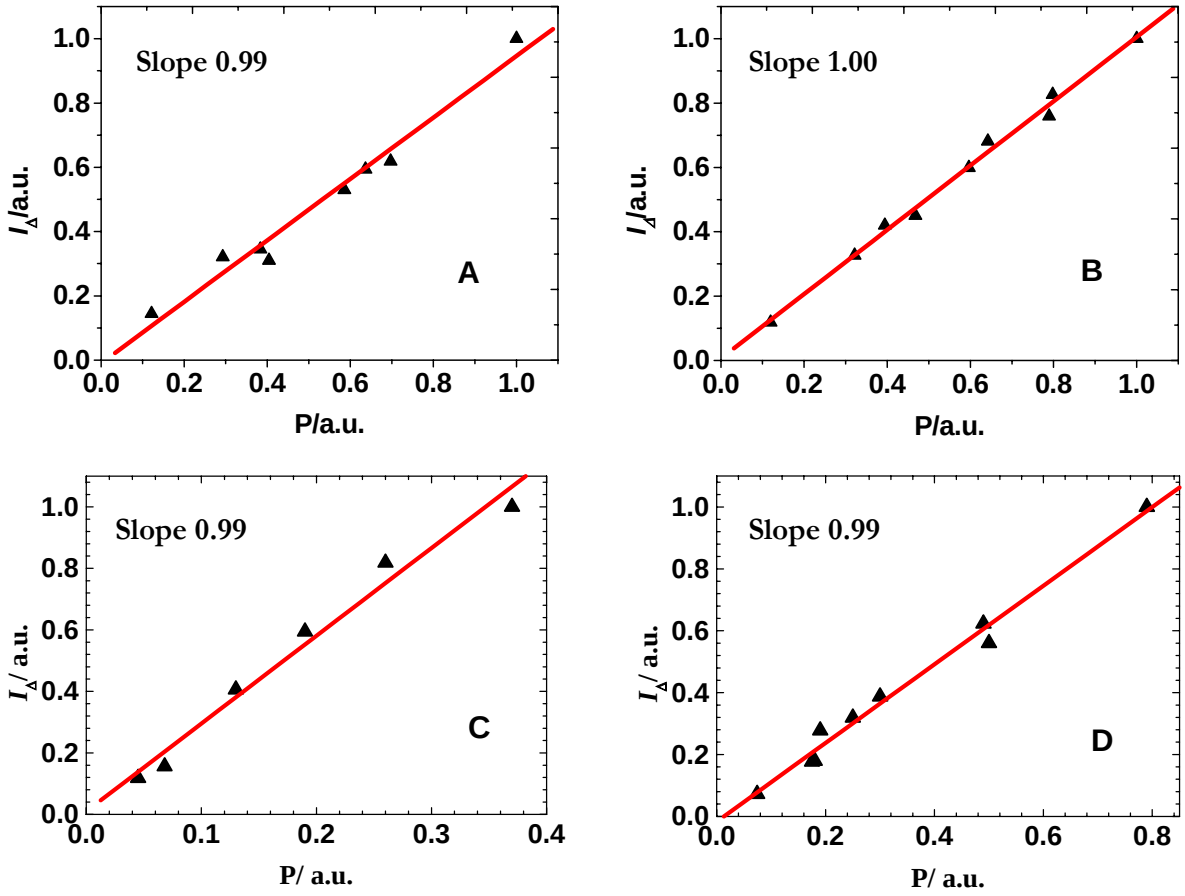

Figure 36. Dependence of singlet oxygen phosphorescence intensity under, I_Δ, under 1PE in ACN on the excitation power, P, at $^{abs}\lambda_{max}$: A) PS-1, B) PS-2, C) PS-3, D) PS-4.

4.1.3 Singlet Oxygen Generation under Two-Photon Excitation

The efficiency of 2PA of PS **1-4** was determined by the open aperture Z-scan method[156] using a picosecond Nd:YAG laser (PL 2143 B Ekspla) coupled to an optical parametric generator (OPG 401/SH). Pulse energies were measured with a Laserstar power meter (Ophir Optronics, Inc.). Two-photon induced average phosphorescence intensities of $^1O_2$ was measured

using the PTI Quantamaster spectrofluorimeter and the cooled PMT under femtosecond laser excitation (Clark-MXR, CPA-2001), with pulse duration ≈ 140 fs (FWHM), repetition rate 1 kHz, output wavelength 775 nm, and average power ≤ 200 mW. The laser beam was focused into 10 mm path length fluorometric quartz cuvettes to a waist radius of ≈ 1.5 mm. No evidence of white-light continuum generation was observed in the solutions under the experimental conditions. Concentrations of the investigated PS in ACN were in the range $10^{-4} \leq C \leq 10^{-3}$ M. The quantum yields of $^1O_2$ sensitization under two-photon excitation, $^{2PA}\Phi_\Delta$, were determined by the same relative steady-state method as in the case of linear, one-photon, singlet oxygen generation. The averaged phosphorescence of singlet oxygen produced by two-photon absorption of PS **1**-**4** was measured in comparison with the corresponding phosphorescence intensity from a solution of 3,3'-(2-(benzo[d]thiazol-2-yl)-7-nitro-9H-fluorene-9,9-diyl)dipropanoic acid, used as a standard under the same experimental geometry and average power of the laser beam. In this case, the values of $^{2PA}\Phi_\Delta$ can be calculated from Equation 7.

$$^{2PA}\Phi_\Delta = {}^{2PA}\Phi_\Delta^R \left(\frac{I_\Delta^S \times \delta_{2PA}^R}{I_\Delta^R \times \delta_{2PA}} \right) \quad (7)$$

Equation 7. Calculation for determining singlet oxygen quantum yield by 2PA.

Where I_Δ, I^R_Δ, δ_{2PA}, and δ^R_{2PA} are the average steady-state phosphorescence emission of singlet oxygen from the PS solutions and 2PA cross-sections of the sample and reference PS at the excitation wavelength (λ_{exc} = 775 nm), respectively. The $^{2PA}\Phi_\Delta{}^R$ is the quantum yield of $^1O_2$ sensitization under two-photon excitation of the reference PS. The typical phosphorescence signal of $^1O_2$ produced under two-photon excitation of PS **1**-**4** in ACN is shown in Figure 37.

These signals are proportional to I_Δ and were used for the determination of ${}^{2PA}\Phi_\Delta$. The value of I_Δ exhibited a linear dependence on the square of excitation power for all the investigated PS, consistent with pure 2PA processes and low quenching efficiency (Figure 38).

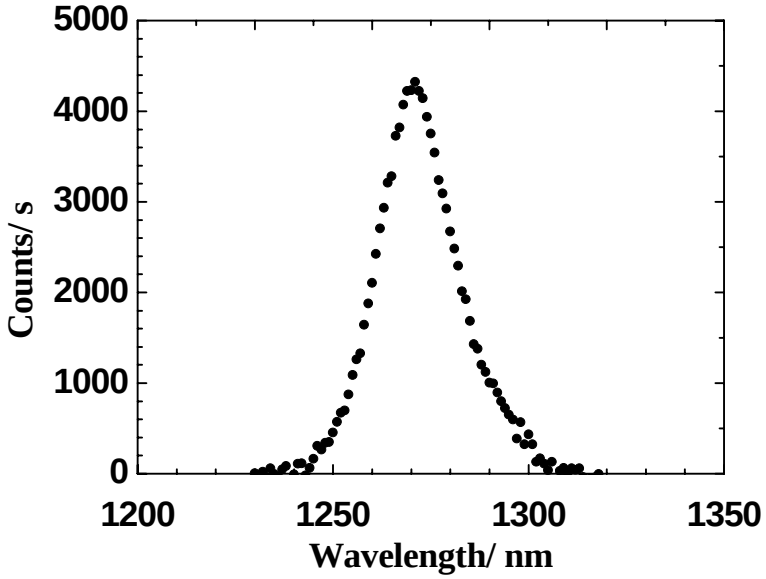

Figure 37. Average phosphorescence signal of singlet oxygen produced by PS 4 in ACN under femtosecond two-photon excitation at 775 nm.

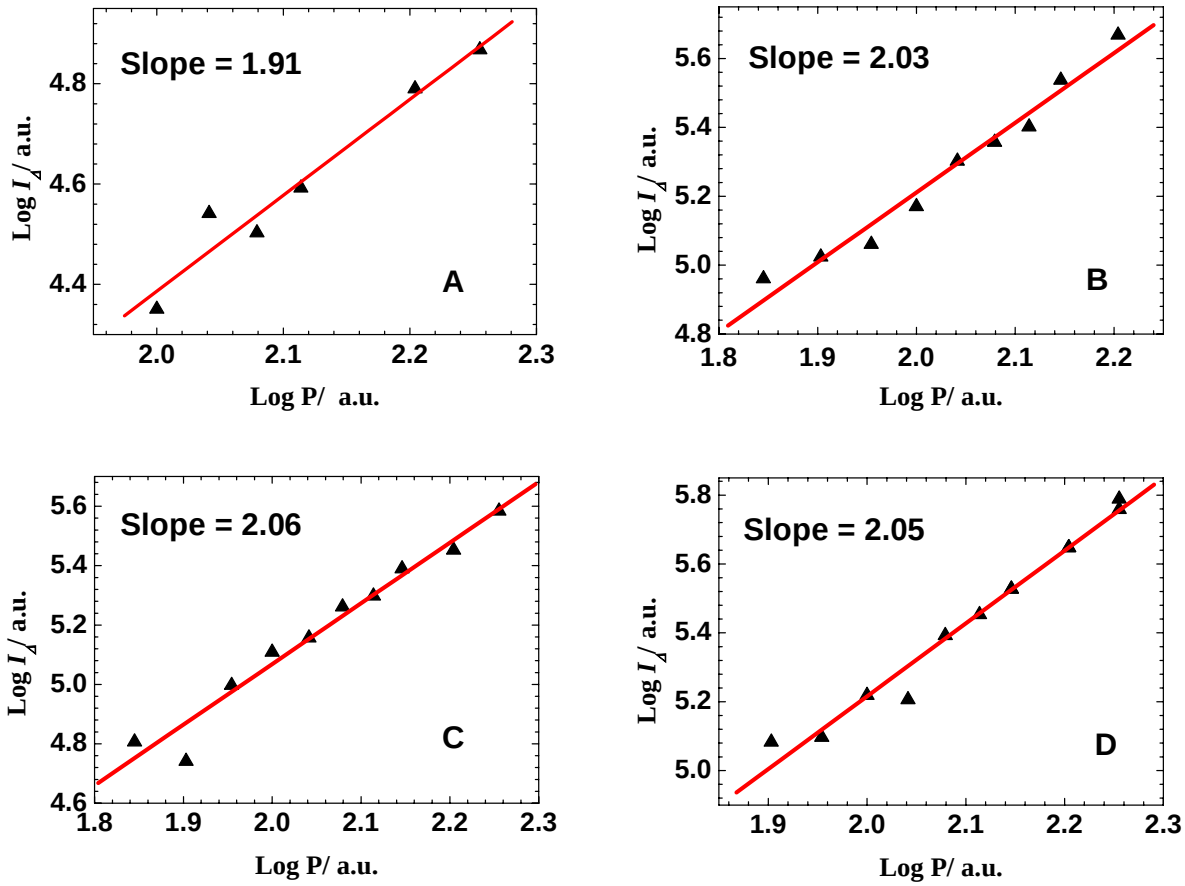

Figure 38. Dependence of singlet oxygen phosphorescence intensity, I_Δ, under 2PE in ACN on the excitation power, P, at 775 nm: A) PS-1, B) PS-2, C) PS-3, D) PS-4.

2PA cross-sections, δ_{2PA}, of PS **1-4** in ACN were measured at 775 nm by the open aperture Z-scan method and are presented in Table 4. Relatively low values of δ_{2PA} were obtained for PS **1** and **3** at 775 nm. This wavelength corresponds to the long wavelength edge of their main absorption band. Although 775 nm is not optimal for two-photon photosensitization, this wavelength was used since it is the fundamental output of the Clark-MXR Ti:sapphire laser, and possessed sufficient intensity for 2PA-induced singlet oxygen quantum yield determination. The quantum yields, ${}^{2PA}\Phi_\Delta$, were determined from Equation (7) for PS **1-4** in ACN and are

presented in the same table. This work represents the first direct 2PA singlet oxygen quantum yield determination by the singlet oxygen phosphorescence method. Previous reports involved either one-photon singlet oxygen quantum yield measurements, indirect singlet oxygen quantum yield determination via photochemical methods upon 2PE, or only qualitative 2PE singlet oxygen generation. PS **1-4** all possessed relatively high two-photon quantum yields, ${}^{2PA}\Phi_{\Delta} \approx 0.3$ - 0.45, which are nearly equal to half of the corresponding Φ_{Δ} values obtained under linear, one-photon, excitation. Values for ${}^{2PA}\Phi_{\Delta}$ that are half of the corresponding Φ_{Δ} values are expected since twice the number of photons are absorbed in a 2PA process relative to 1PA. This indicates that the processes of singlet oxygen production for all the investigated PS start from the same vibronic levels of S_1 and are nearly independent of the type of excitation. This research successfully identified a class of PS compounds that exhibit high singlet oxygen quantum efficiency under both one- and two-photon excitation. Future work will be directed at structural modification to increase the δ_{2PA}.

Table 4. Singlet oxygen quantum yields by 2PE, ${}^{2PA}\Phi_{\Delta}$, and 2PA cross-sections, δ_{2PA}, of PS **1-4** at 775 nm in ACN.

	PS 1	PS 2	PS 3	PS 4
${}^{2PA}\Phi_{\Delta}$	0.40 ± 0.20	0.35 ± 0.10	0.30 ± 0.15	0.45 ± 0.15
δ_{2PA}, GM	9 ± 4	50 ± 15	10 ± 4	60 ± 20

CHAPTER 5: CONCLUSION AND FUTURE WORK

5.1 Conclusion

The research presented in this dissertation focused on the synthesis and photophysical characterization of new, hydrophilic two-photon absorbing fluorene-based singlet oxygen photosensitizers. A synthetic strategy was adopted to impart water solubility, large $^1O_2$ QYs, and moderately high 2PA cross sections. Hydrophilicity was accomplished by incorporating alkyl carboxylic acid or ethyleneoxy motifs pendant to the main fluorene architecture without perturbing the central π conjugation of the chromophore. Large $^1O_2$ QYs were achieved by incorporating heavy atom halogens and/or nitro groups to promote intersystem crossing to the triplet state. Increase of the 2PA δs was obtained by extending the conjugation of the chromophore with an electron withdrawing benzothiazole group. Thorough photophysical characterization of each sensitizer was performed at room and low temperature (77 K) to better understand their spectral properties and to evaluate the efficiency of $^1O_2$ sensitization by one- and two-photon excitation. Photophysical characterization revealed important features and characteristics of the sensitizers that can be used to help direct future development of fluorene based $^1O_2$ sensitizers having large 2PA cross sections at wavelengths extending into the near IR region. This work represents the first direct 2PA singlet oxygen quantum yield determination by the singlet oxygen phosphorescence method. The successful development of 2PA singlet oxygen sensitizers is particularly important in the field of photodynamic therapy and could have a dramatic impact on addressing such issues as specificity of $^1O_2$ formation, efficiency, and ability to penetrate deeper into tissue.

Very good water solubility was accomplished by incorporating alkyl carboxylic acid or ethyleneoxy groups into the 9 position of the fluorene ring without significantly perturbing the photophysical properties of the sensitizer. The carboxylic acid derivatives (PS **1**-**2**) afforded high aqueous solubility under biological conditions (PBS, pH 7.2) while maintaining high $^1O_2$ QYS (0.4-0.34). Typically, the efficiency of $^1O_2$ production decreases as the polarity of the solvent is increased, and often the $^1O_2$ QY in water is << 0.20. The ethyleneoxy derivatives (PS **3**-**4**) were not as water soluble as PS **1**-**2** but still quite hydrophilic. PS **3**-**4** were soluble in a DMSO water mixture or in ethanol.

The synthesis of fluorene derivatives with heavy atoms was accomplished using iodo and/or nitro groups, resulting in large $^1O_2$ QYs. The use of iodo, and other halogens, is often used to promote intersystem crossing to the triplet state. It is interesting to note that the nonhalogen containing sensitizers (PS **2** and **4**) had the highest $^1O_2$ QYs, 0.93 and 0.92, respectively. The linear photophysical characterization of the sensitizers revealed a large amount of charge transfer character in the iodo derivatives (PS **1** and **3**) which could be responsible for the lower $^1O_2$ QYs, 0.65 and 0.74, respectively. When trying to promote the heavy atom effect it is important to locate the heavy atom/group near the location (part of the molecule) where the electronic transition occurs. Hence, the halogen or nitro group does not need to be directly inline with the conjugation to enhance intersystem crossing as it is when it is placed in the 2 or 7 position of the fluorene ring. Moving the heavy atom group to the 4 position and placing a group in the 2 or 7 position that does not increase the charge transfer character significantly may be a good alternative to increasing the $^1O_2$ QY of the sensitizer via the heavy atom effect.

Substitution of the iodo group with benzothiazole shifted the main absorption band to longer wavelengths by about 20 nm. This is not very significant considering the ideal location

for the main absorption band should be around 400-500 nm (800-1000 nm for 2PE). However, the benzothiazole group reduced the charge transfer character of the sensitizer and increased the 2PA cross section 5-6 times compared to the iodo nitro derivatives. Based on these results, the best approach may be to extend the conjugation by insertion of a styryl group between fluorene and benzothiazole and to include a heavy atom/group in the 4 position or on the styryl system to promote intersystem crossing to the triplet state. The main absorption band can be shifted to longer wavelengths by extending the conjugation, and fluorescence can be reduced by promoting intersystem crossing to the triplet state.

Clearly PS **1-4** are efficient $^1O_2$ sensitizers under the conditions studied. The QY value of singlet oxygen generation by 1PE for each sensitizer did not change over a broad region of wavelengths, revealing no spectral dependence on the $^1O_2$ QY. Analysis of the power dependence on $^1O_2$ luminescence intensity revealed a linear dependence, indicating no other photophysical processes occurred. This is particularly important in demonstrating that singlet oxygen is not being formed by quenching of the sensitizer singlet state.

Singlet oxygen formation by 2PE was demonstrated. The quantum yields were about half (~0.3-0.45) of the corresponding singlet oxygen quantum yields obtained under 1PE, indicating $^1O_2$ formation proceeds from the lowest excited S_1 state regardless of the type of excitation (1PE or 2PE). A value of half is expected since twice the number of photons are required for 2PA relative to 1PA. A quadratic dependence on the excitation power was observed for the singlet oxygen luminescence intensity under 2PE, demonstrating that no other nonlinear effects were present. Under high irradiation intensities it is possible to observe reabsorption from the sensitizer excited state, which results in lower $^1O_2$ luminescence intensities as the power is increased. Additionally, no photobleaching of the sensitizers were observed during any of the

experiments under 1PE or 2PE. Moderate 2PA δ were reported (~10-60 GM). It is important to note that these values were obtained at a wavelength (775 nm) at the far edge of their main two-photon absorption band. To be useful as a PDT sensitizer it will be necessary to push this main absorption band to longer wavelengths (800-1000 nm) where much larger 2PA cross sections are expected.

5.2 Future Work

The usefulness of fluorene as a central chromophore platform, from which a vast array of derivatives can be obtained, has been demonstrated by our group. The rest of this chapter discusses a new synthetic strategy to build upon the work that has been presented in this dissertation. A series of reactive chromophore units will be proposed where issues such as shifting the main absorption band to longer wavelengths and increasing the 2PA cross section of the sensitizer will be addressed. Each chromophore unit will contain a reactive nitrile functional group to allow easy attachment to fluorene in the 2 or 7 position. This will allow the synthesis of a diverse group of symmetrical and unsymmetrical fluorene derivatives. The reactive chromophore units will permit mixing and matching of the units to modulate the photophysical properties of each individual sensitizer.

The main objectives of the proposed synthetic strategy is to produce a variety of chromophore units utilizing a uniform synthetic procedure, extend the chromophore conjugation while maintaining photostability, and incorporate heavy atoms and functional groups to promote intersystem crossing while minimizing fluorescence emission. The chromophore will be extended by inserting functionalized styryl benzene units between fluorene and an electron

withdrawing or donating group such as benzothiazole or diphenylamine. The use of styryl groups has been demonstrated to be an effective method to increase the conjugation of 2PA chromophores in addition to having the ability to be functionalized.[55, 99, 106, 113, 117, 118] There are a number of synthetic routes commonly used to obtain conjugated styryl derivatives such as Horner-Wadsworth-Emmons, Heck, and Ullmann reactions among others. A particularly useful route is to use base-catalyzed condensation of aromatic aldehydes with functionalized acetonitriles, where the carbon-carbon bond formation results in an alkene with a vinyl nitrile linking the two desired groups (Figure 39).[169, 170] Placement of the nitrile group is of particular importance since it has been demonstrated that vinyl nitriles can impart photostability against oxidation of the styryl benzene derivatives.[171, 172]

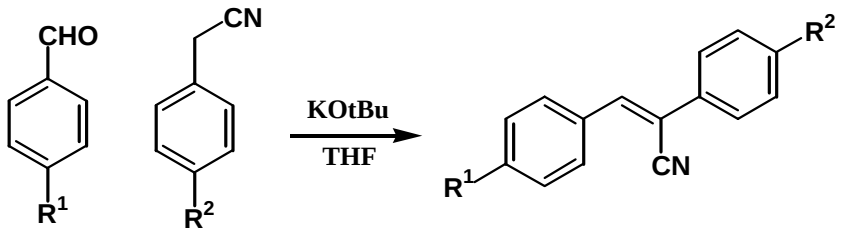

Figure 39. Base catalyzed condensation of an aromatic aldehyde with a functionalized derivative of acetonitrile.

The synthesis of six functionalized chromophore units (Figure 40) can then be prepared where heavy atoms and functional groups have been strategically placed to enhance intersystem crossing. In addition, each proposed unit contains a different degree of extended conjugation resulting in a highly conjugated chromophore with electron donating or withdrawing character. Several fundamental reactions utilizing commercially available starting materials result in

maintaining a uniform synthetic approach. Most importantly, each unit will contain a reactive functionalized acetonitrile group for direct attachment to a bis-aldehyde derivative of fluorene[19, 169] (Figure 41), allowing the synthesis of 21 different possible combinations, several of which are illustrated in Figure 42.

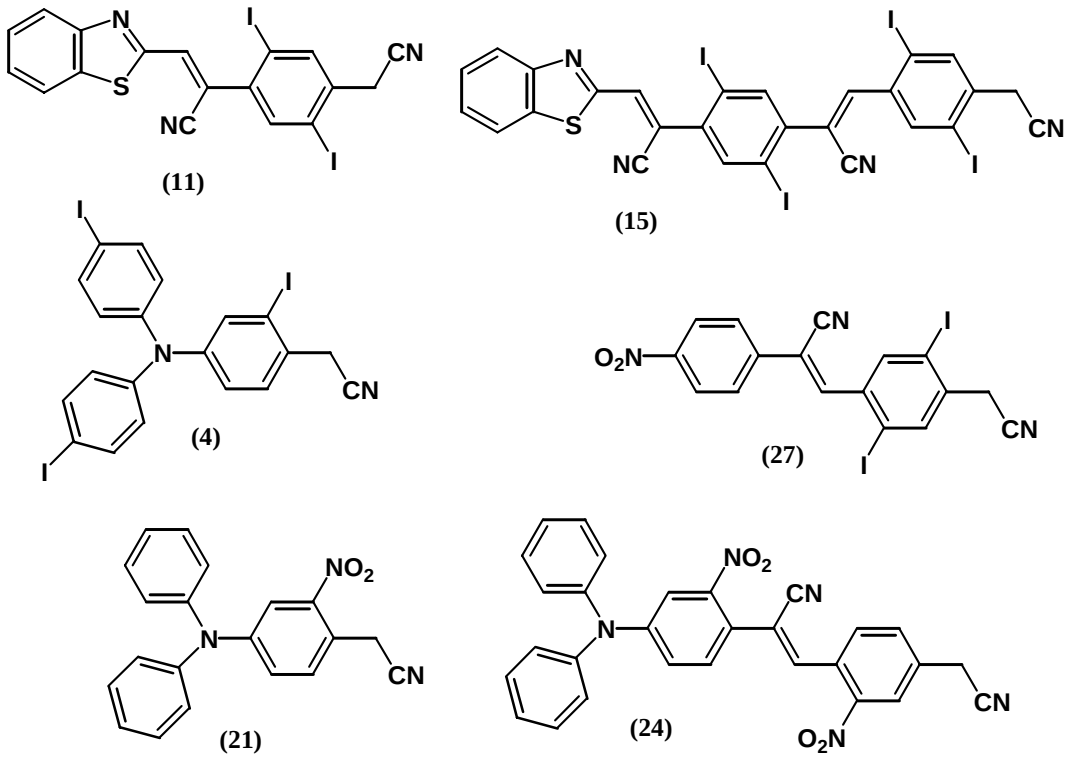

Figure 40. Proposed chromophore precursors for the synthesis of fluorene based singlet oxygen sensitizers.

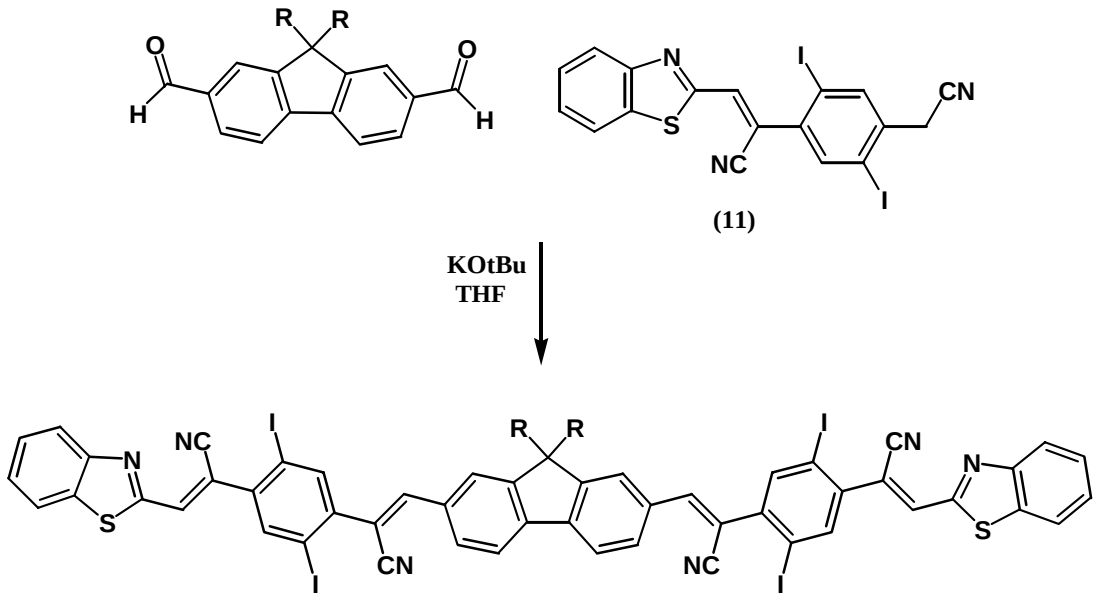

Figure 41. Synthesis of photosensitizer via bis-aldehyde condensation with nitrile intermediate.

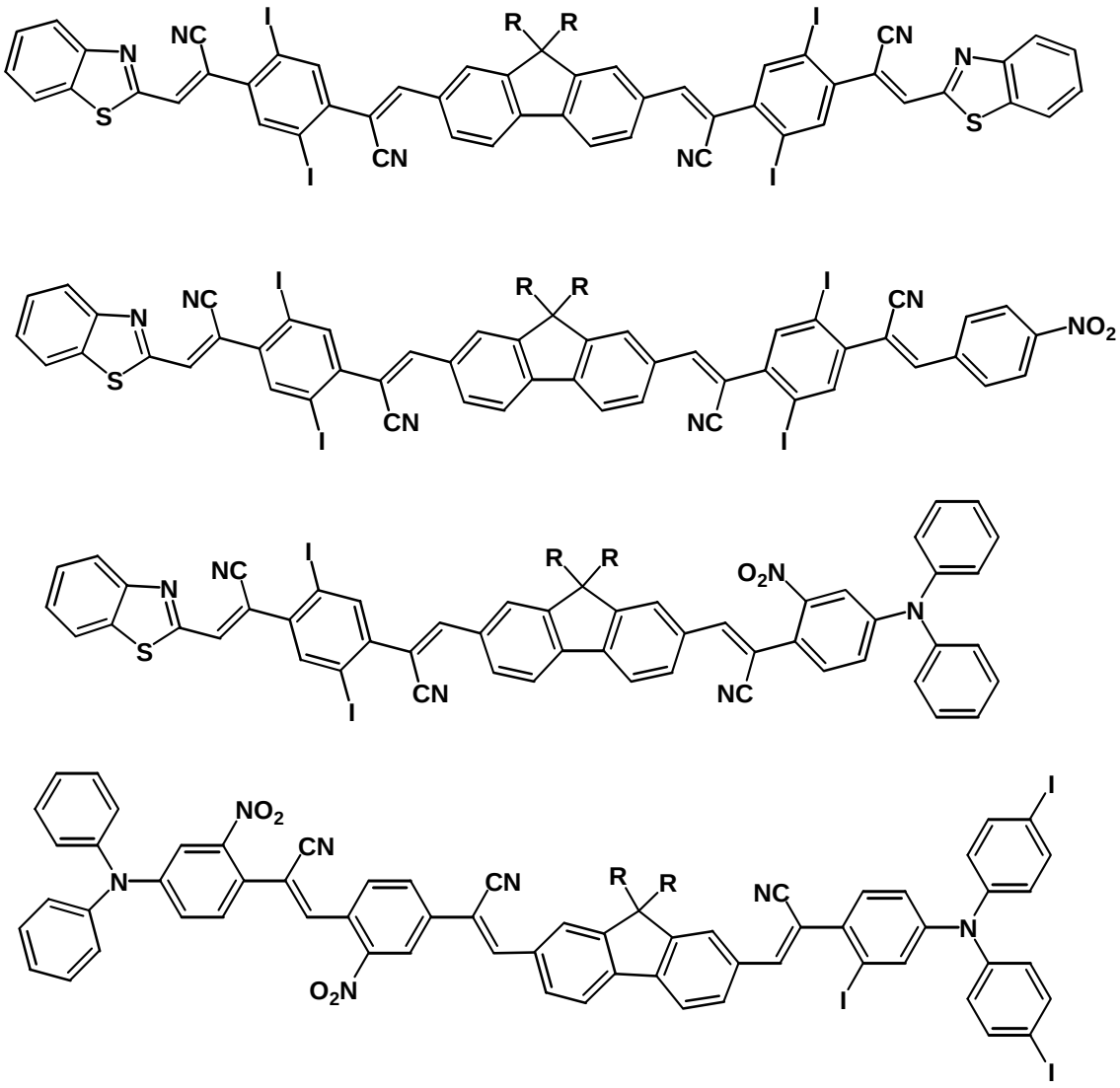

Figure 42. Example of new fluorene-based photosensitizers.

LIST OF REFERENCES

1. Khan, A. U.; Kasha, M., Red Chemiluminescence of Molecular Oxygen in Aqueous Solution. *The Journal of Chemical Physics* **1963,** 39, (8), 2105-2106.

2. Schweitzer, C.; Mehrdad, Z.; Noll, A.; Grabner, E. W.; Schmidt, R., Mechanism of Photosensitized Generation of Singlet Oxygen during Oxygen Quenching of Triplet States and the General Dependence of the Rate Constants and Efficiencies of Formation on Sensitizer Triplet State Energy and Oxidation Potential. *J. Phys. Chem. A* **2003,** 107, (13), 2192-2198.

3. Clennan, E. L.; Pace, A., Advances in singlet oxygen chemistry. *Tetrahedron* **2005,** 61, (28), 6665-6691.

4. Ian J. Macdonald, T. J. D., Basic principles of photodynamic therapy. *Journal of Porphyrins and Phthalocyanines* **2001,** 5, (2), 105-129.

5. Spikes, J. D.; van Lier, J. E.; Bommer, J. C., A comparison of the photoproperties of zinc phthalocyanine and zinc naphthalocyanine tetrasulfonates: model sensitizers for the photodynamic therapy of tumors. *Journal of Photochemistry and Photobiology A: Chemistry* **1995,** 91, (3), 193-198.

6. Henderson, B. W.; Dougherty, T. J., How does photodynamic therapy work? *Photochem Photobiol* **1992,** 55, (1), 145-57.

7. Ochsner, M., Photophysical and photobiological processes in the photodynamic therapy of tumours. *Journal of Photochemistry and Photobiology B: Biology* **1997,** 39, (1), 1-18.

8. Liu, W.; Oseroff, A. R.; Baumann, H., Photodynamic Therapy Causes Cross-linking of Signal Transducer and Activator of Transcription Proteins and Attenuation of Interleukin-6 Cytokine Responsiveness in Epithelial Cells. *Cancer Res* **2004,** 64, (18), 6579-6587.

9. Morgan, J.; Potter, W. R.; Oseroff, A. R., Comparison of photodynamic targets in a carcinoma cell line and its mitochondrial DNA-deficient derivative. *Photochem Photobiol* **2000,** 71, (6), 747-57.

10. Wild, P. J.; Krieg, R. C.; Seidl, J.; Stoehr, R.; Reher, K.; Hofmann, C.; Louhelainen, J.; Rosenthal, A.; Hartmann, A.; Pilarsky, C.; Bosserhoff, A. K.; Knuechel, R., RNA expression profiling of normal and tumor cells following photodynamic therapy with 5-aminolevulinic acid-induced protoporphyrin IX in vitro. *Mol Cancer Ther* **2005,** 4, (4), 516-528.

11. Wong, T.-W.; Tracy, E.; Oseroff, A. R.; Baumann, H., Photodynamic Therapy Mediates Immediate Loss of Cellular Responsiveness to Cytokines and Growth Factors. *Cancer Res* **2003,** 63, (13), 3812-3818.

12. Zheng Huang, M. D., Ph.D., A Review of Progress in Clinical Photodynamic Therapy. *Technology in Cancer Research and Treatment* **2005,** 4, (3), 283-293.

13. Jacques, S. L. P., S.A., Absorption spectra for biological tissues. In Oregon Graduate Institute: 1998.

14. Chen, B.; Pogue, B. W.; Hasan, T., Liposomal delivery of photosensitising agents. *Expert Opin Drug Deliv* **2005,** 2, (3), 477-87.

15. Lacerda, S. H. D.; Abraham, B.; Stringfellow, T. C.; Indig, G. L., Photophysical, Photochemical, and Tumor-selectivity Properties of Bromine Derivatives of Rhodamine-123. *Photochemistry and Photobiology* **2005,** 81, (6), 1430-1438.

16. Qian Peng, T. W., Kristian Berg, Johan Moan, Magne Kongshaug, Karl-Erik Giercksky, Jahn M. Nesland, 5-Aminolevulinic acid-based photodynamic therapy. *Cancer* **1997,** 79, (12), 2282-2308.

17. Göppert-Mayer, M., Elementary Actions with two Quantum Leaps. *Annals of Physics* **1931,** 9, 273-294.

18. Belfield, K.; Corredor, C.; Morales, A.; Dessources, M.; Hernandez, F., Synthesis and Characterization of New Fluorene-Based Singlet Oxygen Sensitizers. *Journal of Fluorescence* **2006,** 16, (1), 105-110.

19. Belfield, K. D.; Morales, A. R.; Kang, B. S.; Hales, J. M.; Hagan, D. J.; VanStryland, E. W.; Chapela, V. M.; Percino, J., Synthesis, Characterization, and Optical Properties of New Two-Photon-Absorbing Fluorene Derivatives. *Chem. Mater.* **2004,** 16, (23), 4634-4641.

20. Schafer-Hales, K. J.; Belfield, K. D.; Yao, S.; Frederiksen, P. K.; Hales, J. M.; Kolattukudy, P. E., Fluorene-based fluorescent probes with high two-photon action cross-sections for biological multiphoton imaging applications. *Journal of Biomedical Optics* **2005,** 10, (5), 051402-8.

21. Dolmans, D. E. J. G. J.; Fukumura, D.; Jain, R. K., TIMELINE: Photodynamic therapy for cancer. *Nature Reviews Cancer* **2003,** 3, (5), 380.

22. Lewis, G. N., The Magnetochemical Theory. *Chem. Rev.* **1924,** 1, (2), 231-248.

23. Mulliken, R. S., Interpretation of the Atmospheric Oxygen Bands: Electronic Levels of the Oxygen Molecule. *Nature* **1928,** 122, 505.

24. Ellis J. W., K. H. O., Combination relations in the absorption spectrum of liquid oxygen *Zeitschrift fuer Physik* **1933,** 86, 583-591

25. Schaap, A. P., *Singlet molecular oxygen* Dowden, Hutchinson & Ross Stroudsburg, PA, 1976; Vol. 5, p 399.

26. Fritzsche, J., Note sur les Carbures d'hydrogene Solides, Tires du Goudron de Houille. *COMPTES RENDUS CHIMIE* **1867,** 64, 1035-1037.

27. Moureu C., D. C., Dean P. M., un Peroxyde Organique Dissociable: Le Peroxyde de Rubrene. *COMPTES RENDUS CHIMIE* **1926,** 182, 1584-1587.

28. A. Windaus, J. B., Über die photochemische Oxydation des Ergosterins. *Justus Liebig's Annalen der Chemie* **1928,** 460, (1), 225-235.

29. Kautsky, H.; de Bruijn, H., Die Aufklärung der Photoluminescenztilgung fluorescierender Systeme durch Sauerstoff: Die Bildung aktiver, diffusionsfähiger Sauerstoffmoleküle durch Sensibilisierung. *Naturwissenschaften* **1931,** 19, (52), 1043-1043.

30. Alexander, S., Notiz über die photochemische Bildung von Biradikalen. *Justus Liebig's Annalen der Chemie* **1935,** 518, (1), 299-302.

31. Foote, C. S.; Wexler, S., Olefin Oxidations with Excited Singlet Molecular Oxygen. *J. Am. Chem. Soc.* **1964,** 86, (18), 3879-3880.

32. Foote, C. S.; Wexler, S., Singlet Oxygen. A Probable Intermediate in Photosensitized Autoxidations. *J. Am. Chem. Soc.* **1964,** 86, (18), 3880-3881.

33. Corey, E. J.; Taylor, W. C., A Study of the Peroxidation of Organic Compounds by Externally Generated Singlet Oxygen Molecules. *J. Am. Chem. Soc.* **1964,** 86, (18), 3881-3882.

34. Günther; Günther; Schenck, O.; Ziegler, K., Die Synthese des Ascaridols. *Naturwissenschaften* **1944,** 32, (14), 157-157.

35. Dufraisse C., E. S., Photooxydation sur Cycle Pentagonal: Photooxydiphenylisobenzofuran. *Comptes Rendus Chimie* **1946,** 223, 735-737.

36. Merkel, P. B.; Kearns, D. R., Direct measurement of the lifetime of $O_2(^1\Delta_g)$ oxygen in solution. *Chemical Physics Letters* **1971,** 12, (1), 120-122.

37. Wilson, T., Excited Singlet Molecular Oxygen in Photooxidation. *J. Am. Chem. Soc.* **1966,** 88, (13), 2898-2902.

38. Nickon, A.; Bagli, J. F., PHOTOSENSITIZED OXYGENATION OF MONO-OLEFINS. *J. Am. Chem. Soc.* **1959,** 81, (23), 6330-6330.

39. Seliger, H. H., A photoelectric method for the measurement of spectra of light sources of rapidly varying intensities. *Analytical Biochemistry* **1960,** 1, (1), 60-65.

40. Browne R. J., O. E. A., Chemiluminescence from the Reaction of Chloride with Aqueous Hydrogen Peroxide. *Proceedings of the Chemical Society* **1964,** 101-128, 117.

41. Gollnick K., S. G. O., Mechanism and Stereoselectivity of Photosensitized Oxygen Transfer Reactions. *Pure and Applied Chemistry* **1964,** 9, 507-525.

42. Snelling, D. R., Production of singlet oxygen in the benzene oxygen photochemical system. *Chemical Physics Letters* **1968,** 2, (5), 346-348.

43. Andrews, L. J.; Abrahamson, E. W., Formation of $O_2(^1\Sigma_g^+)$ by 1-fluoronaphthalene sensitization. *Chemical Physics Letters* **1971,** 10, (2), 113-116.

44. Adams D. R., W. F., Lifetime of singlet oxygen in liquid solution *Chemical Society, Faraday Transactions 2* **1972,** 68, 586-593.

45. Krasnovsky, J. A. A., Photosensitized Luminescence of Singlet Oxygen in Solution. *Biofizika* **1976,** 21, (4), 748-749.

46. Hurst, J. R.; McDonald, J. D.; Schuster, G. B., Lifetime of singlet oxygen in solution directly determined by laser spectroscopy. *J. Am. Chem. Soc.* **1982,** 104, (7), 2065-2067.

47. Ogilby, P. R.; Foote, C. S., Chemistry of singlet oxygen. 36. Singlet molecular oxygen $O_2(^1\Delta_g)$ luminescence in solution following pulsed laser excitation. Solvent deuterium isotope effects on the lifetime of singlet oxygen. *J. Am. Chem. Soc.* **1982,** 104, (7), 2069-2070.

48. Parker, J. G.; Stanbro, W. D., Optical determination of the collisional lifetime of singlet molecular oxygen $O_2(^1\Delta_g)$ in acetone and deuterated acetone. *J. Am. Chem. Soc.* **1982,** 104, (7), 2067-2069.

49. Wilkinson, F. B., James G., Rate constants for the decay and reactions of the lowest electronically excited singlet state of molecular oxygen in solution. *Journal of Physical and Chemical Reference Data* **1981,** 10, (4), 809-999.

50. Wilkinson, F.; Helman, W. P.; Ross, A. B., Quantum Yields for the Photosensitized Formation of the Lowest Electronically Excited Singlet-State of Molecular-Oxygen in Solution. *Journal of Physical and Chemical Reference Data* **1993,** 22, (1), 113-262.

51. Schmidt, R.; Bodesheim, M., Time-Resolved Measurement of $O_2(^1\Sigma^+_g)$ in Solution. Phosphorescence from an Upper Excited State. *J. Phys. Chem.* **1994,** 98, (11), 2874-2876.

52. Schweitzer, C.; Schmidt, R., Physical mechanisms of generation and deactivation of singlet oxygen. *Chem Rev* **2003,** 103, (5), 1685-757.

53. Frederiksen, P. K.; Jorgensen, M.; Ogilby, P. R., Two-Photon Photosensitized Production of Singlet Oxygen. *J. Am. Chem. Soc.* **2001,** 123, (6), 1215-1221.

54. Andersen L. K., O. P. R., Time-resolved Detection of Singlet Oxygen in a Transmission Microscope. *Photochemistry Photobiology* **2001,** 73, (5), 489-492.

55. Frederiksen, P. K.; McIlroy, S. P.; Nielsen, C. B.; Nikolajsen, L.; Skovsen, E.; Jorgensen, M.; Mikkelsen, K. V.; Ogilby, P. R., Two-Photon Photosensitized Production of Singlet Oxygen in Water. *J. Am. Chem. Soc.* **2005,** 127, (1), 255-269.

56. Skovsen E., S. J. W., Ogilby P. R. , Two-Photon Singlet Oxygen Microscopy: The Challenges of Working with Single Cells. *Photochemistry and Photobiology* **2006,** 82, (5), 1187-1197.

57. Charles Moureu, C. D., Paul Marshall Dean, Un Peroxyde Organique Dissociable: Le Peroxyde De Rubrene. *Compt. Rend.* **1926,** 182, 1584-1587.

58. Fritzsche, M., Note Sur Les Carbures D'Hydrogene Solides, Tires Du Goudron De Houille. *Compt. Rend.* **1867,** 64, 1035-1037.

59. Foner, S. N.; Hudson, R. L., Metastable Oxygen Molecules Produced by Electrical Discharges. *The Journal of Chemical Physics* **1956,** 25, (3), 601-602.

60. Foote C. S., W. S., Olefin Oxidations with Excited Singlet Molecular Oxygen. *Journal of American Chemical Society* **1964,** 86, 3879-3880.

61. Evans, D. F., Oxidation by photochemically produced singlet states of oxygen. *Journal of the Chemical Society D: Chemical Communications* **1969**, (7), 367-368.

62. Murray, R. W.; Kaplan, M. L., Singlet oxygen sources in ozone chemistry. Chemical oxygenations using the adducts between phosphite esters and ozone. *J. Am. Chem. Soc.* **1969,** 91, (19), 5358-5364.

63. Hideg Éva, K. T., Kós Péter B., Asada Kozi, Hideg Kálmán, Singlet Oxygen in Plants—Its Significance and Possible Detection with Double (Fluorescent and Spin) Indicator Reagents. *Photochemistry Photobiology* **2006,** 82, (5), 1211-1218.

64. Scurlock, R. D.; Wang, B.; Ogilby, P. R.; Sheats, J. R.; Clough, R. L., Singlet Oxygen as a Reactive Intermediate in the Photodegradation of an Electroluminescent Polymer. *J. Am. Chem. Soc.* **1995,** 117, (41), 10194-10202.

65. Ali, H.; van Lier, J. E., Metal Complexes as Photo- and Radiosensitizers. *Chem. Rev.* **1999,** 99, (9), 2379-2450.

66. Bonnett, R., Photosensitizers of the porphyrin and phthalocyanine series for photodynamic therapy
Chemical Society Reviews **1995,** 24, 19-33.

67. Danilo Dini, M. B. M. H., Phthalocyanines as Active Materials for Optical Limiting. *European Journal of Organic Chemistry* **2001,** 2001, (20), 3759-3769.

68. Guillaud, G.; Simon, J.; Germain, J. P., Metallophthalocyanines: Gas sensors, resistors and field effect transistors. *Coordination Chemistry Reviews* **1998,** 178-180, (Part 2), 1433-1484.

69. Law, K. Y., Organic photoconductive materials: recent trends and developments. *Chem. Rev.* **1993,** 93, (1), 449-486.

70. Torre G. de la, V. P., Agulló-López F., Torres T., Phthalocyanines and related compounds:organic targets for nonlinear optical applications. *Journal of Materials Chemistry* **1998,** 8, 1671-1683.

71. Abdel-Shafi, A. A.; Bourdelande, J. L.; Ali, S. S., Photosensitized generation of singlet oxygen from rhenium(i) and iridium(iii) complexes. *Dalton Transactions* **2007**, (24), 2510-2516.

72. Farmilo A, W. F., Mechanism of quenching of singlet oxygen in solution. *Photochemistry and Photobiology* **1973,** 18, (6), 447-450.

73. Furue Hiroshi, R. K. E., Deactivation of singlet oxygen and triplet pentacene by transition metal complexes. *Canadian Journal of Chemistry* **1978,** 56, (12), 1595-1601.

74. Mehrdad, Z.; Noll, A.; Grabner, E. W.; Schmidt, R., Sensitization of singlet oxygen via encounter complexes and via exciplexes of pi pi* triplet excited sensitizers and oxygen. *Photochemical & Photobiological Sciences* **2002,** 1, (4), 263-269.

75. Schmidt, R.; Shafii, F., Influence of Charge Transfer Interactions on the Sensitization of Singlet Oxygen: Formation of $O_2(^1\Sigma^+_g)$, $O_2(^1\Delta_g)$, and $O_2(^3\Sigma^-_g)$ during Oxygen Quenching of Triplet Excited Biphenyl Derivatives. *J. Phys. Chem. A* **2001,** 105, (39), 8871-8877.

76. Schmidt, R.; Shafii, F.; Schweitzer, C.; Abdel-Shafi, A. A.; Wilkinson, F., Charge-transfer and non-charge-transfer processes competing in the sensitization of singlet oxygen: Formation of $O_2(^1\Sigma^+_g)$, $O_2(^1\Delta_g)$, and $O_2(^3\Sigma^-_g)$ during oxygen quenching of triplet excited naphthalene derivativest. *Journal of Physical Chemistry A* **2001,** 105, (10), 1811-1817.

77. Schweitzer, C.; Mehrdad, Z.; Shafii, F.; Schmidt, R., Charge transfer induced quenching of triplet sensitizers by ground state oxygen and of singlet oxygen by ground state sensitizers: A common deactivation channel. *Physical Chemistry Chemical Physics* **2001,** 3, (15), 3095-3101.

78. Wasserman, H. H.; Scheffer, J. R.; Cooper, J. L., Singlet oxygen reactions with 9,10-diphenylanthracene peroxide. *J. Am. Chem. Soc.* **1972,** 94, (14), 4991-4996.

79. Castro, C.; Dixon, M.; Erden, I.; Ergonenc, P.; Keeffe, J. R.; Sukhovitsky, A., Dye-sensitized photooxygenation of the carbon-nitrogen double bond. *J. Org. Chem.* **1989,** 54, (15), 3732-3738.

80. He, Y.-Y.; An, J.-Y.; Jiang, L.-J., Synthesis of a new water-soluble phototherapeutic sensitizer from hypocrellin B with enhanced red absorption. *Dyes and Pigments* **1999,** 41, (1-2), 93-100.

81. Schaap, A. P.; Thayer, A. L.; Blossey, E. C.; Neckers, D. C., Polymer-based sensitizers for photooxidations. II. *J. Am. Chem. Soc.* **1975,** 97, (13), 3741-3745.

82. Detty, M. R.; Merkel, P. B., Chalcogenapyrylium dyes as potential photochemotherapeutic agents. Solution studies of heavy atom effects on triplet yields, quantum efficiencies of singlet oxygen generation, rates of reaction with singlet oxygen, and emission quantum yields. *J. Am. Chem. Soc.* **1990,** 112, (10), 3845-3855.

83. Paczkowski, J.; Neckers, D. C., Polymer-based sensitizers for the formation of singlet oxygen: new studies of polymeric derivatives of rose bengal. *Macromolecules* **1985,** 18, (6), 1245-1253.

84. Milgrom, L. R., *The Colours of Life: an introduction to the chemistry of porphyrins and related compounds*. Oxford University Press: New York, 1997; p 249.

85. Gupta, I.; Ravikanth, M., Synthesis and photophysical studies of covalently linked porphyrin-21-thiaporphyrin dyads. *Inorganica Chimica Acta* **2007,** 360, (5), 1731-1742.

86. Kadish K. M. , S. K., Guilard R. , *The Porphyrin Handbook*. Academic Press: San Diego, 2000.

87. Kozaki, M.; Akita, K.; Okada, K., Enhanced Electron Transfer by Dendritic Architecture: Energy Transfer and Electron Transfer in Snowflake-Shaped Zn Porphyrin Dendrimers. *Org. Lett.* **2007,** 9, (8), 1509-1512.

88. Mori, G.; Aratani, N.; Osuka, A., Synthesis of three-dimensionally arranged porphyrin arrays via intramolecular meso-meso coupling. *Tetrahedron* **2007,** 63, (33), 7916-7925.

89. Nah, M. K.; Oh, J. B.; Kim, H. K.; Choi, K. H.; Kim, Y. R.; Kang, J. G., Photophysical Properties and Energy Transfer Pathway of Er(III) Complexes with Pt-Porphyrin and Terpyridine Ligands. *J. Phys. Chem. A* **2007,** 111, (28), 6157-6164.

90. Rogers, J. E.; Nguyen, K. A.; Hufnagle, D. C.; McLean, D. G.; Su, W.; Gossett, K. M.; Burke, A. R.; Vinogradov, S. A.; Pachter, R.; Fleitz, P. A., Observation and Interpretation of Annulated Porphyrins: Studies on the Photophysical Properties of Tetraphenylmetalloporphyrins. *J. Phys. Chem. A* **2003,** 107, (51), 11331-11339.

91. DeRosa, M. C.; Crutchley, R. J., Photosensitized singlet oxygen and its applications. *Coordination Chemistry Reviews* **2002,** 233-234, 351-371.

92. Darwent, J. R.; Douglas, P.; Harriman, A.; Porter, G.; Richoux, M. C., Metal Phthalocyanines and Porphyrins as Photosensitizers for Reduction of Water to Hydrogen. *Coordination Chemistry Reviews* **1982,** 44, (1), 83-126.

93. Guldi, D. M.; Mody, T. D.; Gerasimchuk, N. N.; Magda, D.; Sessler, J. L., Influence of Large Metal Cations on the Photophysical Properties of Texaphyrin, a Rigid Aromatic Chromophore. *J. Am. Chem. Soc.* **2000,** 122, (34), 8289-8298.

94. Soncin, M.; Busetti, A.; Biola, R.; Jori, G.; Kwag, G.; Li, Y.-S.; Kenney, M. E.; Rodgers, M. A. J., Photoinactivation of amelanotic and melanotic melanoma cells sensitized by axially substituted Si-naphthalocyanines. *Journal of Photochemistry and Photobiology B: Biology* **1998,** 42, (3), 202-210.

95. Demas J. N., H. E. W., McBride R. P. , Energy Transfer from Luminescent Transition Metal Complexes to Oxygen. *Journal of American Chemical Society* **1977,** 99, (11), 3547-3551.

96. Gao R., H. D., Hernandez B., Selke M., Murphy D., Djurovich P. I., Thompson M. E., Bis-Cyclometalated Ir(III) Complexes as Efficient Singlet Oxygen Sensitizers. *Journal of American Chemical Society* **2002,** 124, 14828-14829.

97. Selke, M.; Karney, W. L.; Khan, S. I.; Foote, C. S., Reactions of Singlet Oxygen with Organometallic Complexes. 3. Kinetics and Scope of the Oxidative Addition Reaction of Singlet Oxygen with Iridium(I), Rhodium(I), and Platinum(II) Complexes. *Inorg. Chem.* **1995,** 34, (23), 5715-5720.

98. Goyan, R. L.; Cramb, D. T., Near-Infrared Two-Photon Excitation of Protoporphyrin IX: Photodynamics and Photoproduct Generation&para. *Photochemistry and Photobiology* **2000,** 72, (6), 821-827.

99. Albota, M.; Beljonne, D.; Bredas, J. L.; Ehrlich, J. E.; Fu, J. Y.; Heikal, A. A.; Hess, S. E.; Kogej, T.; Levin, M. D.; Marder, S. R.; McCord-Maughon, D.; Perry, J. W.; Rockel, H.; Rumi, M.; Subramaniam, G.; Webb, W. W.; Wu, X. L.; Xu, C., Design of organic molecules with large two-photon absorption cross sections. *Science* **1998,** 281, (5383), 1653-6.

100. Cumpston, B. H.; Ananthavel, S. P.; Barlow, S.; Dyer, D. L.; Ehrlich, J. E.; Erskine, L. L.; Heikal, A. A.; Kuebler, S. M.; Lee, I. Y. S.; McCord-Maughon, D.; Qin, J.; Rockel, H.; Rumi, M.; Wu, X.-L.; Marder, S. R.; Perry, J. W., Two-photon polymerization initiators for three-dimensional optical data storage and microfabrication. *Nature* **1999,** 398, (6722), 51-54.

101. Karotki, A.; Kruk, M.; Drobizhev, M.; Rebane, A.; Nickel, E.; Spangler, C. W., Efficient singlet oxygen generation upon two-photon excitation of new porphyrin with enhanced nonlinear absorption. *Selected Topics in Quantum Electronics, IEEE Journal of* **2001,** 7, (6), 971-975.

102. Spangler, C. W., Recent development in the design of organic materials for optical power limiting. *Journal of Materials Chemistry* **1999,** 9, (9), 2013-2020.

103. Drobizhev, M.; Karotki, A.; Kruk, M.; Mamardashvili, N. Z.; Rebane, A., Drastic enhancement of two-photon absorption in porphyrins associated with symmetrical electron-accepting substitution. *Chemical Physics Letters* **2002,** 361, (5-6), 504-512.

104. Karotki Aliaksandr, D. M., Kruk Mikalai, Spangler Charles, Nickel Erik, Mamardashvili Nugzar, Rebane Aleksander, Enhancement of Two-Photon Absorption in Tetrapyrrolic Compounds. *Journal of the Optical Society of America B* **2003,** 20, (2), 321-332.

105. Kruk, M.; Karotki, A.; Drobizhev, M.; Kuzmitsky, V.; Gael, V.; Rebane, A., Two-photon absorption of tetraphenylporphin free base. *Journal of Luminescence* **2003,** 105, (1), 45-55.

106. Ishi-i Tsutomu, T. Y., Kato Shin-ichiro, Shigeiwa Motoyuki, Gorohmaru Hideki, Maeda Shuuichi, Mataka Shuntaro, Singlet Oxygen Generation by Two-Photon Excitation of Porphyrin Derivatives Having Two-Photon-Absorbing Benzothiadiazole Chromophores. *Journal of Materials Chemistry* **2007,** 17, 3341-3346.

107. Dichtel, W. R.; Serin, J. M.; Edder, C.; Frechet, J. M. J.; Matuszewski, M.; Tan, L. S.; Ohulchanskyy, T. Y.; Prasad, P. N., Singlet Oxygen Generation via Two-Photon Excited FRET. *J. Am. Chem. Soc.* **2004,** 126, (17), 5380-5381.

108. Dichtel, W. R.; Hecht, S.; Frechet, J. M. J., Functionally Layered Dendrimers: A New Building Block and Its Application to the Synthesis of Multichromophoric Light-Harvesting Systems. *Org. Lett.* **2005,** 7, (20), 4451-4454.

109. Oar, M. A.; Dichtel, W. R.; Serin, J. M.; Frechet, J. M. J.; Rogers, J. E.; Slagle, J. E.; Fleitz, P. A.; Tan, L. S.; Ohulchanskyy, T. Y.; Prasad, P. N., Light-Harvesting Chromophores with Metalated Porphyrin Cores for Tuned Photosensitization of Singlet Oxygen via Two-Photon Excited FRET. *Chem. Mater.* **2006,** 18, (16), 3682-3692.

110. Oar, M. A.; Serin, J. M.; Dichtel, W. R.; Frechet, J. M. J.; Ohulchanskyy, T. Y.; Prasad, P. N., Photosensitization of Singlet Oxygen via Two-Photon-Excited Fluorescence Resonance Energy Transfer in a Water-Soluble Dendrimer. *Chem. Mater.* **2005,** 17, (9), 2267-2275.

111. Tan, L.-S.; Kannan, R.; Matuszewski, M. J.; Khur, I. J.; Feld, W. A.; Dang, T. D.; Dombroskie, A. G.; Vaia, R. A.; Clarson, S. J.; He, G. S.; Lin, T.-C.; Prasad, P. N. In *Functionalization of heterocyclic diphenylamino-based two-photon absorbing materials for microfabrication, data storage, and upconverted imaging*, Multiphoton Absorption and Nonlinear Transmission Processes: Materials, Theory, and Applications, Seattle, WA, USA, 2003; SPIE: Seattle, WA, USA, 2003; pp 171-178.

112. Norman, P.; Luo, Y.; Agren, H., Large two-photon absorption cross sections in two-dimensional, charge-transfer, cumulene-containing aromatic molecules. *The Journal of Chemical Physics* **1999,** 111, (17), 7758-7765.

113. Poulsen, T. D.; Frederiksen, P. K.; Jorgensen, M.; Mikkelsen, K. V.; Ogilby, P. R., Two-Photon Singlet Oxygen Sensitizers: Quantifying, Modeling, and Optimizing the Two-Photon Absorption Cross Section. *J. Phys. Chem. A* **2001,** 105, (51), 11488-11495.

114. Wang, C.-K.; Macak, P.; Luo, Y.; Agren, H., Effects of pi centers and symmetry on two-photon absorption cross sections of organic chromophores. *The Journal of Chemical Physics* **2001,** 114, (22), 9813-9820.

115. Arnbjerg, J.; Jimenez-Banzo, A.; Paterson, M. J.; Nonell, S.; Borrell, J. I.; Christiansen, O.; Ogilby, P. R., Two-Photon Absorption in Tetraphenylporphycenes: Are Porphycenes Better Candidates than Porphyrins for Providing Optimal Optical Properties for Two-Photon Photodynamic Therapy? *J. Am. Chem. Soc.* **2007,** 129, (16), 5188-5199.

116. Arnbjerg, J.; Paterson, M. J.; Nielsen, C. B.; Jorgensen, M.; Christiansen, O.; Ogilby, P. R., One- and Two-Photon Photosensitized Singlet Oxygen Production: Characterization of Aromatic Ketones as Sensitizer Standards. *J. Phys. Chem. A* **2007,** 111, (26), 5756-5767.

117. McIlroy, S. P.; Clo, E.; Nikolajsen, L.; Frederiksen, P. K.; Nielsen, C. B.; Mikkelsen, K. V.; Gothelf, K. V.; Ogilby, P. R., Two-Photon Photosensitized Production of Singlet Oxygen: Sensitizers with Phenylene-Ethynylene-Based Chromophores. *J. Org. Chem.* **2005,** 70, (4), 1134-1146.

118. Nielsen, C. B.; Johnsen, M.; Arnbjerg, J.; Pittelkow, M.; McIlroy, S. P.; Ogilby, P. R.; Jorgensen, M., Synthesis and Characterization of Water-Soluble Phenylene-Vinylene-Based Singlet Oxygen Sensitizers for Two-Photon Excitation. *J. Org. Chem.* **2005,** 70, (18), 7065-7079.

119. Foote, C. S., Guest Editorial, Definition of Type I and Type II Photosensitized Oxidation. *Photochemistry and Photobiology* **1991,** 54, (5), 659.

120. Krasnovsky, J. A. A. In *Detection of photosensitized singlet oxygen luminescence in systems of biomedical importance: steady-state and time-resolved measurements based on application of S-1 photomultiplier tubes*, Physiological Imaging, Spectroscopy, and Early-Detection Diagnostic Methods, Los Angeles, CA, USA, 1993; SPIE: Los Angeles, CA, USA, 1993; pp 177-186.

121. Lakowicz, J. R., *Principles of Fluorescence Spectroscopy*. Second ed.; Kluwer: New York, 1999; p 698.

122. Telfer, A.; Dhami, S.; Bishop, S. M.; Phillips, D.; Barber, J., beta-Carotene quenches singlet oxygen formed by isolated photosystem II reaction centers. *Biochemistry* **1994,** 33, (48), 14469-74.

123. Telfer, A.; Bishop, S. M.; Phillips, D.; Barber, J., Isolated photosynthetic reaction center of photosystem II as a sensitizer for the formation of singlet oxygen. Detection and quantum

yield determination using a chemical trapping technique. *J Biol Chem* **1994,** 269, (18), 13244-53.

124. Abdel-Shafi, A. A.; Wilkinson, F., Electronic to vibrational energy conversion and charge transfer contributions during quenching by molecular oxygen of electronically excited triplet states. *Physical Chemistry Chemical Physics* **2002,** 4, (2), 248-254.

125. Schmidt, R., The balance between charge transfer and non-charge transfer pathways in the sensitization of singlet oxygen by pi pi* triplet states. *Photochemical & Photobiological Sciences* **2005,** 4, (6), 481-486.

126. Shafii, F.; Schmidt, R., Determination of rate constants of formation of $O_2(^1\Sigma^+_g)$, $O_2(^1\Delta_g)$, and $O_2(^3\Sigma^-_g)$ in the quenching of triplet states by O_2 for compounds with incomplete intersystem crossing. *Journal of Physical Chemistry A* **2001,** 105, (10), 1805-1810.

127. Wilkinson, F.; Abdel-Shafi, A. A., Mechanism of quenching of triplet states by molecular oxygen: Biphenyl derivatives in different solvents. *Journal of Physical Chemistry A* **1999,** 103, (28), 5425-5435.

128. Schmidt, R., Photosensitized Generation of Singlet Oxygen. *Photochemistry and Photobiology* **2006,** 82, (5), 1161-1177.

129. Mehrdad, Z.; Schweitzer, C.; Schmidt, R., Formation of $O_2(^1\Sigma^+_g)$, $O_2(^1\Delta_g)$, and $O_2(^3\Sigma^-_g)$ during oxygen quenching of n π* triplet phenyl ketones: The role of charge transfer and sensitizer-oxygen complex structure. *Journal of Physical Chemistry A* **2002,** 106, (2), 228-235.

130. Kawaoka, K.; Khan, A. U.; Kearns, D. R., Role of Singlet Excited States of Molecular Oxygen in the Quenching of Organic Triplet States. *The Journal of Chemical Physics* **1967,** 46, (5), 1842-1853.

131. H. Tappeiner, H. J., Therapeutische Versuche mit fluoreszierenden Stoffen. *Munch. Med. Wschr.* **1903,** 50, 2042-2044.

132. Jesionek H., T. H., Zur Behandlung der Hautcarcinome mit fluoreszierenden Stoffen *Dtsch. Arch. Klin. Med.* **1905,** 82, 223-226.

133. Meyer-Betz, F., Wirkung des Hamatoporphyrins und anderer Derivate des Blut- und Gallenfarbstoffs. *Dtsch. Arch. Klin. Med.* **1913,** 112, 476-503.

134. Dougherty, T. J., Henderson, B. W. , *In Historical Perspective in Photodynamic Therapy*. Maurice Dekker: New York, 1992.

135. Nowak-Sliwinska, P.; Karocki, A.; Elas, M.; Pawlak, A.; Stochel, G.; Urbanska, K., Verteporfin, photofrin II, and merocyanine 540 as PDT photosensitizers against melanoma cells. *Biochemical and Biophysical Research Communications* **2006,** 349, (2), 549-555.

136. Parkhots, M. V.; Lapina, V. A.; Butorina, D. N.; Sobchuk, A. N.; Lepeshkevich, S. V.; Petrov, P. T.; Krasnovski; ibreve; Jr, A. A.; Dzhagarov, B. M., Spectral and Photochemical Characteristics of the Photosensitizers Chlorin and Photolon in the Presence of Melanin. *Optics & Spectroscopy* **2005,** 98, (3), 374-382.

137. Woodburn, K. W.; Engelman, C. J.; Blumenkranz, M. S., CME photodynamic therapy for choroidal neovascularization - A review. *Retina-the Journal of Retinal and Vitreous Diseases* **2002,** 22, (4), 391-405.

138. Datta, S. N.; Loh, C. S.; MacRobert, A. J.; Whatley, S. D.; Matthews, P. N., Quantitative studies of the kinetics of 5-aminolaevulinic acid-induced fluorescence in bladder transitional cell carcinoma. *Br J Cancer* **1998,** 78, (8), 1113-8.

139. Brown, S. B., The role of light in the treatment of non-melanoma skin cancer using methyl aminolevulinate. *Journal of Dermatological Treatment* **2003,** 14, 11.

140. Kearn, S. J.; Scott, L. J.; Curran, M. P., Verteporfin: A Review of its Use in the Management of Subfoveal Choroidal Neovascularisation. *Drugs* **2003,** 63, (22), 2521-2554.

141. Drobizhev, M.; Stepanenko, Y.; Dzenis, Y.; Karotki, A.; Rebane, A.; Taylor, P. N.; Anderson, H. L., Extremely strong near-IR two-photon absorption in conjugated porphyrin dimers: quantitative description with three-essential-states model. *J Phys Chem B Condens Matter Mater Surf Interfaces Biophys* **2005,** 109, (15), 7223-36.

142. Karotki, A.; Khurana, M.; Lepock, J. R.; Wilson, B. C., Simultaneous Two-photon Excitation of Photofrin in Relation to Photodynamic Therapy. *Photochemistry and Photobiology* **2006,** 82, (2), 443-452.

143. Karotki, A.; Khurana, M.; Lepock, J. R.; Wilson, B. C., Simultaneous two-photon excitation of photofrin in relation to photodynamic therapy. *Photochem Photobiol* **2006,** 82, (2), 443-52.

144. Huwyler, J.; Wu, D.; Pardridge, William M., Brain drug delivery of small molecules using immunoliposomes. *PNAS* **1996,** 93, (24), 14164-14169.

145. Matthay, K. K.; Heath, T. D.; Badger, C. C.; Bernstein, I. D.; Papahadjopoulos, D., Antibody-directed Liposomes: Comparison of Various Ligands for Association, Endocytosis, and Drug Delivery. *Cancer Res* **1986,** 46, (10), 4904-4910.

146. Liu, S., Radiolabeled multimeric cyclic RGD peptides as integrin alphavbeta3 targeted radiotracers for tumor imaging. *Mol Pharm* **2006,** 3, (5), 472-87.

147. Mae, M.; Langel, U., Cell-penetrating peptides as vectors for peptide, protein and oligonucleotide delivery. *Curr Opin Pharmacol* **2006,** 6, (5), 509-14.

148. Snyder, E. L.; Dowdy, S. F., Cell penetrating peptides in drug delivery. *Pharm Res* **2004,** 21, (3), 389-93.

149. Takeuchi, T.; Kosuge, M.; Tadokoro, A.; Sugiura, Y.; Nishi, M.; Kawata, M.; Sakai, N.; Matile, S.; Futaki, S., Direct and rapid cytosolic delivery using cell-penetrating peptides mediated by pyrenebutyrate. *ACS Chem Biol* **2006,** 1, (5), 299-303.

150. Ye, Y.; Bloch, S.; Xu, B.; Achilefu, S., Design, synthesis, and evaluation of near infrared fluorescent multimeric RGD peptides for targeting tumors. *J Med Chem* **2006,** 49, (7), 2268-75.

151. Mukamel, S. S., *Principles of nonlinear optical spectroscopy*. Oxford University Press: New York, 1995; Vol. 6.

152. Baldwin, G. C., *An introduction to nonlinear optics* Plenum Press: New York, 1969; p 155.

153. Mikata, Y.; Takagi, S.; Tanahashi, M.; Ishii, S.; Obata, M.; Miyamoto, Y.; Wakita, K.; Nishisaka, T.; Hirano, T.; Ito, T.; Hoshino, M.; Ohtsuki, C.; Tanihara, M.; Yano, S., Detection of 1270 nm emission from singlet oxygen and photocytotoxic property of sugar-Pendant [60] fullerenes. *Bioorganic & Medicinal Chemistry Letters* **2003,** 13, (19), 3289-3292.

154. So, G.; Karotki, A.; Verma, S.; Hauck, T. S.; Wilson, B.; Pritzker, K. P. H.; Chiang, L. In *Singlet oxygen production by amphiphilic C60 derivatives and its correlation to cell cytotoxicity in vitro*, Photonic Applications in Biosensing and Imaging, Toronto, Canada, 2005; SPIE: Toronto, Canada, 2005; pp 59690D-8.

155. Webb, C. X. a. W. W., Measurement of two-photon excitation cross sections of molecular fluorophores with data from 690 to 1050 nm. *Journal of the Optical Society of America B* **1996,** 13, (3), 481-491.

156. Sheik-Bahae, M.; Said, A. A.; Wei, T. H.; Hagan, D. J.; Van Stryland, E. W., Sensitive measurement of optical nonlinearities using a single beam. *Quantum Electronics, IEEE Journal of* **1990,** 26, (4), 760-769.

157. Morales, A. R.; Belfield, K. D.; Hales, J. M.; VanStryland, E. W.; Hagan, D. J., Synthesis of Two-Photon Absorbing Unsymmetrical Fluorenyl-Based Chromophores. *Chem. Mater.* **2006,** 18, (20), 4972-4980.

158. Pond, S. J. K.; Rumi, M.; Levin, M. D.; Parker, T. C.; Beljonne, D.; Day, M. W.; Bredas, J. L.; Marder, S. R.; Perry, J. W., One- and Two-Photon Spectroscopy of Donor-Acceptor-Donor Distyrylbenzene Derivatives: Effect of Cyano Substitution and Distortion from Planarity. *J. Phys. Chem. A* **2002,** 106, (47), 11470-11480.

159. Frederiksen, P. K.; Jorgensen, M.; Ogilby, P. R., Two-photon photosensitized production of singlet oxygen. *J Am Chem Soc* **2001,** 123, (6), 1215-21.

160. Ogawa, K.; Hasegawa, H.; Inaba, Y.; Kobuke, Y.; Inouye, H.; Kanemitsu, Y.; Kohno, E.; Hirano, T.; Ogura, S.; Okura, I., Water-soluble bis(imidazolylporphyrin) self-assemblies with large two-photon absorption cross sections as potential agents for photodynamic therapy. *Journal of Medicinal Chemistry* **2006,** 49, (7), 2276-2283.

161. Cohanoschi, I.; Belfield, K. D.; Toro, C.; Yao, S.; Hernandez, F. E., The impact of the pi-electron conjugation length on the three-photon absorption cross section of fluorene derivatives. *The Journal of Chemical Physics* **2006,** 124, (19), 194707-5.

162. Belfield, K. D.; Liu, Y.; Negres, R. A.; Fan, M.; Pan, G.; Hagan, D. J.; Hernandez, F. E., Two-Photon Photochromism of an Organic Material for Holographic Recording. *Chem. Mater.* **2002,** 14, (9), 3663-3667.

163. Belfield, K. D.; Ren, X.; Van Stryland, E. W.; Hagan, D. J.; Dubikovsky, V.; Miesak, E. J., Near-IR Two-Photon Photoinitiated Polymerization Using a Fluorone/Amine Initiating System. *J. Am. Chem. Soc.* **2000,** 122, (6), 1217-1218.

164. C. C. Corredor, Z. L. H. K. D. B., Two-Photon 3D Optical Data Storage via Fluorescence Modulation of an Efficient Fluorene Dye by a Photochromic Diarylethene. *Advanced Materials* **2006,** 18, (21), 2910-2914.

165. Gollnick K., F. G., Doerhoefer S., Doerhoefer G., Photosensitized Oxygenation as a Function of the Triplet Energy of Sensitizers. *Annals of the New York Academy of Sciences* **1970,** 171, 89-107.

166. Belfield, K.; Konté, M.; Przhonska, O., Singlet Oxygen Quantum Yield Determination for a Fluorene-Based Two-Photon Photosensitizer. *Journal of Fluorescence* **2006,** 16, (1), 111-117.

167. Marhevka, V. C.; Ebner, N. A.; Sehon, R. D.; Hanna, P. E., Mechanism-based inactivation of N-arylhydroxamic acid N,O-acyltransferase by 7-substituted-N-hydroxy-2-acetamidofluorenes. *J. Med. Chem.* **1985,** 28, (1), 18-24.

168. Grantham, P. H.; Weisburger, E. K.; Weisburger, J. H., Ionization Constants of Derivatives of Fluorene and Other Polycyclic Compounds2. *J. Org. Chem.* **1961,** 26, (4), 1008-1017.

169. Holm, M. J.; Zienty, F. B.; Terpstra, M. A., Condensation of aromatic and heterocyclic aldehydes with benzenediacetonitriles. *J. Chem. Eng. Data* **1968,** 13, (1), 70-74.

170. Lim, S. J.; An, B. K.; Park, S. Y., Bistable Photoswitching in the Film of Fluorescent Photochromic Polymer: Enhanced Fluorescence Emission and Its High Contrast Switching. *Macromolecules* **2005,** 38, (15), 6236-6239.

171. Dam, N.; Scurlock, R. D.; Wang, B.; Ma, L.; Sundahl, M.; Ogilby, P. R., Singlet Oxygen as a Reactive Intermediate in the Photodegradation of Phenylenevinylene Oligomers. *Chem. Mater.* **1999,** 11, (5), 1302-1305.

172. Ma, L.; Wang, X.; Wang, B.; Chen, J.; Wang, J.; Huang, K.; Zhang, B.; Cao, Y.; Han, Z.; Qian, S.; Yao, S., Photooxidative degradation mechanism of model compounds of poly(p-phenylenevinylenes) [PPVs]. *Chemical Physics* **2002,** 285, (1), 85-94.